UNIVERSITY OF OKLAHOMA

GRADUATE COLLEGE

DEVELOPMENT OF MULTI-OBJECTIVE OPTIMIZATION MODEL OF COMMUNITY RESILIENCE ON MITIGATION PLANNING

A DISSERTATION

SUBMITTED TO THE GRADUATE FACULTY

in partial fulfillment of the requirements for the

Degree of

DOCTOR OF PHILOSOPHY

By

YUNJIE WEN
Norman, Oklahoma
2021

DEVELOPMENT OF MULTI-OBJECTIVE OPTIMIZATION MODEL OF COMMUNITY RESILIENCE ON MITIGATION PLANNING

A DISSERTATION APPROVED FOR THE
SCHOOL OF INDUSTRIAL AND SYSTEMS ENGINEERING

BY THE COMMITTEE CONSISTING OF

Dr. Charles Nicholson, Chair

Dr. Theodore Trafalis

Dr. Andrés González

Dr. Andrew H. Fagg

Dr. Yifu Li

© Copyright by YUNJIE WEN 2021
All Rights Reserved

Acknowledgment

I could not finish this study without the members of my doctoral committee. First, I would like to express my gratitude to my advisor, Dr. Charles D. Nicholson, who has been an extraordinary mentor for me. He treats me with kindness, patience, and respect throughout my whole doctoral study. Additionally, I gratefully acknowledge the funding Dr. Nicholson provided that made my graduate study possible. I appreciate all the time and effort he had devoted to me. His support and inspiration are highly invaluable to my research. I could not have finished my research without Dr. Nicholson. I also want to extend my gratitude to Dr. Andrés González, who has been helping me through this study. He led by example and showed me how to be a great researcher. I want to acknowledge Dr.Theodore Trafalis and Dr. Andrew H. Fagg for their support and guidance on my course study. Last and not least, I would like to thank Dr. Yifu Li's support in being my committee member.

Many other people have also helped me with this study. Dr. Cutler Harvey, Dr. John van de Lindt, and Brad Hartmen (Colorado State University), Wang Chen (National Center for Supercomputing Applications), Dr.Nathanael Rosenheim (Texas A&M University) also provided help when I had questions regarding their researches. I want to acknowledge Lisa Wang (Colorado State University) for providing the 22 tornado events for my study through IN-CORE.

Besides my academic support, I would like to thank my friends during my years' school life. I appreciate that the school has provided so many opportunities to know many wonderful people. Emi Kiyotake has been a wonderful friend through the last two years of

my study. She has sacrificed her time to help me with my writing. Lauran Hale is always a rock to mentally support me during the most challenging time of my life. Safa Namiq has offered so many supports whenever I asked.

My family has been very supportive throughout my six years of school. Unfortunately, my parents passed away before I could finish my doctoral study. I would like to thank my parents take me back to school after I failed university qualification exam 26 years ago. I would have never thought I could finish the doctoral program one day in the US. I think they would be very proud of me for making it so much further than they would have expected. My Sister, Yujie Wen, had sacrificed her time and family to take care of my parents while they were in critical conditions and to arrange funerals for them while I could not. Finally, I would like to thank my husband, Dan Dirks, for being very supportive mentally and financially of my study. I don't think it is possible I could finish my study without him. He never complained, and always 100% supported my decision. I could not ask for a better partner than him.

I want to thank everyone I mentioned above again. Thank you for making me the better person I am now. I will carry all memory from this journey to my next one.

Table of Contents

List of Figure

List of Tables

Abstract

Mitigation planning in many disaster-prone areas has shown success in helping the community to withstand hazardous events, reducing the recovery time and costs, and preventing life losses. This research proposes a multi-objective optimization framework to enhance decision-making to mitigate risk from potential hazards in an integrated and quantitative manner.

First, this study introduces an optimization framework that can integrate different dimensions of community resilience in one model as competing objectives to measure the potential impacts and damage from hazard events. To the best of our knowledge, this framework is the only framework that can provide flexibility on some major components. The decision makers can apply the proposed framework to various hazards without changing the mathematical formulation. The framework's objectives can be determined by the people who are involved in decision-making. Moreover, the number of objectives also can vary according to the actual needs of decision makers.

Second, the proposed framework is applied to tornado mitigation in the city of Joplin, Missouri, USA, to demonstrate how the retrofitting strategies reduce the potential impacts of direct economic loss (economic dimension), population dislocation (social dimension), and building functionality (physical infrastructure). The results analyses illustrate how the decision makers can utilize the information from the optimal solutions to determine the appropriate retrofitting solution for the community.

Finally, a machine learning (ML) model is developed to predict potential economic damage on domestic supply, employment, migration, and household income by using input

data of the computable general equilibrium (CGE) model. This ML model can act as a surrogate model to help the non-CGE expert to interpret the relationship between the capital shock by sector and economic impact from hazards shock on capitals. The predicted impact on domestical supply, employment, migration, and household income from this ML model can act as coefficients of objectives functions (domestical supply, employment, migration, and household income) of the proposed multi-objective optimization model.

1 Introduction

1.1 Background

The increasing number of natural disasters constantly test the resilience of communities every year. Most recently, in 2020 alone, there were 22 weather/climate related disasters with losses exceeding $1 billion each, and the combined cost for these 22 events exceeds $95 billion. Most of the areas that endured the disaster events are well-populated, but the communities in those areas are not resilient to the high frequency of hazards. In 2017, after hurricane Maria, some of the residents in Puerto Rico lost their power for over a year. Over 200,000 Puerto Ricans left the mainland. Katrina displaced 770,000 residents and left $250 billion in damaged to the local community. Fourteen years later, some residents were still rebuilding their homes. Scientists and researchers have reached consensus that effective mitigation can reduce the potential impact from future hazards to the communities. However, to date, there is no generalized and hazard agnostic multi-objective optimization framework to guide the decision makers to determine and evaluate mitigation strategies in a quantitative and integrated manner.

Future hazards are inevitable, yet the frequency and magnitude of the hazard events are growing. As cities and communities continue to expand, the hazards might cause more damage. Fortunately, pre-hazard mitigation is a proactive measure to prepare in advance for future hazards. Mitigation measures can reduce the impact, help the communities bounce back faster, and lower the recovery cost. The ongoing efforts in the National Institute of Standards and Technology (NIST) funded the multi-university Center of Excellence for Risk-based Community Resilience Planning (CoE) are developing the

measurement science to support community resilience assessment. The major work of the CoE is to develop a comprehensive computational platform with a fully integrated supporting database called IN-CORE (Interdependent Networked Community Resilience Modeling Environment) that models the impact and recovery of natural hazards on communities, evaluates community resilience goals, and optimizes resilience enhancement/planning strategies. This dissertation provides an essential component of IN-CORE modules on optimization analysis.

The optimization framework plays a vital role in mitigation planning. The goal of the optimization framework is not only to prioritize the mitigation strategies but also to help the communities allocate limited resources. Ultimately, the framework is used as a risk-informed decision tool for the decision makers, who should determine the mitigation plan among all solutions. However, the components (e.g., objectives functions, the granularity of decision-making, type of hazards) of the existing frameworks were missing decision makers' perspective, and the mitigation solutions produced by these frameworks might not be practical to improve the resilience of the communities.

To facilitate decision-making on mitigating the risk and vulnerability from potential hazards, the framework of multi-objective optimization should allow the decision makers to have a certain degree of freedom to determine the framework components related to the decision-making. This framework must act as a framework to allow decision-making to define the factors that help the communities to make better decisions according to the needs of the communities.

1.2 Research Scope

The scope of this dissertation includes three parts: (1) to design an integrated multi-objective optimization framework that optimizes community resilience goals to obtain retrofitting strategies for communities to mitigate potential risk and vulnerability, and to facilitate the decision-making by analyzing the results provided from the model; (2) to demonstrate the implementation of the optimization model through a case study; and (3) to develop a surrogate model to predict overall economic impact using the information from a CGE model and use the predicted results to connect the CGE model with optimization model.

The dissertation will focus on the following tasks:

- Develop a hazard agnostic framework to produce optimal retrofitting strategies to mitigate the risk from potential hazards considering multiple community resilience goals.
- Provide a complete analysis procedure by applying the framework to tornado hazard in the city of Joplin, MO, by optimizing the three community resilience goals: direct economic loss, population dislocation, and building functionality.
- Develop machine learning models to estimate economic impact based on the economic sector inputs and output results from CEG model and connect the CGE model with an optimization model to showcase the generalization of the framework of the first task.

This dissertation has meaningful academic contributions and implications in the optimization of community resilience and mitigation planning. The proposed framework can be applied to many hazard preventions without limitation on the type of community

resilience goals, type of hazards, and the decision level. With the further development of the open-source platform, this framework will have a practical influence on the real-world mitigation problems of community resilience.

1.3 Structure of Dissertation

In Chapter 2, a multi-objective optimization model is proposed for providing retrofitting plans based on the measurement of community resilience goals defined by decision makers. The methodology of decision-making support provides the methods for evaluating the mitigation strategies among all optimal solutions and identifying the vulnerable areas in the communities. Chapter 3 demonstrates the application of the framework proposed in Chapter 2 in the city of Joplin, Missouri, on tornado mitigation that has fewer studies and attention from scientists and researchers compared with other types of hazards. In Chapter 4, a linear machine learning model is developed as a surrogate model to estimate the overall economic impact based on the input data and output results from the CGE model for designed hazards. The results analysis suggests the linear regression models (OLS, Ridge, Elastic Net, LASSO) all can perform well on adequate prediction on economic impacts (i.e., Domestic Supply, Employment, Migration, Household Income). Additionally, an optimization model is designed to apply the building retrofit strategies on economic sectors. Chapter 5 summarizes the major contribution of this dissertation and suggests future research.

2 Multi-objective optimization model of community resilience on mitigation planning

2.1 Introduction

The challenges of current resilience frameworks are generalization on hazard types, correlation between social and economic attributes, and optimization and prioritization of retrofit solutions (Koliou, et al., 2018). To enhance the resilience of a community in an integrated manner, a framework should have flexibility and the ability to adjust the essential components to fit specific needs from decision makers. First, the objectives of the optimization framework should reflect the primary interest of the decision makers. The number of objectives and the determination of objectives should be defined by the people involved in the decision-making, not those who design the framework. If decision makers select economic loss and recovery time as objectives, the optimization model is a bi-objective optimization problem. Second, a generic framework should not only target one specific hazard. The characteristics of a hazard should be provided though the input data to the model, not the model itself. Third, a framework should have the ability to integrate different systems to measure the potential impact on these systems. The primary potential impact from hazard events typically includes the evaluation of the damage to social, economic and physical infrastructure systems. Many metrics have been derived for each system, for example, direct economic loss (Zhang and Nicholson, 2016), indirect economic loss (Fujimi and Tatano, 2012), population dislocation (Rosenheim, et al., 2021), household well-being loss (Markhvida, et al., 2020), and building functionality (Koliou and van de Lindt, 2020). The decision makers of the community should determine

appropriate metrics for the framework. Finally, one rising challenge is how to determine the retrofitting planning among all optimal solutions. Decision-making support should be provided to explore the options for decision makers to target vulnerability reduction and to provide criteria on prioritizing those options.

2.2 Highlights

This chapter proposes an optimization framework to mitigate potential impacts from hazard events for the community. This model is designed with flexibility that allows the decision makers to define what community resilience goals should be included and which type of hazard is considered if the requirements for the input data are met. The decision makers can choose the community resilience goals that are appropriate to the needs and interests of the community at a considered hazard. To increase the scalability of the framework, three considerations are in place for this purpose. First, a set of pre-defined combination of allowable retrofit strategies reduces the size of input data, which is one of factors can impact the run-time of the model. Second, in comparison to a non-linear model, a linear design of the mathematical model allows problem to be solved in efficient way. Third, while the epsilon constraints approach, would take exponential number of steps if number of objectives were increased, but epsilon constraint method can solve problems more efficiently comparing with some metaheuristic algorithms and genetic algorithm. The decision-making support from the analysis of the results provides arrays of options for decision makers to select the appropriate retrofitting planning for the community. The upcoming analysis section illustrates how the results can be utilized to facilitate the process of decision-making.

2.3 Multiple dimensions of community resilience

The US National Institute of Standards and Technology (NIST) defines community resilience as a community's ability "to prepare for anticipated hazards, adapt to changing conditions, and withstand and recover rapidly from disruptions" (NIST, 2015). Given the observed increasing intensity, impact, and frequency of significant hazards, enhancing community resilience is a critical mission. However, communities are complex entities with many facets and the resilience goals and effective strategies should reflect the multiple and important aspects of the communities. Researchers have worked to identify the most salient dimensions. Bruneau, et al. (2003) conceptualized resilience from four interrelated dimensions: technical, organization, social, and economic. Renschler, et al. (2010) introduced seven dimensions for assessing community resilience: population and demographics, environment/ecosystem, organized governmental service, physical infrastructure, lifestyle and community competence, economic development, and social-cultural capital. Miles and Chang (2011) demonstrated that damage associated with a hazard event impacted three critical elements of community resilience: physical infrastructure functionality, financial and economic performance, and individual well-being. Alshehri, et al. (2014) focused on six resilience attributes: social, economic, physical and environmental, governance, health and well-being, and information and communication. The NIST Community Resilience Planning Guide provided a framework that included setting goals for three distinct community elements: physical (i.e., built environment), social, and economic systems (NIST, 2015). These various studies underscore the significance of addressing community resilience from a multidimensional perspective. Achieving resilience objectives along different dimensions may be further

complicated if the objectives are conflicting and/or the necessary interventions are competing for the same set of limited resources, e.g., budget, time, labor resources.

Various decision frameworks and mathematical models can help provide decision-support for the complex issues associated with enhancing community resilience. For example, Zhang and Nicholson (2016) developed a multiple objective optimization mathematical program that integrated direct economic damage (economic dimension) and population dislocation (social dimension) measures to improve community resilience. Ellingwood, et al. (2016) demonstrated the possibility of fully integrating physical, social, and economic infrastructure systems. In particular, this study investigated the interaction between physical infrastructure systems and socio-economic systems within a community. Both Zhang and Nicholson (2016) and Ellingwood et al. (2016) demonstrated their work on Centerville – a virtual community, designed specifically to evaluate multiple disciplinary approaches to resilience (for additional analyses on Centerville see Cutler, et al. (2016b), Guidotti, et al. (2016), Unnikrishnan and van de Lindt (2016)). Sutley, et al. (2017a) developed a multiple objective optimization problem that coupled various socio-economic characteristics and built environment factors to support decision making for seismic retrofit strategies at a community level. Üstün and Anagün (2015), Tapia and Padgett (2016), and Sadeghi, et al. (2017) demonstrated the potential impact of multiple objective optimization modeling coupled with the multifaceted attributes of communities to enhance resilience.

2.4 Multi-objective optimization

Multi-objective optimization (MOO) problems have two or more objectives that typically compete for the same resources (e.g., budget, labor, time, etc.) and are conflicting, i.e., no single solution optimizes all objectives. Figure 2-1 depicts an objective space for a bi-objective minimization problem with two competing objectives, $f_1(x)$ and $f_2(x)$, where x denotes a decision variable for the problem. Solution x_2 dominates solution x_1 since $f_1(x_2) < f_1(x_1)$ and $f_2(x_2) < f_1(x_1)$. However, both x_1 and x_2 are dominated by x_3 and x_4. The solutions x_3 and x_4 are said to be non-dominated since for both solutions, one objective cannot be improved without degrading the other. The set of all non-dominated solutions form the Pareto frontier (shown in Figure 2-1 as the solid dots). All solutions along the Pareto frontier are considered equally good from a mathematical perspective and it is up to a decision-maker to determine the tradeoff appropriate for the problem at-hand.

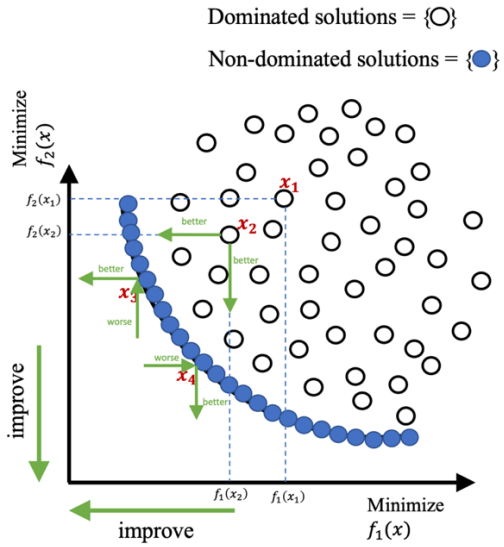

Figure 2-1. Objective space of bi-objective optimization problem

Various studies have employed MOO techniques for community resilience. Zhang and Nicholson (2016) proposed a multi-objective optimization model to provide a retrofit plan to mitigate social (i.e., population dislocation) and economic impacts (i.e., immediate cost from structural damage) in communities to seismic events in a built environment. The case study was applied to a virtual city, Centerville, comprised of over 15,000 buildings. Calle (2019) extended this effort by integrating an enhanced, non-linear method to estimate population dislocation. The case study was implemented on a community with over 300,000 buildings including 11 distinct structural types. Sutley, et al. (2017a) studied a community-level mitigation problem coupling socio-economic and engineering systems for seismic retrofit planning. The authors incorporated four resilience metrics—initial loss, economic loss, morbidities, and recovery time. In the companion paper, Sutley, et al. (2017b) presented the multi-objective optimization formulation and results exemplified on 100,000 wood frame buildings in Los Angeles County, CA. However, the studies from Sutley, et al. (2017a) and Sutley, et al. (2017b) were only designed for seismic mitigation. Moreover, the objectives that represent the resilience metrics in the studies above only measured specific aspects of systems, such as population dislocation and morbidities measuring the social system, economic impact measuring the monetary loss of community. Neither these objectives nor the number of objectives can be altered per the actual needs of the problems. Therefore, none of these studies can act as a framework to be applied to the different types of problems (e.g., tornado mitigation considering economic and social impacts, flooding mitigation considering economic, social and physical systems, tsunami mitigation only considering economic impact, etc.).

2.5 Building inventory as an interface between the built environment and human welfare

The built environment includes residential, commercial, and governmental buildings; utility networks providing water power, and gas; and, the network of roads, rails, and bridges that contribute to the transportation system, among others. Often the various elements of a community's built environment are depicted as interdependent layers. These relationships are often complex, and many researchers have investigated how the functionality of the physical system as a whole is impacted by disruptions in the subsystems (Masoomi and van de Lindt, 2018; Wang, et al., 2018; Zhang, et al., 2018; Wang, et al., 2021). For instance, the water network may be affected by power outages disrupting pumps or treatment centers (Adachi and Ellingwood, 2008); disruptions in the transportation system may impact the recoverability of other systems by impeding access of repair and construction crews (Liu, et al., 2020). The functionality of the building inventory, i.e., the ability of the buildings in a community to be used for their intended purpose, is dependent both on the building's structural integrity and of the availability of the critical utilities (Almufti and Willford, 2013; Lin and Wang, 2017).

Fundamentally, the built environment exists to support the socio-economic well-being of the community. That is, at least two additional conceptual layers should be added to the community depiction, i.e., layers representing societal welfare and the economic systems. These two layers, while somewhat abstract, are certainly multi-faceted, interdependent, and complex, but also highly dependent on the proper functionality of the built environment. Disruptions anywhere within the built environment may have negative

impacts on the economic systems (e.g., Cutler et al., 2016a; Masoomi et al., 2018) and/or the social systems (Cutter, et al., 2003; Zahran, et al., 2008; Van Zandt, et al., 2012; Karakoc, et al., 2019; Rosenheim, et al., 2021). However, we propose that building inventory as a "layer" within the community depiction plays a distinct and critical role as a principal interface between the built environment and the socio-economic layers (see Figure 2-2). For instance, power, water, and gas utilities are primarily distributed to buildings such as residential units; the transportation system largely serves as a mechanism to convey people and goods from one building to another such as raw materials to manufacturers or finished goods to warehouses. A building is said to be functional if it can support its original purpose (Lin and Wang, 2017). Dysfunctionality then may be due to direct damage to a building or indirect effects. For instance, if the supporting utility services are damaged the effects will be experienced at the building level. Such effects impact human activity, e.g., damaged school buildings impact education services, disrupted power or water services affect local businesses, and gas leaks may cause residents to evacuate homes. While "buildings as an interface" is not entirely a comprehensive depiction (e.g., telecommunication services are less and less tied to buildings and more to mobile devices), it does provide a useful modeling abstraction that both captures important dependencies and reduces problem complexity. Given this role, and the fact that functional buildings are fundamental to life safety, shelter, health, and social stability, our modeling perspective focuses on this interface.

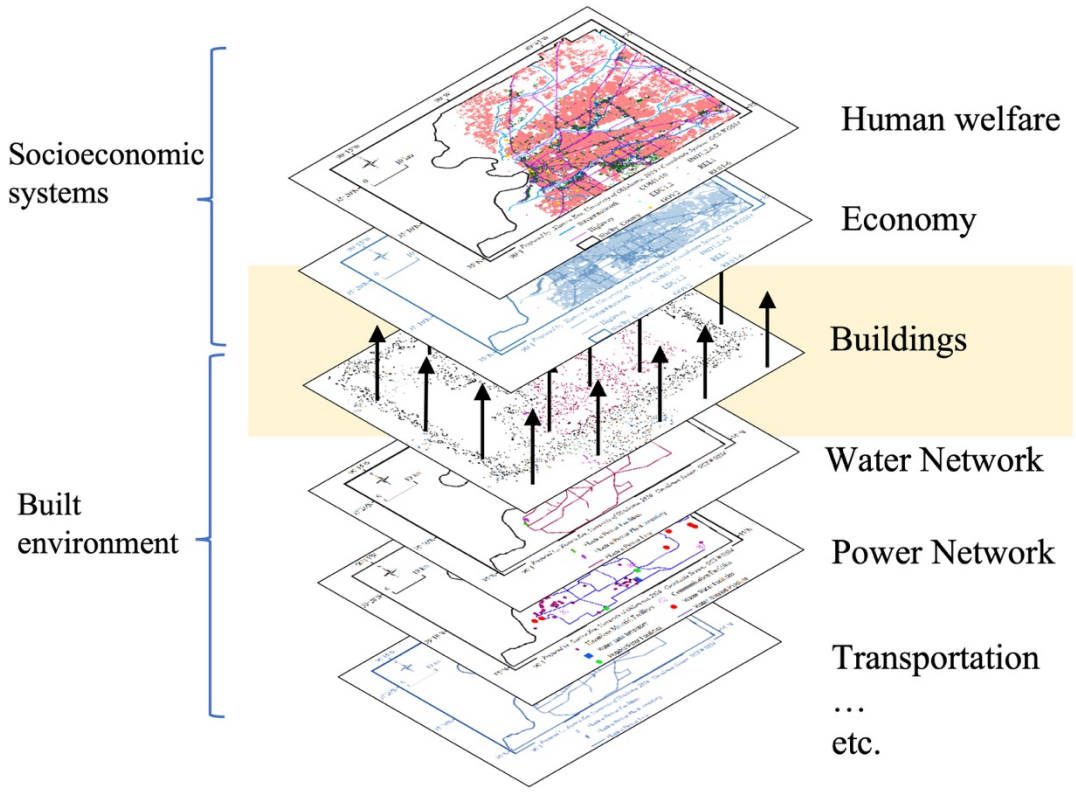

Figure 2-2. Buildings as interface layer within a community

2.6 Research gap and contribution

Hazard mitigation in the past studies of community resilience have focused on the essential individual system. Each field has conducted rich research, for example, hazard impact on the economic system (West, 1995; van der Veen, 2004; Chang and Rose, 2012; Xiao and Nilawar, 2013; Martinelli, et al., 2014; Zhou and Chen, 2020), on the social system (Maguire and Hagan, 2007; Magis, 2010; Wind, et al., 2011), and on the physical system (Gordon, et al., 2004; Adachi and Ellingwood, 2008; Chang, et al., 2008; Zhang and Miller-Hooks, 2014; Lin and Wang, 2016; Unnikrishnan and van de Lindt, 2016; Masoomi, et al., 2018a; Rosenheim, et al., 2021). However, in the past decade, the increasing number of collaborative studies between different systems (Guha, 2011; Gilbert,

et al., 2015; Sutley, et al., 2017a; Wang, et al., 2021) showed more robust assessment and mitigation on community resilience. To identify the research need, several research studies and the research components of their studies have been summarized in Table 2-1. Out of the studies listed in the table, 13 studies conducted a multi-objective optimization model on hazard mitigation. Sutley, et al. (2017b) conducted an integrated model to measure the economic, social, and physical system in one framework. However, the model from Sutley, et al. (2017b) only targeted seismic mitigation. Thus, the gap in the current research is an integrated model measures multiple dimensions of community resilience while further being acceptable to a variety of hazards.

Based on the research gap identified from the studies presented in Table 2-1, the study in Chapter 2 can fill the research gap and contribute to community resilience from the following aspects: (1) the framework can apply to various hazards, (2) the granularity of decision level is determined by needs of decision-making, and (3) the number of objective and objectives are defined by the decision makers.

First, the framework proposed from this study is the first framework among the existing frameworks that integrates all essential systems (i.e., economic, social, and physical) into one framework and is able to be applied to various hazards. It can be applied to various hazards because the hazard characteristics are not designed into the mathematical model but are reflected through the input data, as long as the required data are available and meet the requirements of the framework. Moreover, the primary systems of a community are integrated into the framework in a competitive way that allows decision makers to allocate mitigation resources with a more comprehensive perspective.

Secondly, none of existing studies have the flexibility that allows decision makers to define the granularity of decision level. Sutley, et al. (2017a) introduced four objectives (i.e., initial cost, number of morbidities, economic loss, and recovery time) at building archetype level, which was not able to be changed to any other decision level. In the framework introduced in this study, the granularity of decision level is not designed into the mathematical model, but it is incorporated into the model via the input data.

Third, the frameworks introduced by Zhang and Nicholson (2016) and Sutley, et al. (2017b) did not have ability to allow decision makers to determine the objectives. Furthermore, neither of the frameworks allowed decision-maker to define the number of objectives needed for the decision-making. If a framework cannot reflect the needs/input from the end-user, the framework is limited and may only be applied to a very specific problem. The framework developed here enables decision makers to choose appropriate objectives and number of objectives, which is the first framework of mitigation plan to have flexibility on the model design.

To conclude, the framework introduced in Chapter 2 can enhance the community resilience in a consolidated manner that can engage decision makers to define the objectives, and granularity of decision level. The three aforementioned aspects were not introduced in any existing studies but are all included in the framework introduced in this study.

Table 2-1. Reference related to the research gap

Reference	Hazard agnostic	Optimization Model	Multi-objective	Physical system	Social system	Economic system	User defined granularity level	Flexibility of objective
Dodo, et al. (2005)	Earthquake	✅	❌	❌	❌	✅	❌	❌
Dueñas-Osorio, et al. (2007)	Earthquake	❌	❌	✅	❌	❌	❌	❌
Dong, et al. (2014)	Earthquake	✅	✅	✅	❌	✅	❌	❌
Sadeghi, et al. (2017)	Earthquake	✅	✅	❌	✅	✅	❌	❌
Sutley, et al. (2017b)	Earthquake	✅	✅	✅	✅	✅	❌	❌
Park, et al. (2012)	Flood	✅	✅	✅	❌	❌	❌	❌
Woodward, et al. (2014)	Flood	✅	✅	❌	✅	✅	❌	❌
Arca, et al. (2015)	Wildfire	✅	✅	❌	❌	✅	❌	❌
Wang, et al. (2018)	Tornado	✅	✅	✅	❌	❌	❌	❌
Wang, et al. (2021)	Tornado	❌	❌	✅	✅	✅	❌	❌
Legg, et al. (2013)	Hurricane	✅	❌	✅	❌	❌	❌	❌
Dahal and Dahal (2017)	Hurricane	✅	❌	✅	❌	✅	❌	❌
Faturechi and Miller-Hooks (2013)	✅	✅	❌	✅	❌	❌	❌	❌
González, et al. (2016)	✅	✅	❌	✅	❌	❌	❌	❌
Zhang and Nicholson (2016)	✅	✅	✅	❌	✅	✅	❌	❌
Tapia and Padgett (2016)	✅	✅	✅	❌	✅	✅	❌	❌
Ellingwood, et al. (2016)	✅	❌	❌	✅	✅	❌	❌	❌
Zhang, et al. (2018)	✅	✅	✅	✅	❌	❌	❌	❌
Fang and Zio (2019)	✅	✅	❌	❌	❌	❌	❌	❌
Karakoc, et al. (2019)	✅	✅	✅	✅	✅	❌	❌	❌
RO1	✅	✅	✅	✅	✅	✅	✅	✅

(Note: ✅ indicates the research component is discussed in the reference; ❌ indicates the research component is not include in the reference)

2.7 The Interdependent Networked Community Resilience Modeling Environment

The Interdependent Networked Community Resilience Modeling Environment (IN-CORE) is an open-source research tool to provide novel and comprehensive modeling to support research on the interconnection of physical, social, and economic systems (Gardoni, et al., 2018; van de Lindt, et al., 2018). IN-CORE was designed by the Center for Risk-Based Community Resilience Planning (http://resilience.colostate.edu/) to model the impact and recovery of natural hazards on communities in a computational environment with fully integrated databases. The fundamental process flow of IN-CORE is illustrated in Figure 2-3: (1) a community description is provided to the platform that represents the built environment and the social and economic systems, (2) a hazard such as a tornado, earthquake, or flood is simulated within the system and the resulting physical damage are estimated, (3) the impacts on the social, economic, and physical system functionality are computed based on the current state of the system at a given time j, and (4) recovery models allow a user to advance through time steps $j = 0, \dots, m$ to evaluate the effects of restoration models on the community. Additionally, IN-CORE provides detailed decision support to optimize mitigation or recovery interventions with respect to community defined goals (step 5) to identify a suite of Pareto optimal solutions (in steps 6,7,8) that respect the community defined resource availability and constraints. Finally, IN-CORE provides a suite of solution visualizations to support decision-making.

The mathematical optimization modeling approach and general framework presented in this study is designed for implementation in IN-CORE to provide the

aforementioned detailed decision support for enhancing or retrofitting buildings prior to a hazard event. The model can function as either standalone or as an integral element of IN-CORE leveraging the hazard simulation, damage estimates, and expected intervention effects on building-level vulnerability to support any number of community defined objectives. Section 2.7 describes the modeling framework and its relationship to IN-CORE analyses.

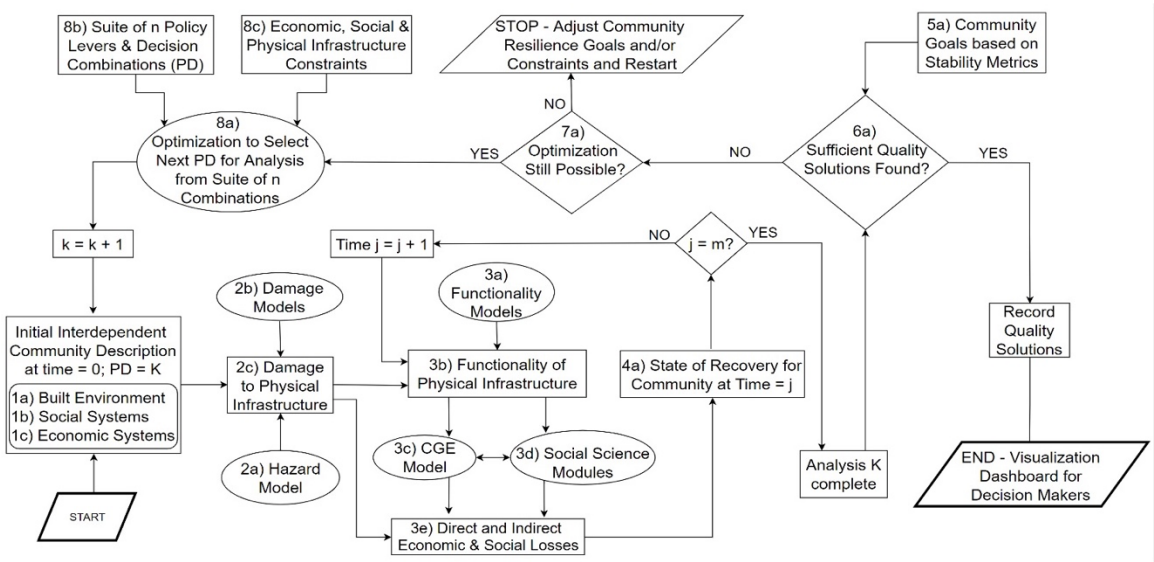

Figure 2-3. The structure of IN-CORE (Ellingwood, et al., 2019)

2.8 Multi-objective mitigation optimization framework

Figure 2-4 provides a graphical overview of the modeling framework and its three primary components, i.e., the (1) required input data and granularity specification, (2) the multi-objective approach and mathematical model specification, and (3) the detailed output that supports a variety of visualization and solution analysis. Each of these components are detailed in the subsequent subsections.

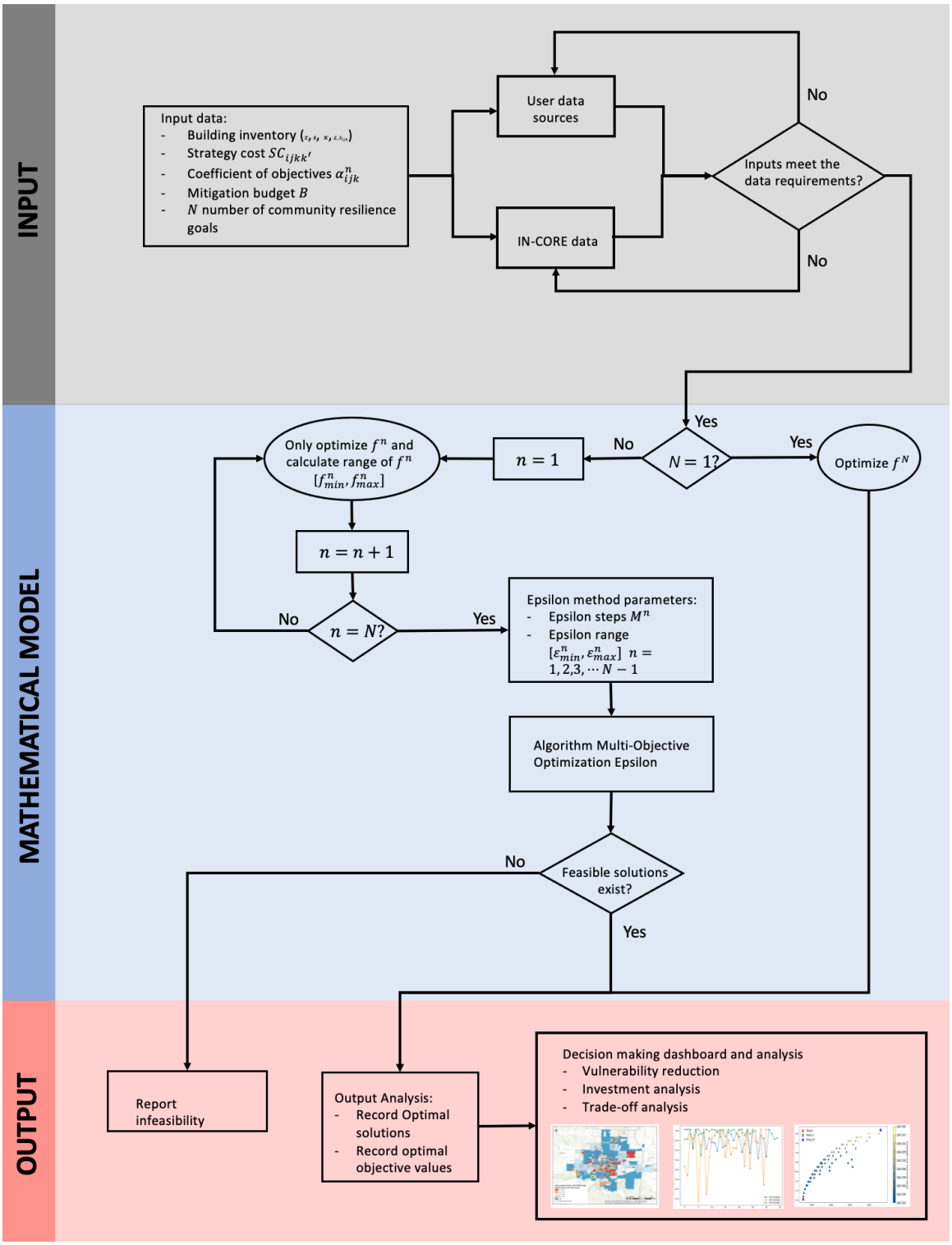

Figure 2-4. Flowchart of the framework

2.8.1 Model input

Communities are geographically defined areas of local jurisdiction such as a counties, cities, or towns. Based on the availability of data, decision-maker needs, scope of intervention authority, the size of the community (specifically, the size of the building inventory), and system computational capabilities, the granularity of the intervention decision support should be defined. For example, a community might desire decision-support at a building-specific level to determine exactly which school buildings, commercial businesses, and/or residential units should be retrofit. However, if the building inventory is large or the decision makers are not interested in such detail, it is typically computationally easier to provide modeling support if the buildings are assigned to logical groups. These groups can be defined as sets of buildings at various levels of detail, e.g., blocks, block groups, census tracts, or public use microdata areas (PUMAs), etc. Additionally, the groups need not be contiguous. For example, the groupings can be based on topographical elevation – a key building characteristic when considering flood hazards – with buildings across the community within a certain elevation range grouped together. The proposed model permits any level of granularity that a user desires, requiring only that each building in the analysis is assigned to exactly one group. Typically speaking, the tradeoff is that more specific granularity provides more detail at the expense of increased computational burden. Let $\mathcal{Z}$ denote the set of building groups.

A building's vulnerability to a hazard is often modeled based on a fragility curve that provides probabilistic information regarding the resulting damage state of the structure after experiencing a hazard of some given magnitude. The fragility curves are specific to classes of buildings. For example, a single-story wood frame residential home will likely

have a distinct fragility from a steel framed high rise for most hazards. The optimization model permits flexibility relating to the structural vulnerabilities of the building inventory (either at an individual building level or a group of buildings with identical fragility functions for a hazard scenario.) That is, a given subset of buildings $i \in \mathcal{Z}$ may be further classified into distinct building taxonomies. The optimization model is agnostic as to how the building types are defined (e.g., commercial vs. residential, wood frame vs. steel frame, archetype 1 vs. archetype 2, etc.). Typically, these identifiers are associated with unique fragility functions for a specified hazard. Let $\mathcal{S}$ denote the set of building types for a community.

Appropriate building-specific mitigation interventions should reflect the building type, material, occupational use, and specific hazard vulnerabilities. Strategies may include various building retrofits, code enforcement, or even building relocation, among others. For instance, depending on the building type, seismic mitigation may include reinforcing buildings with cross bracing, reinforcing buildings using shear walls, or installing shear anchors, etc. For a tsunami, building relocation may be the only suitable intervention due to the severe risk within the inundation zone. For a tornado, different types of roof covering, roof sheathing nailing patterns, and/or roof-to-wall connections might represent different strategies. Let $\mathcal{K}$ denote the set of mitigation strategies. The set $\mathcal{K}$ includes the current status quo level or building code of the existing building inventory. Data are required on the cost and expected benefit for each strategy $k \in \mathcal{K}$ that is applicable to buildings in group $i \in \mathcal{Z}$ of type $j \in \mathcal{S}$. The cost may be expressed in dollars, as time, or as some other community resource. The benefit of strategy $k \in \mathcal{K}$ must be computable in terms of

reduced vulnerability to a building, e.g., the shape of the fragility curve describes a lower probability of greater levels of damage for a specified hazard intensity level.

The sets $\mathcal{Z}$, $\mathcal{S}$, and $\mathcal{K}$ define the granularity of the optimization model and subsequent decision-support. All input data must be specified at least at this level of detail. This includes the baseline building inventory prior to any mitigation efforts. Specifically, let the parameter b_{ijk} denote the total number of buildings in group $i \in \mathcal{Z}$ of type $j \in \mathcal{S}$ at the baseline (pre-intervention) at level $k \in \mathcal{K}$. Table 2-2 provides an example of baseline building inventory data. Here, in group 1, there are five multi-family buildings with strategy $k = 0$ implemented, ten multi-family buildings using strategy 2, 40 single family homes where $k = 2$, and two schools with strategy 4 in place prior to mitigation intervention. All values in the sets $\mathcal{Z}$, $\mathcal{S}$, and $\mathcal{K}$ are categorical, i.e., no order is implied in the numbering of groups or strategies. The sum of the building count column represents the total number of buildings for which mitigation decision support is sought.

The cost to implement a mitigation strategy on a single building (e.g., retrofitting the building to higher code level, modifying the roof sheathing nail pattern, etc.) is denoted as $SC_{ijkk'}$ and represents the average cost of enhancing a building of type $j \in \mathcal{S}$ located in group $i \in \mathcal{Z}$ from the baseline strategy $k \in \mathcal{K}$ to enhanced level $k' \in \mathcal{K}$. The costs may be estimated in terms of dollars, time, labor resources, etc. and may be function of appraised value, building square footage, available labor, and/or material costs, among other factors. Table 2-3 provides an example input data file for the strategy implementation costs, $SC_{ijkk'}$, in terms of dollars. A "do nothing" plan for a building in which $k = k'$ has no associated intervention costs and is always possible. Otherwise, all pairwise allowable

modifications within a group and for a building type must be listed. For example, in Table 2-3, it is possible to change multi-family homes in group 1 from strategy 1 to 2, from 1 to 3, and from 2 to 3. However, it is impossible (or not worth modeling) to allow those same residential structures to move from strategy 2 to 1, 3 to 1, or 3 to 2. The cost column represents the average cost per building for the associated implementation. For example, from Table 2-3, there are five multi-family buildings in group 1 with a baseline level of $k = 1$ and the average cost to modify one of these buildings to $k = 2$ is estimated at $30,000. Regardless of the units of the strategy implementation cost (e.g., money, time, laborers, etc.), the assumption is that resource is limited. Let B denote the value of the input parameter for the community budget of the associated limited resource available during the mitigation intervention time frame.

Communities may have multiple resilience related objectives that they would like to optimize. For any intervention to be worthwhile, it must have a computable benefit relevant to one or more of these objectives. If there N objectives are identified (e.g., minimize population dislocation, minimize direct economic loss, minimize negative impacts on employment, etc.), let α_{ijk}^{n} denote the conditional expected impact on objective $n \in \{1, \dots, N\}$ given the hazard scenario's effect on the buildings in group $i \in Z$, of type $j \in S$, at possible strategy $k \in \mathcal{K}$. For instance, α_{ijk}^{n} may reflect the expected direct economic loss (objective n) due to damage to single story wood frame single-family homes (building type j) located in the inundation zone (group i) of a 500-year return period tsunami hazard. Table 2-4 provides the example file for α_{ijk}^{n} in which objective $n = 1$ is associated with direct economic loss. The objective coefficient α_{ijk}^{n} of $150,000 is the

expected value loss of multi-family homes in group 1 which have strategy $k = 1$ implemented at time of hazard.

Table 2-2. Building inventory data file example

Group $i \in \mathcal{Z}$	**Building type** $j \in \mathcal{S}$	**Strategy** $k \in \mathcal{K}$	**Building count** b_{ijk}
1	Multi-family	1	5
1	Multi-family	2	10
1	Single-family	2	40
1	School	4	2
2	Single-family	1	10
3	Church	2	2
3	Single-family	1	60
3	Shopping mall	1	1
3	Office building	2	5

Table 2-3. Strategy cost example data

Group $\boldsymbol{i \in \mathcal{Z}}$	**Building type** $\boldsymbol{j \in \mathcal{S}}$	**Baseline strategy** $\boldsymbol{k \in \mathcal{K}}$	**Enhanced strategy** $\boldsymbol{k' \in \mathcal{K}}$	**Strategy implementation cost ($)** $\boldsymbol{SC_{ijkk'}}$
1	Multi-family	1	1	0
1	Multi-family	1	2	30,000
1	Multi-family	1	3	45,000
1	Multi-family	2	3	20,000
1	Single-family	2	2	0
1	Single-family	2	3	10,000
1	School	4	4	0
1	School	4	5	500,000
1	School	4	6	1,150,000
2	Single-family	1	1	0
2	Single-family	1	2	15,000
2	Single-family	3	3	0
2	Single-family	3	7	22,000
3	Church	2	2	0
3	Church	2	3	100,000
…	…	…	…	…

Table 2-4. Objective coefficient example data file

Objective $n \in \{1, \ldots, N\}$	**Group** $i \in \mathcal{Z}$	**Building type** $j \in \mathcal{S}$	**Strategy** $k \in \mathcal{K}$	**Objective coefficient** α_{ijk}^{n}
1	1	Multi-family	1	150,000
1	1	Multi-family	2	100,000
1	1	Multi-family	3	25,000
1	1	Single-family	2	30,000
1	1	Single-family	3	10,000
1	1	School	4	225,000
1	1	School	5	95,000
1	1	School	6	110,000
1	2	Single-family	1	10,000
1	2	Single-family	2	2,000
1	2	Single-family	3	15,000
1	2	Single-family	7	9,000
…	…	…	…	…

Input data sources

The input data can be either created externally or be accessed and/or computed via IN-CORE. The current version of IN-CORE contains multiple community descriptions (i.e., inclusive of building inventory data and building types), which can be used to construct the data reflected in Table 2-2. The building group definitions can be customized based on decision-maker goals or otherwise can be modeled directly in IN-CORE at parcel, block, or block group levels. The costs for interventions can be computed based on building inventory details such as percent of appraised value and/or content value. Using fragility functions for building types, IN-CORE can estimate the impacts from earthquake, tornado, hurricane, tsunami, and flood hazard scenarios on physical, social, and economic systems.

In particular, for physical damage to buildings, IN-CORE computes expected damage and probabilistic damage states; for social systems, population dislocation is estimated; and, for economic impact, the impact on the capital stock due to direct damage and indirect, longer-term effects such as household income and employment rates. To generate the type of data depicted in Table 2-4, the buildings in the community can be set to different interventions strategies and hazard simulations run multiple times as a Monte Carlo simulation to calculate expected impacts.

2.8.2 Mathematical model

Decision variables

Let x_{ijk} be the decision variable indicating the total number of buildings in group $i \in \mathcal{Z}$ of building type $j \in \mathcal{S}$ set at strategy $k \in \mathcal{K}$ after optimal mitigation intervention. The difference between x_{ijk} and b_{ijk} implies the overall change from baseline to optimal policy. More specifically, let $y_{ijkk'}$ denote the number of buildings in group $i \in \mathcal{Z}$ of type $j \in \mathcal{S}$ that are enhanced from level $k \in \mathcal{K}$ to $k' \in \mathcal{K}$. The decision variables are logically integer. However, for larger building groupings, the decision variables can be modeled as continuous to greatly improve computational speed. In particular, when the scale of the solution values (hundreds or thousands) is large and the relative error is small, continuous valued solution policies will be rounded to integer feasible retrofit actions.

Objectives

The objective coefficients α_{ijk}^{n} for objectives $n \in \{1, \ldots, N\}$ and the decision variable x_{ijk} are used to create the set of linear objective functions presented in

$$\min \sum_{(i,j,k) \in \mathcal{T}_n} \alpha_{ijk}^n x_{ijk} \qquad \forall n \in \{1,2,\dots,N\} \quad . \tag{2-1}$$

Let the set $\mathcal{T}_n$ denote the 3-tuple(i,j,k) associated with allowable interventions in group $i \in \mathcal{Z}$ for building type $j \in S$ at strategy $k \in \mathcal{K}$ for $n \in \{1,\dots,N\}$ in which α_{ijk}^n is defined (see Table 2-4). Without loss of generality, any maximization objective can be converted to a minimization problem by changing the sign of the objective coefficient. For instance, maximizing post hazard expected building functionality is mathematically equivalent to minimizing the negative of the same building functionality. The decision vector $\boldsymbol{x}$ must include all possible post-optimization states whether or not a coefficient is defined for some objective $n \in \{1,\dots,N\}$. Let the 3-tuple $\mathcal{T}$ denote the set all possible post-optimization states defined as follows:

$$\mathcal{T} = \bigcup_{n \in \{1,\dots,N\}} \mathcal{T}_n.$$

Constraints

The constraint defined in Equation (2-2) ensures that the costs associated with all mitigation interventions are within the allowable budget B,

$$\sum_{(i,j,k,k') \in \mathcal{U}} SC_{ijkk'} y_{ijkk'} \leq B \tag{2-2}$$

where the set $\mathcal{U}$ is the 4-tuple (i,j,k,k') associated with allowable interventions from strategy k to k' in group $i \in \mathcal{Z}$ for building type $j \in \mathcal{S}$. The set $\mathcal{U}$ is derived from the levels defined in Table 2-3.

The constraint in Equation (2-3) provides the logical relationship between the $\boldsymbol{x}$ and $\boldsymbol{y}$ decision vectors such that the number of building at final state after intervention

equal to the number of building before the intervention. That is, the number of buildings in group $i \in \mathcal{Z}$ of type $j \in \mathcal{S}$ that are at strategy $k \in \mathcal{K}$ after the optimization (i.e., x_{ijk}) is determined by the number of those same buildings originally at that level (i.e., b_{ijk}) plus the number of buildings newly enhanced to strategy k (i.e., $y_{ijk'k}$) minus the number of buildings enhanced from k to another strategy k' (i.e., $y_{ijkk'}$),

$$x_{ijk} = \sum_{k':\,(i,j,k',k)\in\mathcal{U}} y_{ijk'k} + b_{ijk} - \sum_{k':\,(i,j,k,k')\in\mathcal{U}} y_{ijkk'} \quad \forall (i,j,k) \in \mathcal{T}. \tag{2-3}$$

The constraint in Equation (2-4) ensures the total number of buildings in every group and for each type are the same before and after the mitigation intervention,

$$\sum_{k:\,(i,j,k)\in\mathcal{T}} x_{ijk} = \sum_{k:\,(i,j,k)\in\mathcal{T}} b_{ijk} \quad \forall i \in \mathcal{Z}, \forall j \in \mathcal{S}. \tag{2-4}$$

Finally, each decision variable can only take non-negative values:

$$x_{ijk} \geq 0 \quad \forall (i,j,k) \in \mathcal{T} \text{ , and} \tag{2-5}$$

$$y_{ijkk'} \geq 0 \quad \forall (i,j,k,k') \in \mathcal{U}. \tag{2-6}$$

Solution approach

The multiple objective optimization problem described in Equations (2-1) - (2-6) is solved using the epsilon-constraint method (Laumanns, et al., 2006; Mavrotas, 2009). In this method, one objective function is selected to be optimized, while the remaining objective functions are reformulated as constraints. Without loss of generality, let objective

N be selected for optimization, then, using the vector notation, the problem can be reformulated as:

$$\min\ f^N(\boldsymbol{x}), \tag{2-7}$$

subject to all constraints (2-2) – (2-6) and additionally the newly formed constraints:

$$f^n(\boldsymbol{x}) \leq \epsilon^n \quad \forall n \in \{1,2,\dots,N-1\}. \tag{2-8}$$

Let P_ϵ denote the epsilon-constrained multiple objective problem defined by the objective in Equation (2-7), constraints (2-2) – (2-6), and Equation (2-8).

The parameter values $\epsilon^n\ \forall n \in \{1,2,\dots,N-1\}$ enforce quality restrictions on the objectives. For instance, if ϵ^n is set infinitely large for all $n \in \{1,2,\dots,N-1\}$, then the constraints in Equation (2-8) are not restrictive and the solution provides the minimum possible value for f^N. Whereas, for instance, if ϵ^1 is reduced into a meaningful range, then all feasible solutions to P_ϵ ensure a performance requirement on objective f^1. An optimal solution to the reformulated problem provides a point along the Pareto frontier. By iterating over many values of $\epsilon^n\ \forall n \in \{1,2,\dots,N-1\}$, the Pareto frontier can be estimated. To accomplish this, an upper and lower bound is established for each ϵ^n with $n \in \{1,2,\dots,N-1\}$ based on the minimums and maximums of objective function f^n with $n \in \{1,2,\dots,N-1\}$. The minimum values are obtained through single objective optimization of $f^n\ \forall n \in \{1,2,\dots,N-1\}$. The maximums are obtained based on computing the objective function values assuming no mitigation interventions are permitted. Let ϵ^n_{min} and ϵ^n_{max} denote the lower and upper bound of f^n for $n \in \{1,2,\dots,N-1\}$. Problem P_ϵ will be solved many times using different combinations of the epsilon values. Let $\mathcal{E}_n$ denote a set

of values for ϵ^n ranging from ϵ^n_{min} to ϵ^n_{max} for $n \in \{1,2,\dots,N-1\}$. For instance, to create a set with $M+1$ values, one could define $\mathcal{E}_n = \left\{\epsilon^n_{min} + \frac{m}{M}(\epsilon^n_{min} - \epsilon^n_{max}) \middle| m = \{0,1,\dots,M\}\right\}$. Increasing the cardinality of $\mathcal{E}_n$ provides for more detail along the Pareto frontier, but also increases the computational burden. The number of optimization problems to be solved is a function of the number of objectives N and the cardinality of each set $\mathcal{E}_n$ $n \in \{1,2,\dots,N-1\}$, i.e., $\prod_{n=1}^{N-1}|\mathcal{E}_n|$. The algorithm is provided in Figure 2-5.

2.8.3 Outputs of the model

The algorithm in Figure 2-5 generates Pareto optimal solution(s) for the decision variables. For $N > 1$, there will be multiple solutions. Each solution is associated with multiple objectives. Table 2-5 provides an example of an optimal solution of decision variable x_{ijk}. The first column is used to differentiate solutions if the total number of Pareto optimal solution is more than one. For example, there are a total of 100 optimal solutions produced by the model. The solution with Solution Id = 1 is different with the solution with Solution Id = 100. Additionally, the "Solution Id" does not indicate that the solution with Solution Id = 1 is better or worse than the solution with Solution Id = 100. The column "Group $i \in \mathcal{Z}$" is the decision level for mitigation planning. For example, if the group is defined as individual building, the retrofit planning can be executed at the building level. The column "Building type $j \in \mathcal{S}$" indicates the type of buildings considered in the model. The "Final Strategy $k \in \mathcal{K}$" column provides the final state to which the buildings are retrofitted. For instance, there are two school buildings in Table 2-5. One of schools is

retrofitted to strategy 4 and another one is enhanced to strategy 5. The last column of the table, "Decision variable x_{ijk}" is the number of buildings that are retrofitted to strategy $k \in \mathcal{K}$ with building type $j \in \mathcal{S}$ at group level $i \in \mathcal{Z}$, which reflects the final retrofit plans. For example, the solution with Solution Id = 1, shows that 30 single-family buildings are retrofitted to strategy 2 and 10 single-family buildings are enhanced to strategy 3 in group 1. Table 2-6 contains the same information for columns "Solution Id", "Group $i \in \mathcal{Z}$", and "Building type $j \in \mathcal{S}$" as in Table 2-5 does. However, the meaningful purpose of Table 2-6 is to provide the retrofitting details on starting and final strategies. The column "Initial Strategy $k \in \mathcal{K}$" indicates the strategy prior to the retrofitting effort and the column "Final Strategy $k \in \mathcal{K}$" is the final state of retrofitting. The column "Decision variable $y_{ijkk'}$" is the number of buildings retrofitted from $k' \in \mathcal{K}$ to strategy $k \in \mathcal{K}$ with building type $j \in \mathcal{S}$ at group level $i \in \mathcal{Z}$ and implies the final retrofit plan. Following the previous example of Table 2-5, Table 2-6 explicitly shows the initial strategy for 30 single-family building is strategy 2 and the final strategy is also strategy 2, which indicates there is no retrofitting effort implemented on these 30 single-family buildings. In addition, 20 single-family buildings are retrofitted from strategy 2 to strategy 3. This detailed retrofitting plan provided through decision variable $y_{ijkk'}$ is one of the main contributions and benefits of this framework.

Finally, the example objective function output is provided in Table 2-7. Given that each solution is associated with multiple objectives, if there is more than one Pareto optimal solution that exists, the column "Solution Id" correspond with the column "Solution Id" in Table 2-5 and Table 2-6. For instance, the Solution Id = 1 matches the solution with Solution Id = 1 in Table 2-5 and Table 2-6. The "Objective $n \in \{1, \dots, N\}$" column

indicates the number of objectives in this solution. The details provided in Table 2-7 shows there are 3 objectives in this model. The value 1 mean the first objective of the model ($n = 1$) and the value 2 is for the second objective ($n = 2$). The column "Objective Value" provides the optimal values for each objective. Decision support analysis using the details provided from Table 2-5 to Table 2-7 will be discussed in Section 2.9.

Algorithm Multi-Objective Optimization Epsilon-Constraint Method

Input: Problem P_ϵ and $\mathcal{E}_n$ $\forall n \in \{1,2,\dots,N-1\}$

for $\epsilon^1 \in \mathcal{E}_1$

  for $\epsilon^2 \in \mathcal{E}_2$

    …

      for $\epsilon^{N-1} \in \mathcal{E}_{N-1}$

        solve Problem P_ϵ

          if feasible **return** f^n $\forall n \in \{1,2,\dots,N-1\}$, x_{ijk} $\forall (i,j,k) \in \mathcal{T}$, $y_{ijkk'}$ $\forall (i,j,k,k') \in \mathcal{U}$

Output: A set of Pareto optimal objective values and corresponding decision variables values

Figure 2-5. Multi-Objective Optimization Epsilon-Constraint Algorithm

Table 2-5. Pareto optimal solution (x_{ijk}) data file example

Solution Id	**Group $i \in \mathcal{Z}$**	**Building type $j \in \mathcal{S}$**	**Final Strategy $k \in \mathcal{K}$**	**Decision variable x_{ijk}**
1	1	Multi-family	1	0
1	1	Multi-family	2	13
1	1	Multi-family	3	2
1	1	Single-family	2	30
1	1	Single-family	3	10
1	1	School	4	1
1	1	School	5	1
1	2	Single-family	1	2
1	2	Single-family	2	8
…	…	…	…	…

Table 2-6. Pareto optimal solution ($y_{ijkk'}$) data file example

Solution Id	**Group** $\boldsymbol{i \in \mathcal{Z}}$	**Building type** $\boldsymbol{j \in \mathcal{S}}$	**Initial Strategy** $\boldsymbol{k \in \mathcal{K}}$	**Final Strategy** $\boldsymbol{k \in \mathcal{K}}$	**Decision variable** $y_{ijkk'}$
1	1	Multi-family	1	1	0
1	1	Multi-family	1	2	4
1	1	Multi-family	1	3	1
1	1	Multi-family	2	2	9
1	1	Multi-family	2	3	2
1	1	Single-family	2	2	30
1	1	Single-family	2	3	10
1	1	School	4	4	1
1	1	School	4	5	1
1	1	School	4	6	0
…	…	…	…		…

Table 2-7. Pareto optimal objective (f^n) data file example

Solution Id	**Objective** $\boldsymbol{n \in \{1, \ldots, N\}}$	**Objective Value**
1	1	$700,000
1	2	1,600
1	3	0.879
2	1	$2,000,000
2	2	700
2	3	0.910
…	…	…

2.9 Model context

In the context of pre-hazard planning, models are fundamentally an abstraction of reality regardless of the model's complexity and scope. The implication from how models are developed, applied, evaluated, and interpreted can ultimately influence decision-making. Therefore, it is crucial to understand the fundamental assumptions and limitations of the modeling framework proposed in this research effort.

First, we assume that hazard characteristics are independent of the mitigation efforts. For instance, tornado paths and windspeeds, earthquake peak ground acceleration, and tsunami-induced storm surges are not affected by building codes and enhancements. Secondly, we assume the mitigation interventions are independent in terms of resources and benefits. For instance, enhancing two equivalent buildings to a given improvement level costs twice as much as enhancing just one. The contribution of the mitigation interventions is similarly independent, i.e., there is no efficiency gained nor diminishing returns based on the number of interventions. Third, we consider the only first-order effect of hazard events. That is, the model does not specifically address effects from potentially cascading events (i.e., direct damage to one infrastructure element causes damage or dysfunctionality to cascade to one or more different infrastructure elements even if the hazard did not directly impact these elements). That said, some elements of cascading events may be addressed by the framework if these effects are captured in the objective coefficient values. For instance, a computable general equilibrium (CGE) model effectually estimates the indirect effects of hazard damage on the economy, such as increased unemployment and lower household wages. If a CGE model is used to determine objective coefficients for such outcomes, the decision framework implicitly addresses

these indirect outcomes. Finally, all coefficients associated with objectives and costs and the available budget are assumed to be valid and certain. The objective coefficients may be generated through Monte Carlo simulations or other means to reflect expected conditional values with respect to a hazard scenario. The existing approaches to model the uncertainty are Monte Carlo simulation (Smith and Matthews, 2015; Attary et al., 2018; Younesi et al., 2020), scenario-based analysis (Klibi and Martel, 2012; Lv et al., 2013; Zhang et al., 2018b), Bayesian update (Chen et al., 2010; Wang et al., 2013; Rahman, 2019). However, given that the mathematical modeling framework is based on linear programming, these objective values are not considered stochastically.

The downside to this certainty assumption is that there is substantial uncertainty in any real-world scenario: uncertainty concerning the hazard type, severity, and impact region, as well as uncertainty to the cost and effectiveness of any mitigation strategy. As such, assuming certainty is a significant simplification to the resilience problem. We posit that in the present problem space, such a simplification is likely necessary. While methods such as robust optimization and stochastic programming are algorithmically possible, given the size of the typical community instance and the number of potentially uncertain parameters, such techniques have limited practical value due to the computational burden. The framework we propose benefits from the ability to address relatively large problems in a reasonable time (seconds to hours) under various user-defined scenarios (e.g., hazard specifications or budget considerations) and to generate many possible scenario-based solutions for decision makers and subject matter expert analysis. Indeed, given the complexity of the problems at hand, the uncertainty of the input parameters, and the critical nature of the decisions and outcomes the framework is designed to evaluate, it is essential

to remember that any such system exists in a role of *support tool* providing one quantitative perspective on the resilience problem.

2.10 Post-optimization solution analysis

2.10.1 Tradeoff analysis

With multiple objectives, i.e., $N > 1$, there are N potentially competing objectives. If two objectives are competing, then a solution that minimizes one objective does not simultaneously minimize the other. This means that along the Pareto frontier, a decision-maker must make a choice in terms of a tradeoff, i.e., how much should objective f^i be deteriorated to support objective f^j, for $i \neq j$. Figure 2-6 provides an example assuming two objectives: direct economic loss and population dislocation. It is reasonable to assume that these objectives are competing. In particular, damage to residential homes may be the most significant driver of immediate population dislocation, yet damage to the commercial sector buildings is likely to cause the most economic loss due to direct impact to capital stock. A solution, e.g., point A in Figure 2-6 most likely allocates mitigation efforts toward commercial buildings as a priority relative to residential building allocation resulting in a low economic loss value, but suboptimal expected population dislocation. The solution associated with point B is likely allocates more mitigation investment toward residential areas resulting in reduced population dislocation at the expense of direct economic impact. Point C provides a solution that forfeits some of both objectives to provide a more balanced outcome. The solution output from the optimization model provides sufficient detail to quantitatively evaluate such tradeoffs. Consider the possible numerical outcomes

demonstrated in Table 2-8 and Table 2-9. Shifting from the solution associated with point A to that of the solution associated with B, the economic loss increases by $1,300,000 (185.7% increase) but the population dislocation decreases by 900 (56.3% decrease). This is a ratio of $1,444 of increased economic loss per individual *not* dislocated. When comparing solutions A and C, solution C increases the expected economic loss by only $200,000 (28.6% increase) but reduces the expected dislocation by 800 individuals (50% decrease), a ratio of $250 of loss per individual. Solution B is an extreme solution in that it successfully minimizes population dislocation. However, when compared to solution C, solution B only reduces population dislocation by an additional 100 individuals (12.5% decrease) but incurs $1,100,000 (122.2% increase) in economic loss, i.e., $11,000 per individual not dislocated. Such detail provides decision makers information to help quantitatively evaluate tradeoffs.

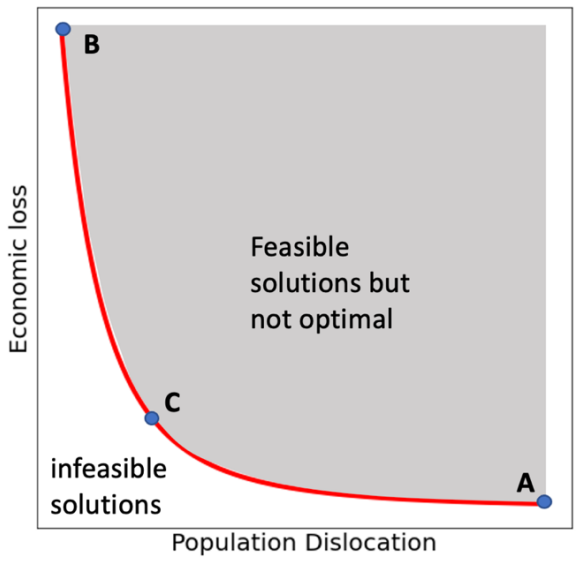

Figure 2-6. Illustration of bi-objective space and tradeoffs

Table 2-8. Numerical example of potential tradeoff values

Solution	Economic loss	Population dislocation
A	$700,000	1,600
B	$2,000,000	700
C	$900,000	800

Table 2-9. Quantitative tradeoff example

Tradeoff Analysis: **Δ economic loss** **Δ pop dislocation**		**To**	
		Point B	Point C
From	Point A	$1,300,000 -900	$200,000 -800
	Point B		-$1,100,000 100

2.10.2 Resource analysis

Increasing or decreasing mitigation resources (e.g., time, money, labor, etc.), impacts the quantity of feasible mitigation interventions. A larger budget leads to more options which may improve one, more, all even all objective functions, whereas a smaller budget likely shifts the Pareto tradeoff surface towards poorer performance. Figure 2-7 depicts two Pareto curves for a bi-objective problem with different budgets. Points A and B are on the curve associated with budget B_1, and points A′ and B′ are on the curve

associated with a smaller budget, B_2. Changing the value of input parameter B in Equation (2-2) allows for optimization assuming a different value of resource budget. Not only does the Pareto surface of a smaller budget solution set shift towards the suboptimal region of the larger budget solution set, the shape of the curve also changes impacting the evaluation of the corresponding tradeoffs. By exploring different budget options, decision makers can determine resource investment levels necessary to achieve community resilience goals.

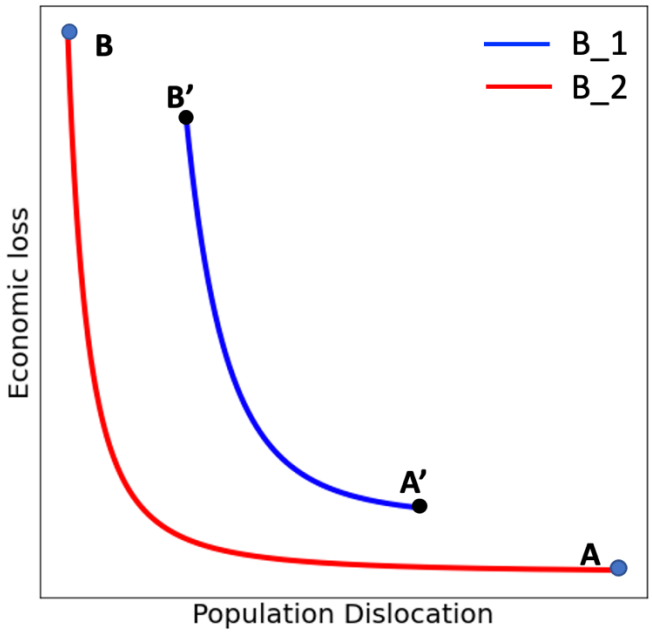

Figure 2-7. Illustration of Pareto curves with two different budgets inputs

2.10.3 Priority analysis

To estimate the Pareto frontier and, potentially, to evaluate options at varying budget levels, the proposed framework generates numerous, distinct solutions. One

valuable analysis is to identify buildings (or groups of buildings or group of buildings of a given type) that are invested in most frequently across the solution sets. If significant resources are allocated to a specific building set for many combinations of epsilon values in Equation (2-8), then this set is important for all the community defined objectives. This may be due to inherent vulnerability of the buildings and/or its value within the community with respect to the various objective functions. Additionally, if a building set is selected for enhancement across many budget levels, from the most restrictive to the least, then the particular set again is deemed as vital with respect to the mathematical model. One possible investment analysis is depicted in Table 2-10 where the relative frequency of retrofitted group across all objective priorities is computed for multiple budgets. In the example, group 4 stands out because the values relative frequency indicate Group 4 is retrofitted more often than other groups across all optimal solutions and for all resource budgets. Other groups, e.g., group 3, may have much less investment allocations from the mathematical framework indicating that potentially these buildings play a little role in improving objective performance, the mitigation interventions in such areas are not cost-effective, and/or the buildings are not vulnerable to the hazard scenario, etc. Evaluating the optimization solution sets with this level of detail allows decision makers a unique quantitative perspective on the community and can identify vulnerable areas to be prioritized. Figure 2-8 provides an example to prioritize the vulnerable areas with the retrofit budget $9 Million dollars, and total 55 optimal solutions in Joplin, MO. The groups with dark red color (relative frequency of unique groups from 0.8 – 1) imply high retrofitting frequency across all 55 solutions, which mean these groups (dark red color)

have appear in 44 solutions in the worst cases. On the contrary, the groups in light yellow are not retrofitted on any solutions.

Table 2-10.Example solution priority analysis with different budget levels

	Relative frequency of retrofitted groups across all objective priorities			
Group	**Budget B_1**	**Budget B_2**	**Budget B_3**	**All Budgets**
1	5.0%	7.9%	7.5%	6.1%
2	2.2%	0.1%	0.0%	1.3%
3	0.2%	0.0%	0.0%	0.1%
4	8.1%	11.7%	15.3%	10.0%
5	2.1%	1.4%	0.0%	1.6%
…	…	…	…	…

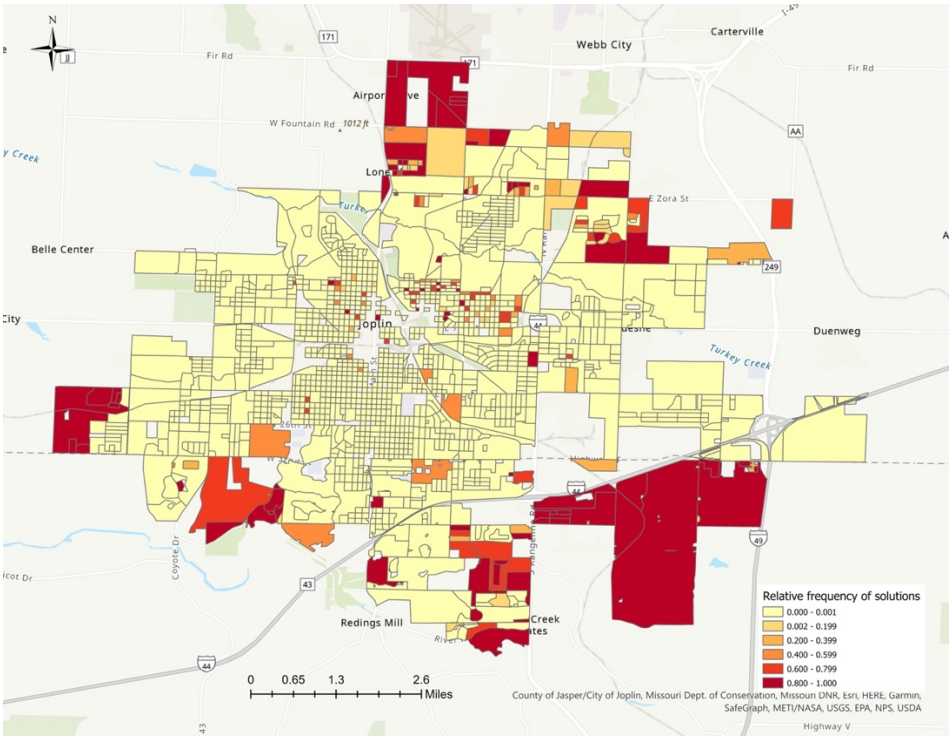

Figure 2-8. Using optimal solution to prioritize vulnerable areas

2.11 Summary

The decision support framework introduced in this chapter features a multi-objective optimization mathematical model designed to work at any level of decision granularity from high level groups of buildings such as PUMAs, census tracts, or block groups, down to the parcel or building level of detail. Building groupings do not have to be spatially contiguous but can be created based on relevant characteristics of the analysis, e.g., digital elevation models could be used to create spatially disparate groups of buildings in elevation ranges with different vulnerability to flooding. Decision granularity for groups of buildings is further refined based on a set of types which may be associated with structural features (e.g., wood frame vs. reinforced masonry, etc.), occupational type (e.g., residential vs. commercial, etc.), or any other category that the decision-maker prefers to define. The specification of type is useful for computing distinct hazard fragilities, related outcomes from a hazard scenario (e.g., population dislocation, school closure, etc.), or to define appropriate mitigation options. For each combination of a building group and type, any number of distinct mitigation interventions are permitted. The interventions should each have an estimated cost (in terms of available resources, such as dollars, time, labor, etc.) and one or more benefits associated with the various community-defined resilience objective functions. The underlying mathematical model is solved using the ϵ-constraint method such that, in the case of competing objectives, a set of Pareto optimal solutions is returned. This set of solutions allows community leaders and researchers to evaluate a spectrum of outcomes and quantitatively evaluate tradeoffs among solutions. Finally, the model itself is hazard agnostic. If the correct objective coefficients are provided (and assuming the validity of the other inputs), the approach produces solutions that are

guaranteed to be optimal for a given set of epsilon values regardless of the hazard intensity or type. The framework is designed to work either as a stand-alone component or as an integral module within the IN-CORE platform. IN-CORE can estimate the impact of numerous hazard types on multiple resilience metrics.

Using linear programming as the mathematical paradigm enhances the practical computational efficiency of the framework and supports multiple investigations in hazard mitigation. The level of detailed decision support from the model, the use of the iterative ϵ-constraint method for multi-objective optimization, and the evaluation of multiple hazard or budget scenarios, result in a considerable quantity of solution data that can be analyzed to further enrich evidence-based decision making. In particular, Pareto solutions sets can be computed for multiple resource budgets to analyze how the location and shape of the tradeoff surface changes. Solving under different budget levels also allows investigators to pinpoint the amount of investment necessary to meet different resilience goals. Solution set analysis can also identify vulnerability vulnerable areas or within the community which may need to be prioritized regardless of the particular resilience objective emphasis. Each of these analyses are explored in detail in the Chapter 3 in a case study for Joplin, Missouri under threat of a severe tornado.

3 Multi-objective optimization application: tornado mitigation

3.1 Introduction

A tornado is considered a minor threat with less damage and low occurrence comparing other hazards (e.g., earthquake, hurricane, flooding). However, in U.S. history, damage from the tornadoes to the local communities is tremendously severe in some events. On May 20, 2013, a mile wide EF5 tornado passed through Newcastle, Moore, and southern Oklahoma City. The post-disaster estimation reported 24 fatalities and $2 billion in damage. On April 25-28, 2011, an estimated 349 tornadoes tore through the South and East of the U.S., with 321 people dead in the event and $11.9 billion in damage. According to NOAA (National Oceanic and Atmospheric Administration), an average of 1,253 tornadoes occur in the United States each year.

Mitigation planning on tornadoes (Smith, et al., 2012; Walsh and Tezak, 2012; Harrison, et al., 2015; Ripberger, et al., 2018) is not studied extensively compared to earthquakes (Berke and Beatley, 1992; Kanamori, et al., 1997; Gupta and Shah, 1998; Dodo, et al., 2007; Xu, et al., 2007; Li, 2012; Oettle and Bray, 2013; Pollyea, et al., 2018), floods (Cuny, 1991; Brody, et al., 2009; Brody and Highfield, 2013; Kousky and Walls, 2014; Yazdi and Salehi Neyshabouri, 2014; Xie, et al., 2017; Tasseff, et al., 2019), and hurricanes (Berke and Stubbs, 1989; Jamieson and Drury, 1997; Peacock, 2003; Leatherman, et al., 2007; Deyle, et al., 2008; Chowdhury, et al., 2009; Pinelli, et al., 2009; Kopp, et al., 2010; Ge, et al., 2011; Legg, et al., 2013; Gatzlaff, et al., 2018). Two reasons are likely in play here. First, tornado mitigation planning and risk reduction are often complex for the public to engage in because there are no immediate threats and dangers to

the community. Even with the advanced technology of tornado prediction and tracking, it is still difficult to predict where and when the tornadoes will occur. Secondly, mitigation planning is designed based on what-if scenarios, which are not immediate concerns for the community. Tornado mitigation measures are enhancement of building structural components such as sheathing, roof covering, and the connection between wall and roof. With the relatively inexpensive enhancement of building codes, the damage imposed from tornadoes can be reduced by 30%, but only one city of the United States has adopted enhancement of building codes against tornado hazard (Ripberger, et al., 2018).

A large body of tornado mitigation studies focused on the improvement of building codes, structural enhancement, structural design to prevent physical building damage for future events (Prevatt, et al., 2012a; Smith, et al., 2012; Simmons, et al., 2015; Ramseyer, et al., 2016; Masoomi, et al., 2018a; Ripberger, et al., 2018; Farokhnia, et al., 2020). Mitigation planning typically restricts limited resources (e.g., budget, time, labors). For the community decision makers, the challenge to prepare the community against future hazards is how to allocate limited resources most effectively. Studies of building structural enhancement are essential for mitigation planning. However, the questions to be asked next are how we can conduct such structural retrofitting through the whole community with a restricted budget and how we can determine appropriate retrofit planning for the communities.

3.2 Research gap and contribution

The challenges of tornado mitigation have drawn research attention from different fields, such as the studies from civil engineering (Prevatt, et al., 2012a; Ramseyer, et al.,

2016; Wang, et al., 2018; Farokhnia, et al., 2020; Koliou and van de Lindt, 2020), economics (Cutler, et al., 2016b), social science (Zahran, et al., 2008; Houston, et al., 2017), and computing science (Strader, et al., 2016; Wang, et al., 2020). But none of studies have conducted tornado mitigation using multi-objective optimization model at a granule level decision support. A research gap is identified by evaluating the research components that were conducted in the studies listed Table 3-1. First, majority of studies of tornado mitigation focused on structural design of individual building and enhancement (Prevatt, et al., 2012a; Amini and van de Lindt, 2014; Kantamaneni, et al., 2017; Farokhnia, et al., 2020). The influence from social and economic aspects of a community was overlooked by these studies. Most recent study from Wang, et al. (2021) discussed that different building strategies impacted the measurement from social, economic, and physical infrastructure (i.e., electrical power network, buildings) using Joplin Tornado as the case study through IN-CORE, but the authors did not apply the multi-objective optimization method to provide strategical retrofitting throughout the city of Joplin. The multi-objective optimization framework proposed by Zhang and Nicholson (2016) did not consider the impact from physical system on mitigation plan. The study conducted in this Chapter is able to fill the research gap identified and contribute on tornado mitigation on the three aspects.

First, this study showcases the application of the framework introduced in Chapter 2. By introducing three essential systems as the competing objectives for the optimization model, this study is the first multi-objective optimization model integrating multi-facet of a community on tornado mitigation. Secondly, this study demonstrates the how to use and adapt the existing models from other fields (i.e., Civil engineering, social science, and

economics) to obtain the required data for the model. For example, by modifying a logistic regression model of the population dislocation to a linear model, we introduced the social objective to the optimization model. Third, the rich information produced from the model provides an array of decision support options to mitigate the risk from the tornado hazard for the city of Joplin, MO, at the block groups level. Lastly, we conduct case study through IN-CORE with 66 simulated tornado events, the results further evaluate the individual optimal retrofit plan.

Table 3-1. Reference list related to research gap

Reference	Tornado Mitigation	Structural design or enhancement	Physical system	Social system	Economic system	Integrated multi-objective optimization
Farokhnia, et al. (2020)	✅	✅	✅	❌	✅	❌
Smith, et al. (2012)	✅	✅	✅	❌	❌	❌
Prevatt, et al. (2012a)	✅	✅	✅	❌	❌	❌
Koliou and van de Lindt (2020)	✅	✅	✅	❌	❌	❌
Masoomi, et al. (2018a)	✅	✅	✅	❌	❌	❌
Wang, et al. (2018)	✅	✅	✅	❌	❌	❌
Prevatt, et al. (2012b)	✅	✅	✅	❌	❌	❌
Masoomi, et al. (2018b)	✅	❌	✅	✅	❌	❌
Ellingwood (2007)	❌	✅	❌	❌	❌	❌
Masoomi and van de Lindt (2016)	✅	✅	❌	❌	❌	❌
Liu and Turner (1990)	✅	✅	❌	❌	❌	❌
van de Lindt, et al. (2013)	✅	✅	❌	✅	❌	❌
Simmons, et al. (2015)	✅	❌	❌	❌	✅	❌
Ripberger, et al. (2018)	✅	❌	❌	❌	❌	❌
Kantamaneni, et al. (2017)	✅	✅	❌	❌	❌	❌
Zhang and Nicholson (2016)	✅	✅	❌	✅	✅	✅
Ramseyer, et al. (2016)	✅	✅	✅	❌	❌	❌
Wang, et al. (2020)	✅	❌	✅	✅	✅	❌
RO2	✅	✅	✅	✅	✅	✅

Note: ✅ indicates the research component is discussed in the reference; ❌ indicates the research component is not included in the reference

3.3 Highlights

This chapter conducts a case study to apply the framework introduced in Chapter 2 on tornado mitigation. The optimization model is designed with three competing objectives to represent potential impacts on economic, social, and physical systems, respectively. The model optimizes the retrofitting strategies on residential buildings in the city of Joplin, Missouri. The study demonstrates how the decision makers can utilize the rich information from the optimal solutions to prioritize the appropriate retrofit planning for the community. Such decision-making support analyses include tradeoff analysis, priority analysis, and resources analysis.

3.4 Application of the optimization model

3.4.1 Community resilience goals

In Chapter 2, the community goals are introduced in the multi-objective optimization model as objectives that can be used to measure the performance of the systems (e.g., economic, social, physical, etc.). Three community goals are designed for this study: direct economic loss, population dislocation, and building functionality. These three community goals are selected based on the recent studies from different fields and the principle of optimization model introduced from Chapter 2. First, the direct economic loss is linked to direct physical damage to a building and expressed as a percentage of the appraisal values of the building (Zhang and Nicholson, 2016). A recent study from Rosenheim, et al. (2021) demonstrated that population stability is strongly tied with the physical integrity of buildings in a community. Lastly, the physical system is the primary

driver of social and economic systems. The results from Wang, et al. (2021) supported that enhancing critical infrastructures reduced the potential impact on social and economic systems. Therefore, building functionality is selected as the third objective to represent the physical system. Building functionality of an individual building can be described as the availability of a building to be used for its intended purpose, and it is a function of its structural integrity and availability of utilities (Almufti and Willford, 2013; Lin and Wang, 2017; Zhang, et al., 2018). Building functionality, $Q(t)$ can be expressed as a percentage of a building's functionality at any time t during the restoration period (Koliou and van de Lindt, 2020). Building functionality and recovery depend on various factors such as the amount of structural damage, damage to the utility network, and available labor, etc. (Filiatrault and Sullivan, 2014; Zhang, et al., 2018; Kim and Reed, 2020).

3.4.2 Case study: Joplin, MO

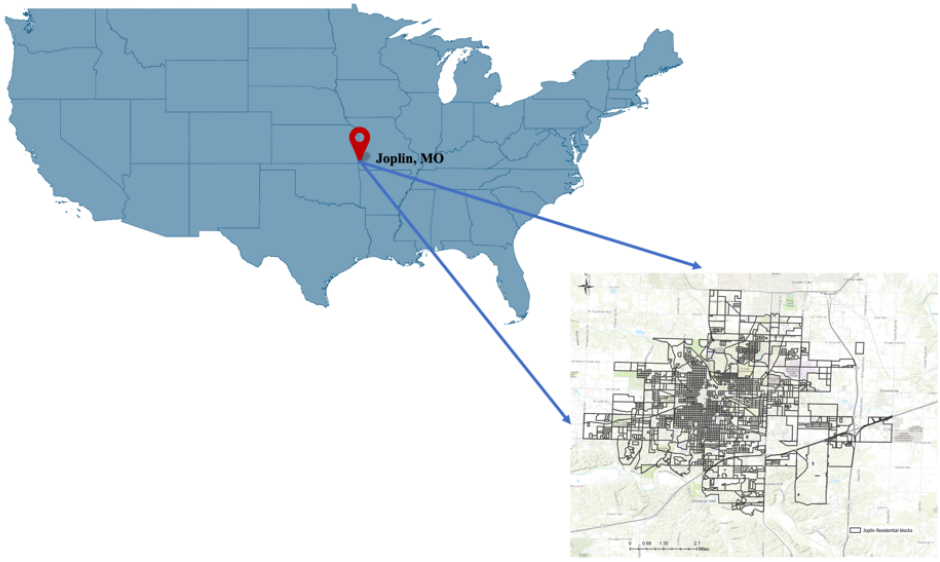

Figure 3-1. Geographic location of Joplin, MO

Joplin is a city located in the southwestern corner of the U.S. state of Missouri (Figure 3-1). As of the 2010 census, the population of Joplin was 50,150. Joplin is also located in an area where consistently experiences a high frequency of tornadoes each year. This area is called Tornado Alley (Concannon, et al., 2000) and refers to the southern plains of the central United States. On May 22 of 2011, an EF-5 rated tornado stroke in Joplin and caused 161 fatalities (out of the total 553 deaths of U.S. tornado deaths in 2011) and over 1,000 injuries, making it a record tornado in 2011. The resulting damage from the built environment and economic loss was recorded as the costliest tornado. The data provided by the Missouri Department of Insurance, Financial Institutions, and Professional Registration reported that insured commercial property losses were $1.228 billion, and residential property losses were $0.552 billion (Kuligowski, et al., 2014). One of the major findings from Kuligowski, et al. (2014) was that 83.8 percent of fatalities were related to building failure, and over 50 percent of building failure-related deaths occurred in residential buildings. Of the buildings damaged in the storm, 7,411 were residential, and 553 were non-residential. 3,069 residential buildings and all 553 non-residential buildings were categorized as heavy or demolished damage degrees. Figure 3-2 shows an example of structural failure observed among residential buildings involving disconnection of components structural systems (roof-to-wall and wall-to-foundation connections) of a single-family wood-frame building that sustained demolished damage during the Joplin tornado.

Although EF0 and EF1 tornadoes occur more frequently, once up to EF2 level, the damage is significantly increased compared with EF1 and EF0 tornadoes. An EF2 tornado can result considerable damage, such as roof torn off frame houses, demolishing of

weakening buildings, trailer housed destroyed, cars being blown off the highway, etc. (McDonald, et al., 2009). Statistically, about 95% of all United States tornadoes are below EF3 intensity, and around 77% are considered weak (EF0 or EF1). To calculate the potential impact from a tornado event, wind speed is necessary to calculate input parameters: direct economic loss and population dislocation. We define wind speed 135 mph in this study as a baseline. For all the buildings in Joplin, the physical damage of a building is computed based on the maximum wind speed of 135 mph, which is the upper bound of wind speed defined for an EF2 tornado. With well-enforced retrofitting strategies, one can still expect numerous broken windows in an EF2 tornado, but the residential structures should remain intact (Simmons, et al., 2015). Table 3-2 provides the detail on Enhanced Fujita Scale for the tornado damage.

Table 3-2. Enhanced Fujita Scales for Tornado damage (Ripberger, et al., 2018)

EF Scale	Wind Speed (MPH)	Characteristic damage to residential wood-frame houses
0	65-85	Threshold of visible damage; loss of roof-covering material (less than 20%), gutters and/or awning; loss of vinyl or metal siding.
1	86-110	Broken glass in doors and windows; uplift of roof deck and loss of significant roof-covering material (20% or more); collapse of chimney; garage doors collapse inward; failure of porch or carport.
2	111-135	Entire house shifts off foundation; large sections of roof structure removed; most walls remain standing; exterior walls collapsed
3	136-165	Most walls collapsed, except small interior rooms
4	166-200	All walls collapsed
5	Over 200	Destruction of engineered and/or well-constructed residence; slab swept clean

Figure 3-2. Residential buildings damage example in Joplin Tornado on May 22, 2011 (Kuligowski, et al., 2014)

3.4.3 Inputs of the framework

Model context

This chapter inherits the assumptions from the framework introduced in the Chapter 2 that interdependencies between different types of buildings are excluded in this paper, and we only consider the first-order effects of the events. It is impossible to predict the exact location, timing, and size of a tornado event compared with other hazards. Also, there is no evidence that tornadoes would occur in one exact location repeatedly. Therefore, retrofitting planning on tornado hazards cannot only consider the areas tornadoes struck in the past within a community. If the historical data show that some areas of the community were exposed to tornado events in the past, then mitigation measures should be applied to all the areas of whole community because one cannot be certain that other areas are safer than the areas where the tornadoes had struck. For example, Moore, the city in Oklahoma, had implemented hurricane clips, which are mental straps often used in construction along the Gulf Coast to keep a roof attached to the walls during the hurricanes, as part of the city's building codes. The city of Moore adopted retrofitting on residential buildings codes that are strong enough to survive EF2 tornadoes after an EF5 tornado devasted the community on May 20, 2013. To model the uncertainty from the input data, we consider each block in Joplin with equal probability to experience tornado events in the future. Therefore, our goal is to compute the conditional expected value of a building's economic, social, and physical systems given an impact by a tornado (i.e., conditioned on experienced windspeed.).

Building stock

In this study, parameter $\mathcal{Z}$ in the model is designed by using the census blocks that are geographically defined areas. Census blocks are the smallest geographic unit used by United States Census Bureau, and "statistical area bounded by visible features, such as streets, roads, streams, and railroad tracks, and by nonvisible boundaries, such as selected property lines and city, township, school district, and county limits and short line-of-sight extensions of streets and road." (U.S. Census Bureau, 2011). The unique identifier for each block follows the block codes defined by U.S. Census Bureau. For example, block "290970101001018" from the building stock contains the information described by Figure 3-3. The identifier for state Missouri remains the same for all blocks, the rest identifiers (County, Census Track, Census Block) differentiate the uniqueness of each block. In Joplin, there are 1,565 blocks (set $\mathcal{Z}$) containing residential buildings, two residential structural types (set $\mathcal{S}$) (i.e., single-family, multi-family) and three retrofitting strategies (set $\mathcal{K}$) above the status quo for residential wood-frame buildings.

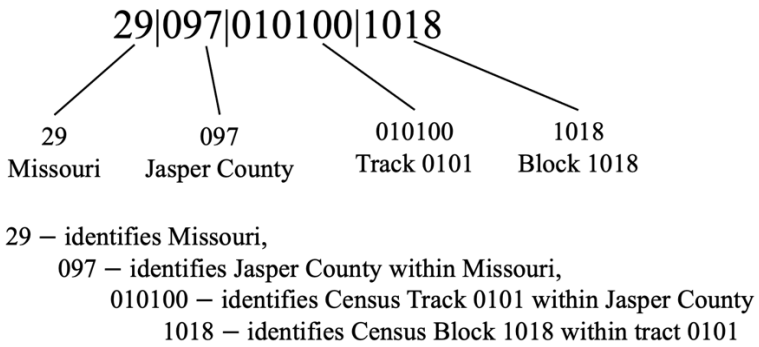

Figure 3-3. Joplin block group identifiers

Retrofitting strategies cost: $SC_{ijkk'}$

Retrofitting a building is making changes to an existing building to reduce the vulnerability of and damage to buildings from hazardous events, such as hurricanes, floods, earthquakes, high winds, etc. Many buildings existing today were built at a time when little was known about where and how regularly hazard events would happen, and how buildings ought to be protected (Federal Emergency Management Agency (FEMA), 2014). In this study, three retrofitting strategies (Table 3-3) are selected from the study proposed by Masoomi, et al. (2018a) that were introduced to enhance residential wood-frame buildings from high wind-related hazards, such as tornadoes, hurricanes.

The cost for hazard mitigation is difficult to be accurately estimated because it depends on many factors such as current design/code, construction practices, structural configuration, local labor costs, and availability of retrofit materials. In this case study, we assume there are no mitigation actions on the buildings before the retrofitting, meaning that the initial retrofitting level (k) for all buildings is 0. Table 3-4 provides the retrofit cost on each strategy of single-family and multi-family wood frame buildings. The retrofit cost for each strategy of each building type is calculated as the percentage of the appraisal value of each building. The retrofit cost information of residential buildings in Joplin is provided by the Civil engineering department from Colorado State University.

Table 3-3. Retrofitting strategies (Masoomi, et al., 2018)

Structural elements	Selection	Retrofit strategy 1	Retrofit strategy 2	Retrofit strategy 3
Roof covering	Asphalt shingles	X	X	–
	Clay tiles	–	–	X
Roof sheathing nailing pattern	8d C6/12	X	–	–
	8d C6/6	–	X	X
Roof-to-wall connection type	Two 16d toe nails	X	–	–
	Two H2.5 clips	–	X	X

Table 3-4. Retrofit cost estimates of residential buildings in Joplin

Retrofit strategies	Archetype	Retrofit cost percentage (%)
1	Single-family	11.41
	Multi-family	8.26
2	Single-family	17.33
	Multi-family	14.34
3	Single-family	35.33
	Multi-family	25.74

Direct economic loss: $\boldsymbol{\alpha_{ijk}^{1}}$

The parameter α_{ijk}^{1} is the coefficient of the objective function of expected direct economic loss with conditional wind speed 135 mph for the buildings in block $i \in \mathcal{Z}$ of archetype $j \in \mathcal{S}$, which at the strategy $k \in \mathcal{K}$. There are three required inputs to estimate the values of α_{ijk}^{1} in this study. The first input is the damage states for each retrofitting strategy considering designated hazard and building type. Damage states are essential information to estimate building damage for structural and non-structural systems of a building. Practically, damage states do not have a continuous scale and describe the building's physical condition. Table 3-5 provides an example of building damage states (Bai, et al., 2009). Another term also is used to describe the building damage states, namely: DS0 (no damage), DS1 (insignificant damage), DS2 (moderate damage), DS3 (heavy damage), and DS4 (destroyed damage state). Masoomi, et al. (2018a) specified four damage states (Table 3-6) for wood-frame buildings under extreme windstorms such as tornadoes and hurricanes. The authors used structural components (i.e., roof covering, window/door, roof sheathing, roof-to-wall connection) to indicate the damage states of wood-frame buildings.

The second input is the corresponding damage factor for each damage state that is essential to assess the cost of structural repairs as a percentage of replacing the structural portion. Table 3-7 provides proposed damage states and the corresponding damage factor for economic loss estimation on tornado hazard based on the approach used in the Hazus Earthquake Model for estimating recovery/reconstruction time as a function of the building damage state (Federal Emergency Management Agency (FEMA), 1999).

The last input for α_{ijk}^{1} estimation resulting from building damage is the fragility curve that is typically developed to evaluate the performance of a building under extreme loads by considering uncertainties in load calculation and resistance estimation. Table 3-8 provides parameters to construct fragility curves used for single-family and multi-family buildings for tornado mitigation when the three retrofit strategies are applied. Figure 3-4, Figure 3-5, and Figure 3-6 represent the fragility curves of a single-family building at strategy 1, strategy 2, and strategy 3 respectively. For a multi-family building, Figure 3-7, Figure 3-8, and Figure 3-9 are the fragility curves for strategy 1, strategy 2, and strategy 3 respectively. Figure 3-10 illustrates the statistical relationship of building damage probability with exceedance probability at damage state DS4 that is associated with the most damage compared with DS1, DS2 and DS3. When the intensity measure (IM) of a hazard is selected, exceedance probabilities associated with different damage states are known from the fragility curve: P_{DS1}, P_{DS2}, P_{DS3}, and P_{DS4}. The expected damage probability of a building can be estimated by the summation of damage probability (i.e., $P_{DS0|IM}$, $P_{DS1|IM}$, $P_{DS2|IM}$, $P_{DS3|IM}$, $P_{DS4|IM}$) multiplying damage factor (i.e., $D_{DS0}, D_{Ds1}, D_{DS2}, D_{DS3}, D_{DS4}$) associated with corresponding damage state. Let parameter M_{ijk} denote the total appraised value of associated buildings. The expected loss is a

function of the appraised value of the structure and expected percent of house value loss with the given damage state from the fragility curve of given building archetypes and wind speed. Therefore, the expected repair cost is expressed as:

$$\alpha_{ijk}^{1} = M_{ijk} \sum_{ds=DS0}^{DS4} P_{ds|IM} * D_{ds} \,. \tag{3-1}$$

Table 3-5. Building damage description associated with damage state (Bai, et al., 2009)

Damage States	Description
No damage (N)	None. No damage is visible, either structural or non-structural.
Insignificant (I)	Damage required no more than cosmetic repair. No structural repairs are necessary. For non-structural elements, repairs could include spackling, partition. Cracks, picking up spilled contents, putting backing fallen ceiling tiles, and righting equipment.
Moderate (M)	Repairable structural damage has occurred. The existing elements can be repaired essentially in place, without substantial demolition or replacement of elements. For non-structural elements, repairs would include minor replacement of damaged partitions, ceilings, contents, and equipment or their anchorages.
Heavy (H)	While the damage is significant, the structure is still standing, and Structural damage would require major repairs, including substantial demolition or replacement of elements. For non-structural elements, repairs would include major replacement of damaged partitions, ceilings, contents, equipment, or their anchorages.
Complete (C)	Damage is so extensive that repair of most structural elements is not feasible. The structure is destroyed, or most of the structural members have reached their ultimate capacities.

Table 3-6. Damage states for the wood-frame building (Masoomi, et al., 2018a)

Damage state	Damage indicators			
	Roof covering failure	Window/door failure	Roof sheathing failure	Roof-to-wall connection failure
DS1	>2% and ≤15%[a]	1[a]	No	No
DS2	>15% and ≤15%[a]	2[a] or 3[a]	1−3[a]	No
DS3	>50%[a]	>3[a]	>3% and ≤35%[a]	No
DS4	Typically > 50%	Typically > 3	>35%[a]	Yes[a]

Note: Each damage state is defined as the occurrence of any of the damage indicators in a given row marked with [a].

Table 3-7. Percentage of replacement/repair cost for Damage States (FEMA, 1999)

Damage state	**Damage factor (%)**
None ($\boldsymbol{D_{DS0}}$)	0
Slight ($\boldsymbol{D_{DS1}}$)	2
Moderate ($\boldsymbol{D_{DS2}}$)	10
Extensive ($\boldsymbol{D_{DS3}}$)	50
Complete ($\boldsymbol{D_{DS4}}$)	100

Table 3-8**.** Building-level tornado fragility curves parameters for residential retrofitting levels (Masoomi, et al., 2018)

Damage state	Retrofitting Strategy	Single-family		Multi-family	
		μ	σ	μ	σ
DS1	1	4.49	0.13	4.56	0.13
	2	4.49	0.14	4.56	0.13
	3	4.74	0.12	4.76	0.12
DS2	1	4.37	0.14	4.46	0.13
	2	4.66	0.12	4.69	0.12
	3	4.80	0.11	4.83	0.11
DS3	1	4.44	0.13	4.51	0.13
	2	4.79	0.11	4.79	0.11
	3	4.88	0.10	4.92	0.10
DS4	1	4.49	0.14	4.45	0.15
	2	4.97	0.13	4.87	0.14
	3	5.10	0.12	5.05	0.13

Note: μ refers to logarithmic mean of curves and σ refers to logarithmic standard deviation of curves, and the unit is mph.

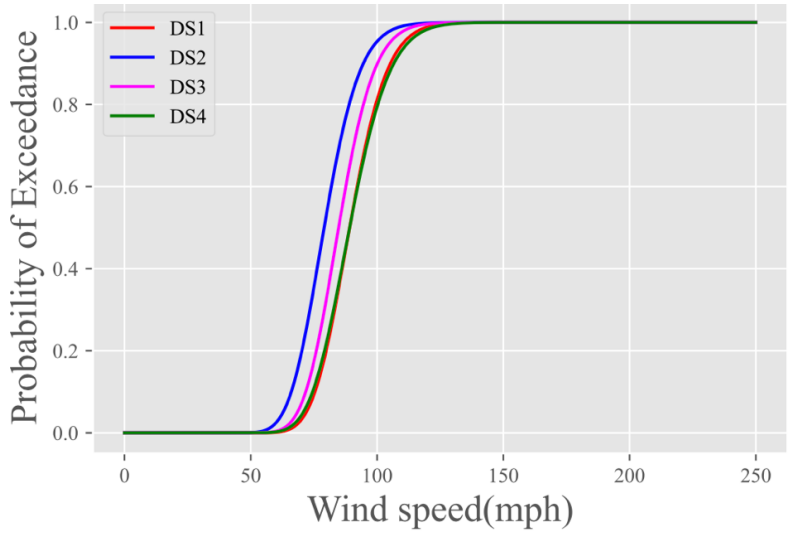

Figure 3-4. Fragility curve of a single-family building at strategy 1

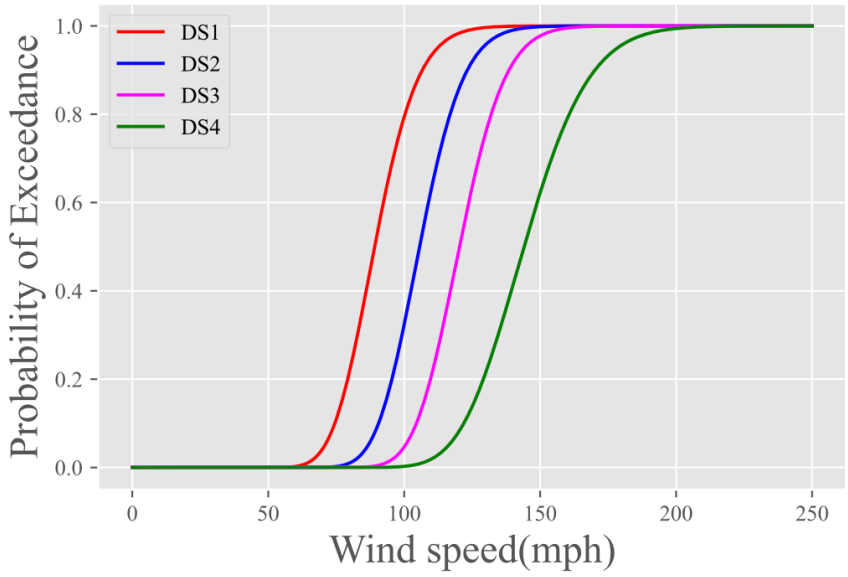

Figure 3-5. Fragility curve of a single-family building at strategy 2

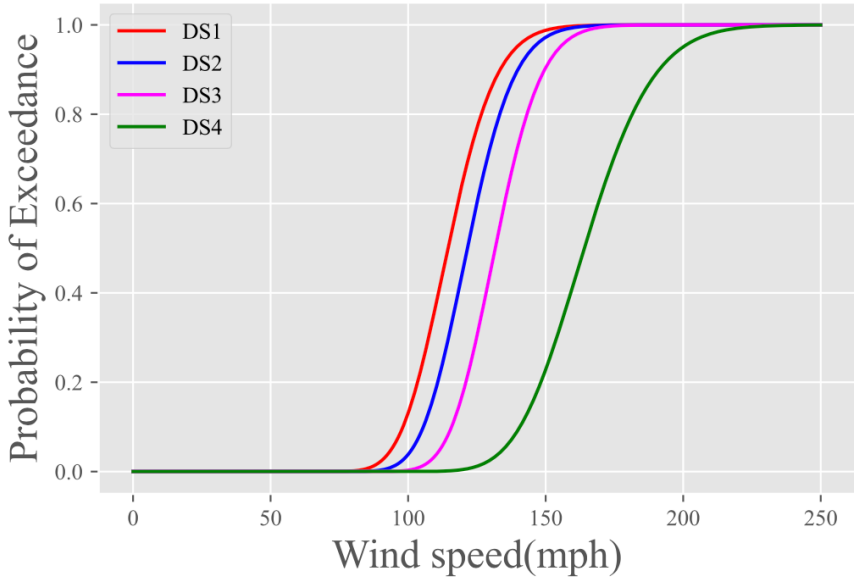

Figure 3-6. Fragility curve of a single-family building at strategy 3

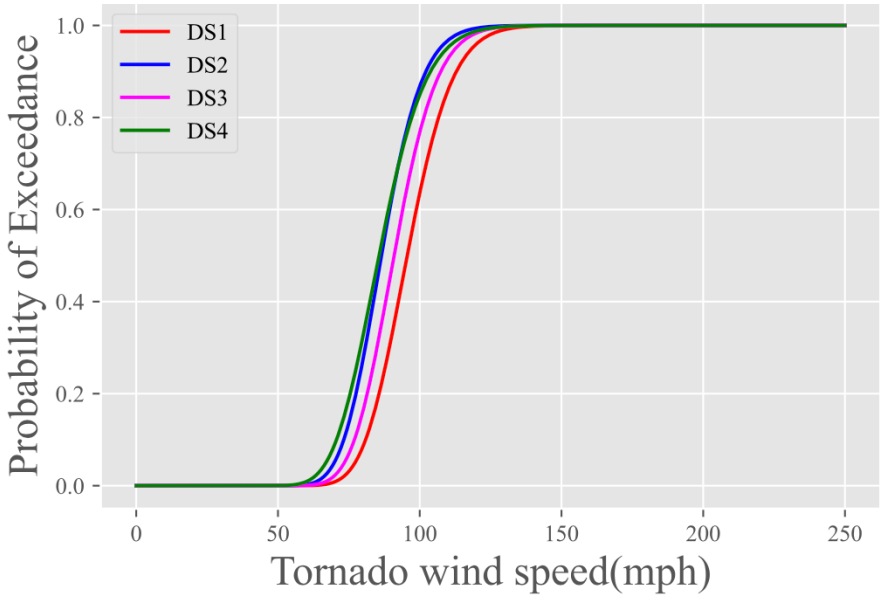

Figure 3-7. Fragility curve for a multi-family building at strategy 1

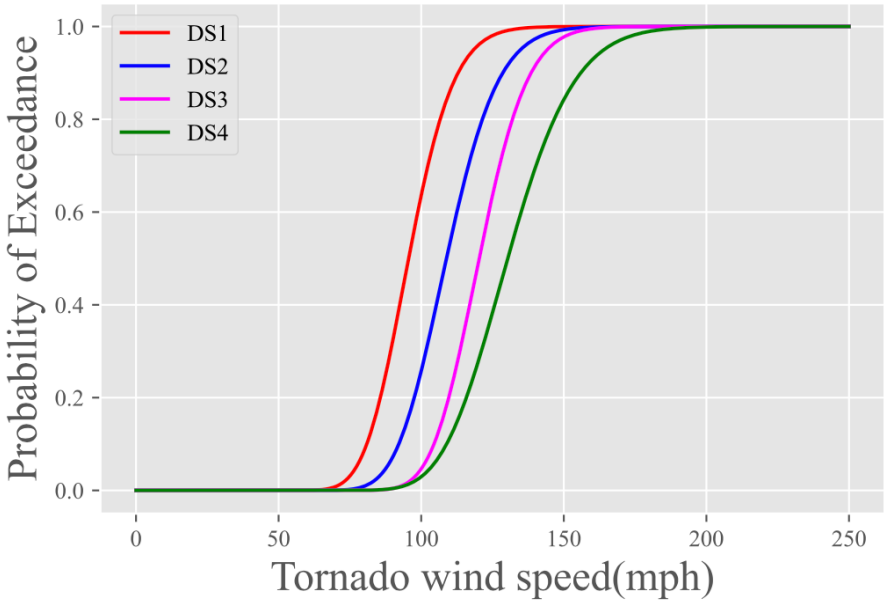

Figure 3-8. Fragility curve of a multi-family building at strategy 2

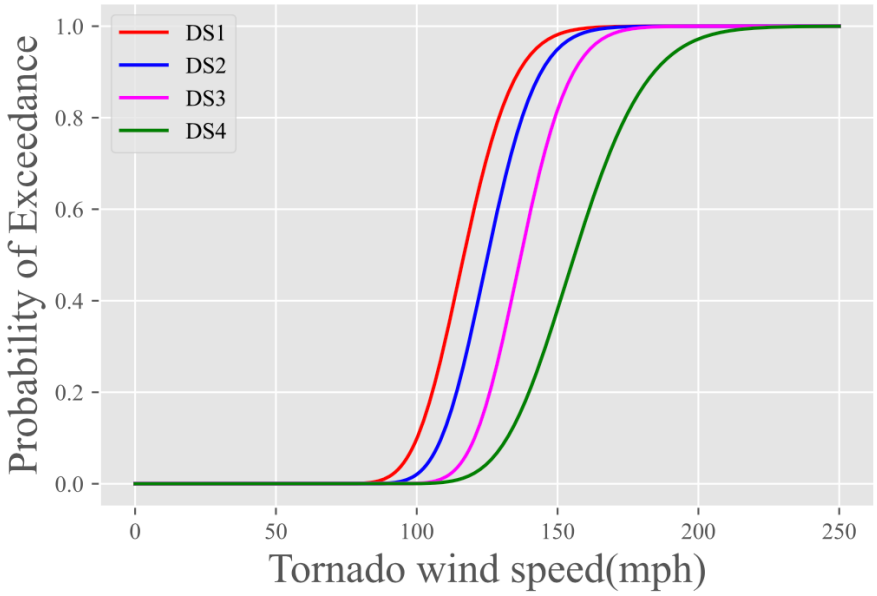

Figure 3-9. Fragility curve of a multi-family building at strategy 3

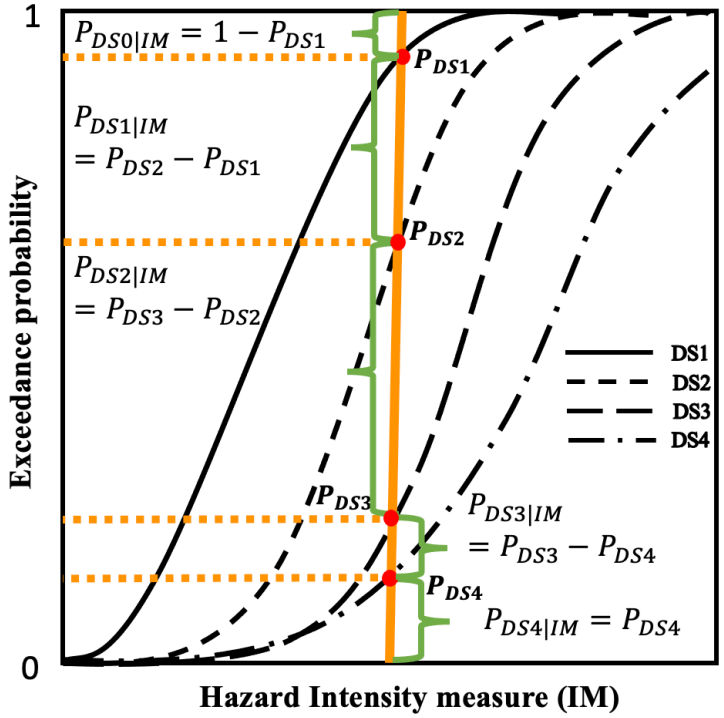

Figure 3-10. Illustration of expected damage probability with different damage state

Figure 3-11 illustrates that enhancement to a single-family building retrofit levels can reduce the probability of the building reaching the damage state DS4. The repair/replacement cost for the building at DS4 damage state is 100% of appraisal value of the building (Table 3-7). One can observe that the probability of exceedance of DS4 for the building with strategy 1 is 100% when wind speed is 135 mph, meaning that the building mitigated with strategy 1 has 100% probability with DS4 damage if the wind speed reaches 135 mph. However, if strategy 2 is implemented on the building, the probability of exceedance of DS4 drops to approximately 30%, and approximately to 5% for strategy 3. For a multi-family building (Figure 3-12) at a wind speed 135 mph, the probability for the building exceeding DS4 is 100% with strategy 1. Strategy 2 improves

the probability of exceedance by approximately 40%, and strategy 3 reduces the probability of the building reaching DS4 to 5%. Figure 3-11 and Figure 3-12 explain the motivation behind the hazard mitigation is to reduce the probability of exceedance of all damage states, and therefore, to reduce the expected damage probability that leads to less direct economic loss ultimately.

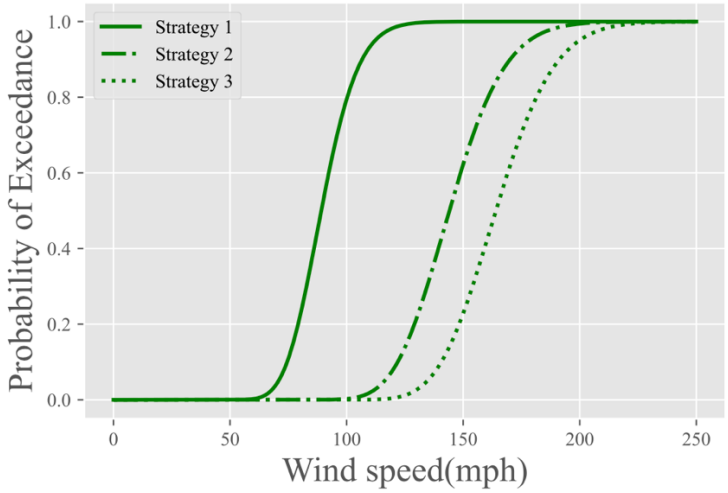

Figure 3-11. Fragility curves of a single-family building with strategy 1, strategy 2, and strategy 3 on damage state DS4

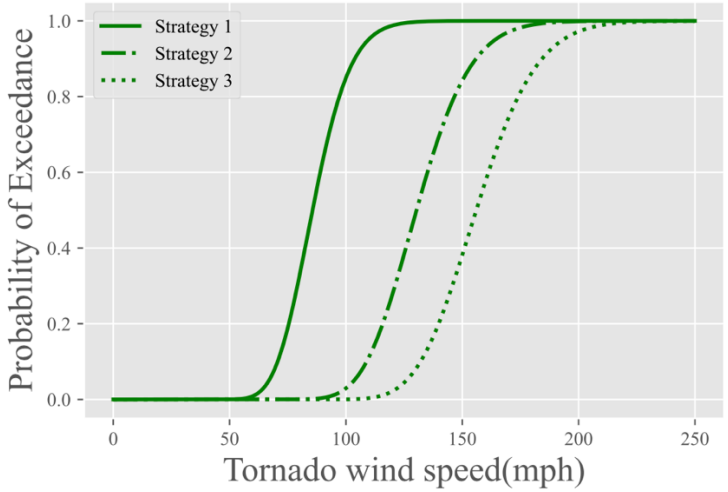

Figure 3-12. Fragility curves of a multi-family building with strategy 1, strategy 2, and strategy 3 on damage state DS4

Population Dislocation: $\boldsymbol{\alpha_{ijk}^{2}}$

The coefficient of population dislocation parameter α_{ijk}^{2} in this framework was adapted from the work proposed by Lin (2009). The author designed population dislocation ($DisF$) as a logistic regression model: a dislocation factor was calculated from probability of dislocation (Pr_{dis}) by the following operation: $DisF = 1$ if $Pr_{dis} \geq 0.5$; $DisF = 0$ otherwise. $DisF$ calculated of the probability of dislocation that is the first term in Equation (3-2). To apply a linear design of the framework introduced in Chapter 2, the dislocation factor is replaced by the probability of dislocation that is associated with four features (i.e., p_{ijk}^{vloss}, DS_j, B_i, H_i). The first feature is the percentage of building value loss due to damage, denoted here as p_{ijk}^{vloss}. The second feature is a binary value DS_j for archetype $j \in \mathcal{S}$ to represent whether the building is a single-family dwelling unit ($DS_j = 1$) or if it is a multi-family dwelling unit ($DS_j = 0$). Thirdly, B_i denotes the percentage of the Black population in block $i \in \mathcal{Z}$. Lastly. H_i represents the percentage of the Hispanic population in block $i \in \mathcal{Z}$. The coefficients $\beta_0, \dots, \beta_4$ are -0.42523, 0.02480, -0.50166, -0.01826, and -0.01198 that are extracted from Lin, et al. (2008). α_{ijk}^{2} is expressed as:

$$\alpha_{ijk}^{2} = \frac{1}{1 + e^{-\left(\beta_0 + \beta_1 p_{ijk}^{vloss} + \beta_2 DS_j + \beta_3 B_i + \beta_4 H_i\right)}} \times nDU_{ij} \times h\overline{DU}_i \tag{3-2}$$

where nDU_{ij} is the average number of dwelling units of archetype $j \in \mathcal{S}$ in block $i \in \mathcal{Z}$, and $h\overline{DU}_i$ represents the average number of households per dwelling unit in block $i \in \mathcal{Z}$. The value p_{ijk}^{vloss} in Equation (3-2) is the only factor that is affected by the decision variable in the model, and it is computed as:

$$p_{ijk}^{vloss} = \frac{l_{ijk}^{-c}}{M_{ij}} \times 100 \quad . \tag{3-3}$$

where l_{ijk}^{-c} is the direct economic loss of a building (excluding content loss) for block $i \in \mathcal{Z}$ and archetype $j \in \mathcal{S}$ that is at strategy $k \in \mathcal{K}$. The parameter M_{ij} indicates the average appraised value for buildings of archetype $j \in \mathcal{S}$ in block $i \in \mathcal{Z}$.

Building functionality parameter: α_{ijk}^{3}

α_{ijk}^{3} is designed as the coefficient of the objective building functionality that measures the performance of the physical system. α_{ijk}^{3} is defined as average building functionality across all buildings in the community and expressed as:

$$\alpha_{ijk}^{3} = \frac{Q_{ijk}^{t}}{\sum_{i \in \mathcal{Z}} \sum_{j \in \mathcal{S}} \sum_{k \in \mathcal{K}} b_{ijk}} \tag{3-4}$$

where Q_{ijk}^{t} is adapted from the study introduced by Koliou and van de Lindt (2020), and is defined as:

$$Q_{ijk}^{t} = \frac{1}{1 + \left(\frac{1}{Q_{ijk}^{0}} - 1\right) e^{-r_{ijk}t}} \quad . \tag{3-5}$$

The definition of Q_{ijk}^{t} is the average functionality at time t ($t \geq 0$) for all the buildings in block $i \in \mathcal{Z}$ and archetype $j \in \mathcal{S}$ that are at strategy $k \in \mathcal{K}$. When $t = 0$, Q_{ijk}^{t} can be represented as Q_{ijk}^{0} that is defined as a starting building functionality right after the immediate tornado event. r_{ijk} is computed based on Q_{ijk}^{0}, and recovery time t needed to achieve 100% building functionality and is expressed as:

$$r_{ijk} = -\frac{1}{t}\ln\frac{\frac{1}{Q_{ijk}^{t}}-1}{\frac{1}{Q_{ijk}^{0}}-1} \quad . \tag{3-6}$$

If Q_{ijk}^{0} and Q_{ijk}^{t} are given, r_{ijk} is a function of recovery time t. However, if Q_{ijk}^{t} is 100%, the ln 0 is mathematically undefined. If Q_{ijk}^{0} equals 0, meaning the building in block $i \in \mathcal{Z}$ and archetype $j \in \mathcal{S}$ that are at strategy $k \in \mathcal{K}$ is completely destroyed, Equation (3-6) is undefined as well. To verify the impact from different values of Q_{ijk}^{0} on the determination of values of r_{ijk}, four sets of values of Q_{ijk}^{0} and Q_{ijk}^{t} are provided in Table 3-9 and are used as parameters in Equation (3-6). The relationship between r_{ijk} and recovery time t is depicted through Figure 3-13. To compute the value of r_{ijk}, recovery time t for the building to reach 100% functionality is the deciding factor. To choose appropriate value of recovery time t in Equation (3-6), two aspects are considered. First, the Equation (3-5) from Koliou and van de Lindt (2020) was developed to account for a slower repair rate immediately after the disaster event, and higher rate in the following days as shown in Figure 3-14. The authors additionally pointed out that for residential buildings (multi-family building) associated with structural and non-structural extensive damage, there is a 50% probability that 180 days are needed for the buildings to reach 100% building functionality. Using t=180 days in Equation (3-6) and four sets values of Q_{ijk}^{0} and Q_{ijk}^{t}, the values of r_{ijk} are achieved as shown in Table 3-9 (column "r_{ijk}"). Secondly, if we consider Q_{ijk}^{t} unknown, using the values of Q_{ijk}^{0} and r_{ijk} in Table 3-9, and recovery time t = 180 days, the recovery trajectory of building functionality is described

in Figure 3-15. Comparing the shape of Q_{ijk}^{t} with parameters provides from Set 2 – Set 4, the building functionality trajectory with parameters from Set 1 has the slower repair rate and higher rate in the later recovery stage. Therefore, the values of parameters Q_{ijk}^{0} and r_{ijk} are defined by the values of Set 1 in Table 3-9.

If a building is destroyed, Q_{ijk}^{0} can be practically defined as 0, meaning that Equation (3-5) is mathematically undefined. Additionally, the starting functionality Q_{ijk}^{0} can determine the value of r_{ijk}. Based on these two considerations, the final equation to compute the building functionality is proposed as:

$$Q_{ijk}^{t} = \begin{cases} \dfrac{1}{1+\left(\dfrac{1}{Q_{ijk}^{0}}-1\right)e^{-r_{ijk}t}} & if\, Q_{ijk}^{0} > 0 \\ \dfrac{1}{1+\left(\dfrac{1}{\omega}-1\right)e^{-r_{ijk}t}} & if\ Q_{ijk}^{0} = 0 \end{cases} \text{, and} \tag{3-7}$$

where ω is defined as a starting parameter if $Q_{ijk}^{0} = 0$. t is the user-defined parameter and defined as the recovery time (unit: days) after the immediate tornado event.

Table 3-9. r_{ijk} values change according to Q_{ijk}^{0} and Q_{ijk}^{t} at recovery time t = 180 days

	Q_{ijk}^{0}	Q_{ijk}^{t}	r_{ijk}
Set 1	10^{-7}	0.9999999	0.1790
Set 2	10^{-5}	0.9999999	0.1535
Set 3	10^{-3}	0.9999999	0.1279
Set 4	10^{-1}	0.9999999	0.0890

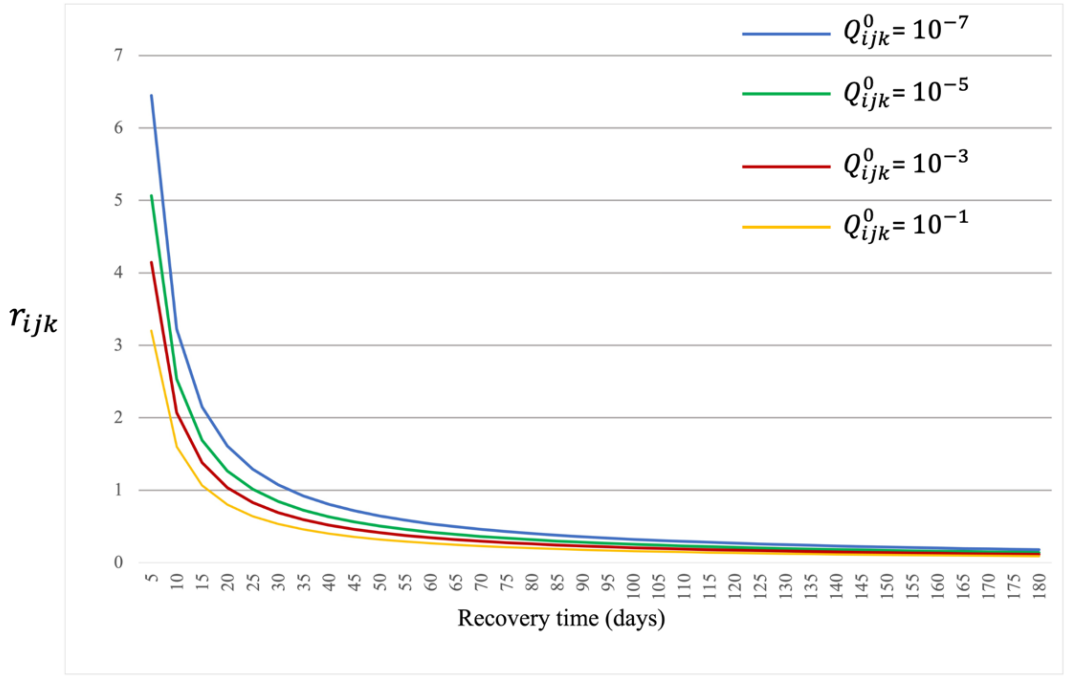

Figure 3-13. r_{ijk} values vary according to different Q_{ijk}^0values when Q_{ijk}^t= 0.9999999

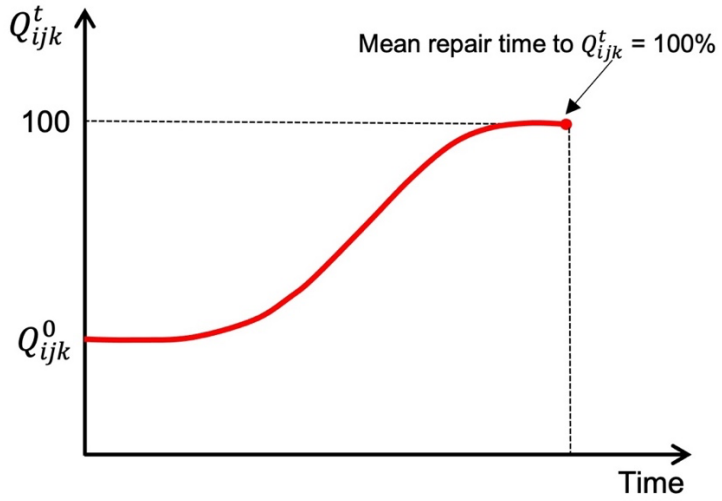

Figure 3-14. Repair time function for quantifying multiple levels of building functionality based on predefine/starting damage levels (Koliou and van de Lindt, 2020)

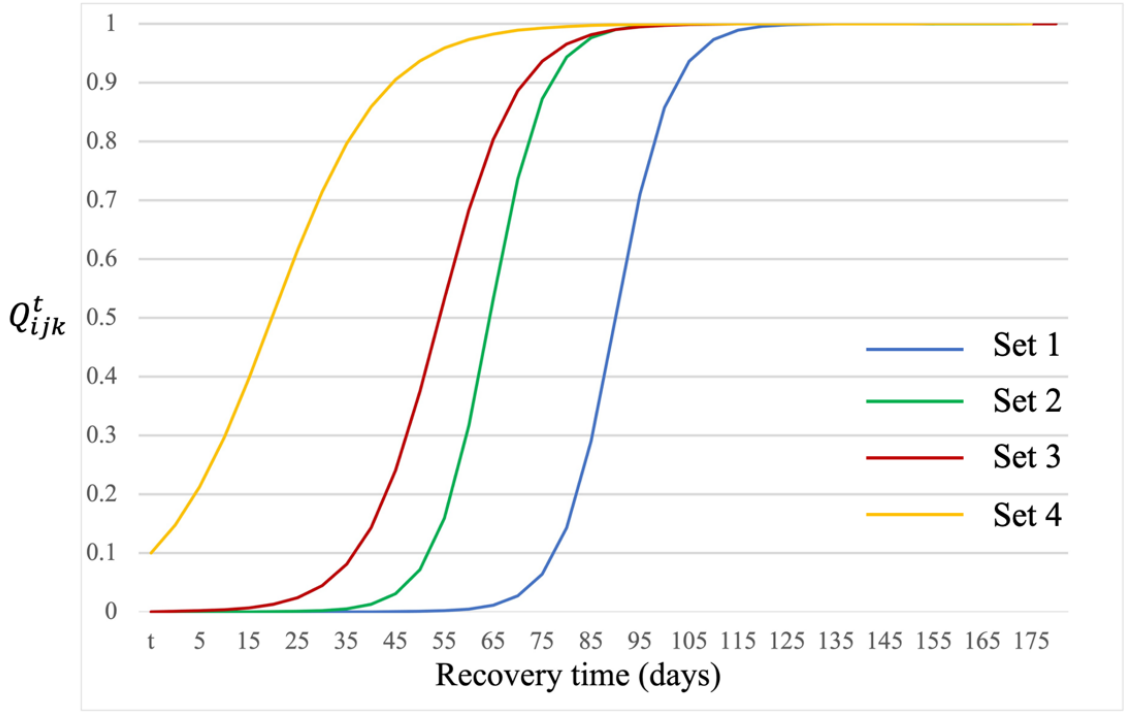

Figure 3-15. Building functionality Q_{ijk}^{t} recovery trajectory Considering different values of Q_{ijk}^{0} and r_{ijk}

3.4.4 Optimization model

We can formulate the optimization problem by following form. The model is coded with Python using Gurobi solver.

Description	Equations	Eq.No.
Input Parameter	Set of locations $i \in \mathcal{Z}$ Set of building types $j \in \mathcal{S}$ Set of retrofitting strategy $k \in \mathcal{K}$ Coefficient of direct economic loss: α_{ijk}^{1} Coefficient of population dislocation: α_{ijk}^{2} Coefficient of building functionality: α_{ijk}^{3} Retrofitting cost: $SC_{ijkk'}$ Retrofitting budget: B	(3-1) (3-2) (3-4)
Decision Variable	The total number of buildings after the mitigation: $\boldsymbol{x_{ijk}}$ the total number of buildings retrofitted from strategy k to k': $\boldsymbol{y_{ijkk'}}$	
Objective 1 Minimize direct economic loss	$\min \sum_{(i,j,k) \in \mathcal{T}_1} \alpha_{ijk}^{1} x_{ijk} \quad n = 1$	(2-7)
Objective 2 Minimize population dislocation	$\min \sum_{(i,j,k) \in \mathcal{T}_2} \alpha_{ijk}^{2} x_{ijk} \quad n = 2$	(2-7)
Objective 3 Minimize the building functionality	$\min \sum_{(i,j,k) \in \mathcal{T}_3} -\alpha_{ijk}^{3} x_{ijk} \quad n = 3$	(2-7)
Constraint 1 Retrofitting budget constraint	$\sum_{(i,j,k,k') \in \mathcal{U}} SC_{ijkk'} y_{ijkk'} \leq B$	(2-2)
Constraint 2 Building constraint of final state after intervention	$x_{ijk} = \sum_{k':(i,j,k',k) \in \mathcal{U}} y_{ijk'k} + b_{ijk} - \sum_{k':(i,j,k,k') \in \mathcal{U}} y_{ijkk'}$ $\forall (i,j,k) \in \mathcal{T}.$	(2-3)
Constraint 3 Building number balance constraint	$\sum_{k:(i,j,k) \in \mathcal{T}} x_{ijk} = \sum_{k:(i,j,k) \in \mathcal{T}} b_{ijk} \quad \forall i \in \mathcal{Z}, \forall j \in \mathcal{S}.$	(2-4)
Constraint 4 Non-negative constraint	$x_{ijk} \geq 0 \quad \forall (i,j,k) \in \mathcal{T}$	(2-5)
Constraint 5 Non-negative constraint	$y_{ijkk'} \geq 0 \quad \forall (i,j,k,k') \in \mathcal{U}.$	(2-6)

Table 3-10 summarizes the notation used in the model.

Table 3-10. Notation for the optimization model

	Description
Set	
$\mathcal{Z}$	A set of unique block groups $i \in \mathcal{Z}$
$\mathcal{S}$	A set of residential building types $j \in \mathcal{S}$
$\mathcal{K}$	A set of intervention strategy associated with tornado mitigation
$\mathcal{T}_n$	A set of combination of 3-tuple (i, j, k)
$\mathcal{T}$	Union of $\mathcal{T}_n$ $n \in \{1, \dots, N\}$
$\mathcal{U}$	A set of combination of 4-tuple (i, j, k, k') associated with allowable interventions from strategy k to k' in group $i \in \mathcal{Z}$ for building type $j \in \mathcal{S}$
Parameters	
α_{ijk}^1	Coefficient of the objective function for direct economic loss in block $i \in \mathcal{Z}$ of structure type $j \in \mathcal{S}$, which are at strategy $k \in \mathcal{K}$
α_{ijk}^2	Coefficient of the objective function for population dislocation in block $i \in \mathcal{Z}$ of structure type $j \in \mathcal{S}$, which are at strategy $k \in \mathcal{K}$
α_{ijk}^3	Coefficient of the objective function for building functionality in block $i \in \mathcal{Z}$ of structure type $j \in \mathcal{S}$, which are at strategy $k \in \mathcal{K}$
B_i	Percentage of the Black population in block $i \in \mathcal{Z}$
B	The total budget available for retrofit efforts
DS_j	Dummy variable for a residential structure. $DS_j = 1$ if the archetype is Single-Family Dwelling $DS_j = 0$ if the archetype is Multi-Family Dwelling
nDU_{ij}	The average number of dwelling units
b_{ijk}	Corresponding quantity of building before any mitigation efforts in block $i \in \mathcal{Z}$ of structure type $j \in \mathcal{S}$, which are at strategy $k \in \mathcal{K}$
H_i	Percentage of the Hispanic population in block $i \in \mathcal{Z}$
$h\overline{DU}_i$	The average number of households per dwelling unit for block i
l_{ijk}^{-c}	The direct economic loss of a building excluding content loss in block $i \in \mathcal{Z}$ of structure type $j \in \mathcal{S}$, which are at code/strategy $k \in \mathcal{K}$
M_{ijk}	The total appraised value of associated buildings in block $i \in \mathcal{Z}$ of structure type $j \in \mathcal{S}$, which are at strategy $k \in \mathcal{K}$
M_{ij}	The average appraised value per building for the building group in block $i \in \mathcal{Z}$ of structure type $j \in \mathcal{S}$
N	Total number of objectives
p_{ijk}^{vloss}	Percentage value loss of a building in block $i \in \mathcal{Z}$ of structure type $j \in \mathcal{S}$, which are at strategy $k \in \mathcal{K}$
Q_{ijk}^0	The functionality of building in block $i \in \mathcal{Z}$ of structure type $j \in \mathcal{S}$, which are at strategy $k \in \mathcal{K}$ at immediate disruption
Q_{ijk}^t	The functionality of building in block $i \in \mathcal{Z}$ of structure type $j \in \mathcal{S}$, which are at strategy $k \in \mathcal{K}$ at time t
r_{ijk}	Parameter related to building functionality
$SC_{ijkk'}$	Strategy cost for strategy $k \in \mathcal{K}$ on building type $j \in \mathcal{S}$ in block $i \in \mathcal{Z}$
Decision Variables	
x_{ijk}	Decision variable, the total number of buildings of structural type $j \in \mathcal{S}$ in block $i \in \mathcal{Z}$ at strategy $k \in \mathcal{K}$ after mitigation
$y_{ijk'k}$	Decision variable, the total number of buildings retrofitted from $(k', k) \in \mathcal{L}$ in block $i \in \mathcal{Z}$ of structure type $j \in \mathcal{S}$ after mitigation

3.4.5 Outputs of the Optimization model

Optimal solutions

Two decision variables x_{ijk} and $y_{ijkk'}$, imply the retrofitting plans. The optimal solutions of x_{ijk} encompass the following 5 pieces of information as shown in Table 3-11: (1) unique I.D. of each solution (column Solution Id); (2) unique I.D. of blocks where buildings are located (column $\mathcal{Z}$); (3) structural type (column $\mathcal{S}$); (4) final retrofitting strategies for the buildings (column $\mathcal{K}$); (5) the number of buildings in block $i \in \mathcal{Z}$ of archetype $j \in \mathcal{S}$, which are at the strategy $k \in \mathcal{K}$ (column x_{ijk}). The rows with the same "Solution Id" in Table 3-11 are unique Pareto optimal solution that is a retrofit plan. The column $\mathcal{Z}$ is defined as the unique census block groups in Joplin, MO, which are the granularity of decision-making for the mitigation planning. Using the information provided from Table 3-11, we can interpret the implementation of this solution as a retrofit plan in Joplin as: (1) 20 single-family buildings are enhanced to strategy 3 in block "290970101001018"; (2) 3 multi-family buildings are enhanced to strategy 2 in block "290970101001018"; (3) 214 single-family buildings are enhanced to strategy 3 in block "290970103002015"; (4) 8 multi-family buildings are enhanced to strategy 3 in block "290970110002039"; (5) There is no retrofit action on 33 single-family buildings in block "290970101001003".

The optimal solutions for decision variable $y_{ijkk'}$ contain the same information comparing to the optimal solution of x_{ijk}, except for the allowable retrofit strategy pair (k', k) in Table 3-12. The column $y_{ijkk'}$ represents the number of buildings for strategy $k \in \mathcal{K}$ retrofitted to strategy $k' \in \mathcal{K}$ on archetype $j \in \mathcal{S}$ in block $i \in \mathcal{Z}$. The information

from $y_{ijkk'}$ shows the methodology of how the final retrofitting strategies are achieved. For example, in Table 3-11, the final strategy of 214 single-family buildings in block "290970103002015" is strategy 3. In Table 3-12, the initial retrofitting strategy for these 214 single-family buildings is revealed at strategy 0, which means there is no prior retrofitting effort on these 214 buildings. The detailed implementation associated with decision variable $y_{ijkk'}$ is valuable information for decision makers. In this example, the decision-making level is at the block group, and it is possible that not all buildings in the same block are retrofitted. The initial strategy information from $y_{ijkk'}$ can differentiate buildings groups if the buildings with same building type are retrofitted to the same final strategy with different starting strategies.

It is possible that there may be more than one optimal solution. For example, using \$181M budget for the retrofitting effort and 20 number of epsilon steps, there are a total of 109 unique Pareto optimal solutions produced by the optimization model and these solutions are equally optimal to achieve the same mitigation effect. Each solution is associated with three objectives (i.e., direct economic loss, population dislocation, building functionality). Table 3-13 shows an example of the optimal values of these objectives. The number of objectives $n \in \{1, \dots, N\}$ is defined in the mathematical model formulation in Section 3.3.4. For example, for solution with Solution Id = 1, the objective values are explained as: (1) the value of the first objective (direct economic loss) is \$1.414M; (2) the value of the second objective (population dislocation) is 22; and (3) the value of the third objective (building functionality) is 0.69.

Table 3-11. x_{ijk} optimal solution example

Solution Id	$\mathcal{Z}$	$\mathcal{S}$	$\mathcal{K}$	x_{ijk}
1	290970101001018	Single-family	3	20
1	290970101001003	Single-family	0	33
1	290970101001081	Multi-family	2	3
1	290970103002015	Single-family	3	214
1	290970110002039	Multi-family	3	8
…	…	…	…	…

Table 3-12. $y_{ijkk'}$ optimal solution example

Solution Id	$\mathcal{Z}$	$\mathcal{S}$	$\mathcal{K}$	$\mathcal{K}'$	$y_{ijkk'}$
1	290970101001018	Single-family	0	3	20
1	290970101001003	Single-family	0	0	33
1	290970101001081	Multi-family	1	2	3
1	290970103002015	Single-family	0	3	214
1	290970110002039	Multi-family	0	3	8
…	…	…	…	…	…

Table 3-13. Pareto optimal objectives data consider all residential blocks

Solution Id	Objective $n \in \{1, \dots, N\}$	Objective Value
1	1	$ 1.414M
1	2	22
1	3	0.69
2	1	$ 1.378M
2	2	28
2	3	0.56
…	…	…

Tradeoff analysis

The outputs of the model include the optimal solutions and the optimal values of three competing objective functions: direct economic loss, population dislocation, and building functionality. Each optimal solution is associated with one set of optimal values for the three objectives. Improving any of these three objectives will reduce the other two objectives. In the previous example, there were a total of 109 unique Pareto optimal solutions using the parameter of a $181M budget for the retrofitting effort, and 20 number of epsilon steps. A Pareto surface can be drawn using the set 109 of optimal objective values (Table 3-13) to describe the tradeoff relationship of these three objectives, which are shown in Figure 3-16. Figure 3-17 provides Pareto curves between average population dislocation per block and average community building functionality. The points with same color scale (the color scale bar) indicate that the direct economic losses of these solutions are at the same level.

To illustrate the tradeoff analysis using the outputs from the model, three solutions were selected from a total of 109 Pareto solutions in Figure 3-16 and Figure 3-17, which are marked as Plan 1, Plan 2, and Plan 3. Table 3-14 provides the objective function values associated with the three solutions. The values of direct economic loss and population dislocation are calculated as average values at the block group level, and the building functionality is shown as the average building functionality across the whole community. Given such information, if decision-maker prefers Plan 2 over Plan 1, the impact on direct economic loss is reduced by $36,000 ($1.414M versus $1.378M) with an 8% improvement (0.69 versus 0.56) on building functionality, but the number of dislocated population is changed from 22 to 23 people. This example demonstrates the tradeoff analysis between

the competing objectives. By improving direct economic loss and building functionality, the population is degraded by such a choice. It can additionally be interpreted that one dislocated population on each block costs $36,000 on direct economics loss and 8% on building functionality. Similarly, if Plan 3 is chosen over Plan 1, direct economic loss is improved by $29,000 ($1.414M versus $1.385M), and building functionality is improved by 13% (0.69 versus 0.56) with increasing one dislocated population. Plan 1 is associated with the highest direct economic loss and the lowest building functionality but leads to the least population dislocated compared to Plan 2 and Plan 3. If Plan 2 is chosen over Plan 3, the building function is improved by 5% while losing $7,000 on direct economic loss. In conclusion, decision makers can use tradeoff information to evaluate different solutions to facilitate the decision-making process on determination of retrofit plans from the available solutions.

Table 3-15 summarizes the tradeoff analysis on the three selected solutions and the negative sign indicates the degradation on the corresponding objectives. Table 3-16 shows the details of the three plans. In Plan 1, there are a total of 14,794 buildings (approximately 60% of total buildings) retrofitted to higher strategy from the initial strategy (strategy 0). In Plan 2, 17,417 single-family buildings (70% of total single-family buildings) are retrofitted to strategy 2, and all 67 multi-family building are retrofitted to strategy 3. However, Plan 3 retrofits the most single-family buildings compared with Plan 1 and Plan 2. Out of a total of 18,760 retrofitted single-family buildings, 1,357 single-family buildings and 21 multi-family buildings are enhanced to strategy 3. Recalling the objective values associated with these three plans (Table 3-14), Plan 3 is associated with higher building functionality than Plan 1 or Plan 2 because Plan 3 retrofitted more buildings (a total of

18,760) than Plan 1 or Plan 2. Figure 3-18 geographically explains such a difference. Each point on the map represents a building, and each layer (buildings with same color) represents a retrofit Plan. Because of the overlapping between the different plans, the majority of retrofitted buildings across the three plans are same; however, Plan 3 (bottom layer in green) covers more areas than Plan 2 (layer in blue) or Plan 1(layer in rosybrown), which validates the fact Plan 3 enhanced the most buildings out of the three plans. Moreover, in Plan 2, the budget spent on retrofitting multi-family buildings is approximately 12% of the total budget of $181M on a total of 67 buildings due to the fact appraisal values of a multi-family building are more expensive than a single-family in most cases. With allocating a higher budget on multi-family buildings, Plan 2 has the least direct economic loss compared with Plan 1 or Plan 3.

The tradeoff analysis illustrates how the information provided from the optimal solutions are utilized to evaluate the differences between retrofit plans. However, the decision-making on selecting the retrofitting plans is determined by decision makers who need to balance the decision factors such as local policies, budget, resources, etc.

Table 3-14. Objective function values of selected three retrofit plans

Retrofit Plan	Average Direct economic loss/block (Million $)	Average Population dislocation/block	Average community building functionality
1	1.414	22	0.56
2	1.378	23	0.64
3	1.385	23	0.69

Table 3-15. Tradeoff analysis on selected retrofit plans

Tradeoff Analysis: Δ economic loss Δ pop dislocation Δ Building functionality		**To**	
		Plan 2	Plan 3
From	Plan 1	$36,000 -1 8%	$29,000 -1 13%
	Plan 2		-$7,000 0 5%

Table 3-16. Details of three selected retrofit plans

Retrofit Plans	Archetype	Retrofit strategy	Number of buildings	Budget allocation ($M)
Plan 1	Single-family	0	10,000	0
	Single-family	2	6,344	72.4
	Single-family	3	8,412	105.9
	Multi-family	0	29	0
	Multi-family	3	38	3.1
Plan 2	Single-family	0	7,339	0
	Single-family	2	17,417	159.9
	Multi-family	0	0	0
	Multi-family	3	67	21.5
Plan 3	Single-family	0	5,996	0
	Single-family	2	17,403	171.3
	Single-family	3	1,357	9.4
	Multi-family	0	46	0
	Multi-family	3	21	0.6

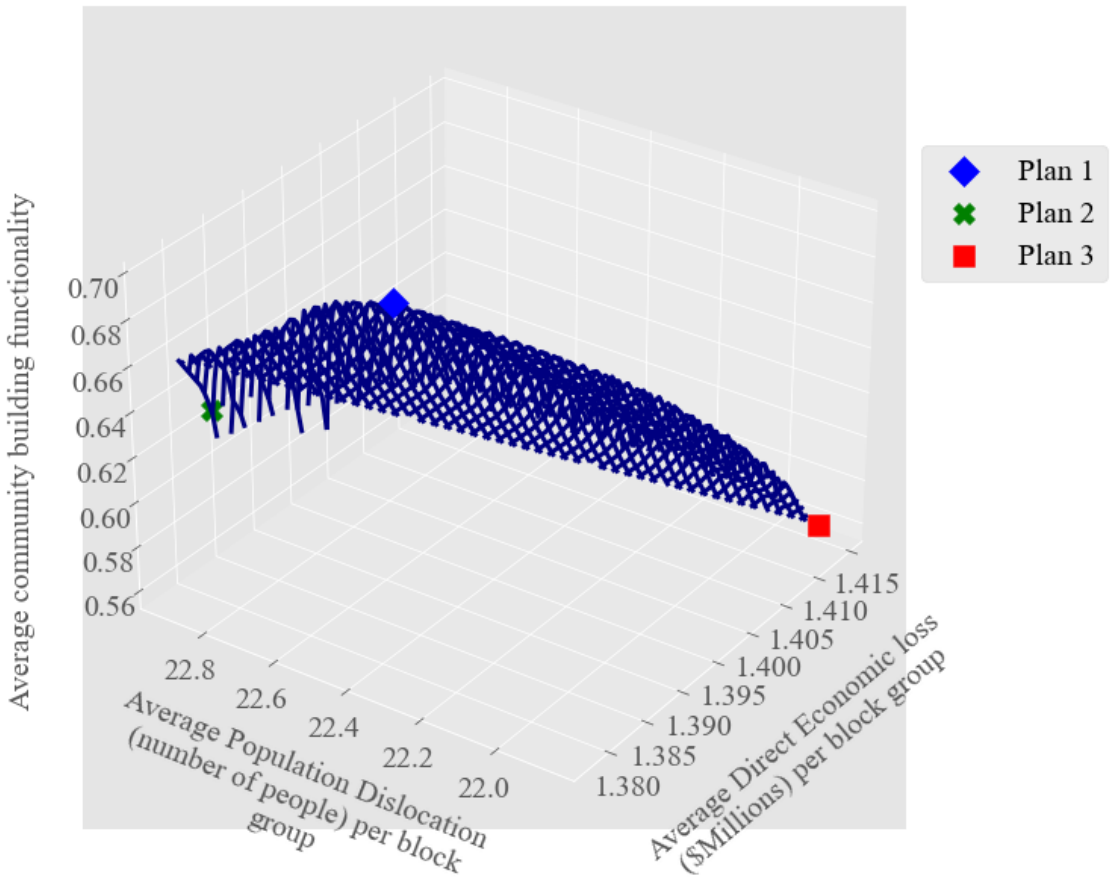

Figure 3-16. Pareto surface from the solutions with $181M budget and recovery time 30 days

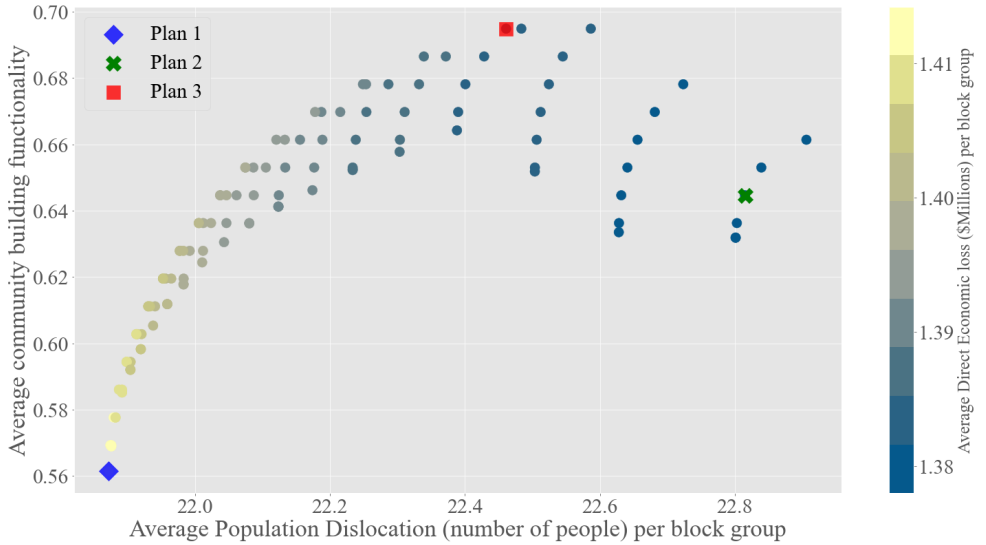

Figure 3-17. Pareto solutions of three competing objectives–direct economic loss, population dislocation, and building functionality with $181M budget and building recovery time 30 days in Joplin

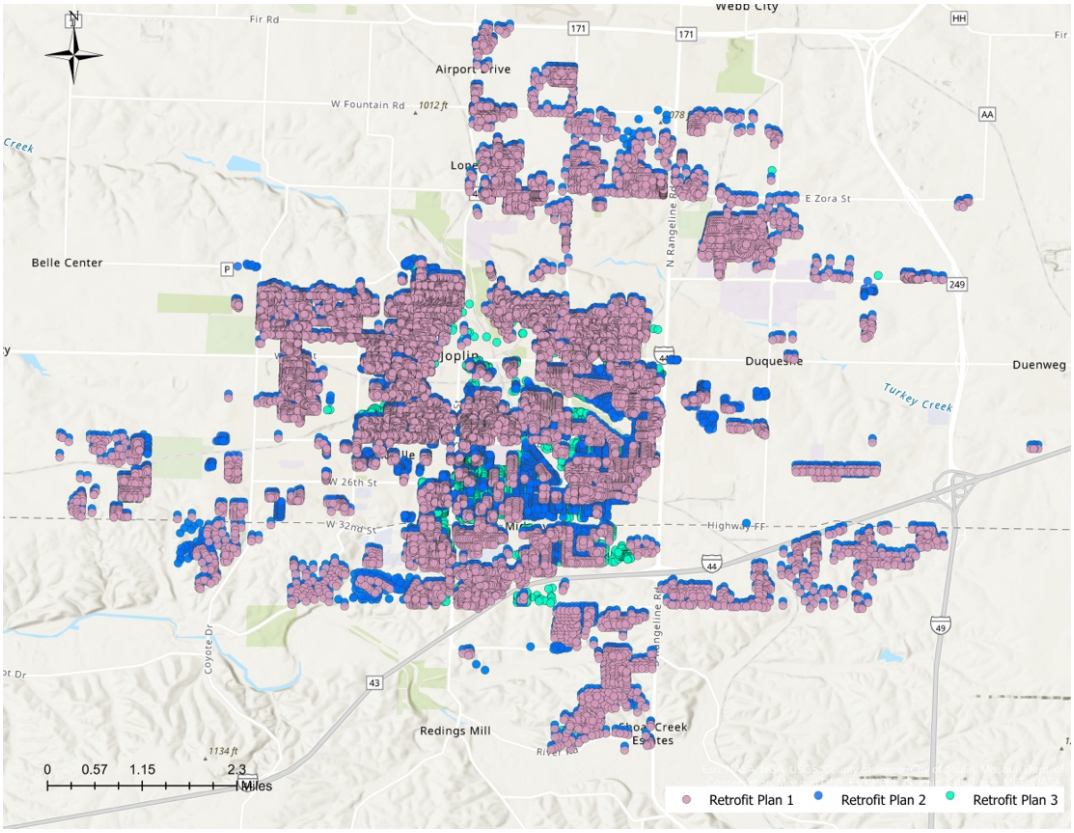

Figure 3-18. Geographic building mapping of three retrofit plans

3.5 Strategies on decision Support

3.5.1 Priority analysis

The priority analysis provided by this study furthers the decision-making on mitigating the potential loss and improve the community resilience. The optimal solutions from Table 3-11 and Table 3-12 include the following information: Block ($\mathcal{Z}$), building structure ($\mathcal{S}$), retrofitting level ($\mathcal{K}$ and $\mathcal{K}'$), and the retrofit plans from decision variables (x_{ijk} and $y_{ijkk'}$). If the number of solutions is produced at a budget level, the frequency of a block appearing in all retrofitting solutions can be used as an indicator to measure if this block is more vulnerable than others. For instance, there are a total of 1,565 blocks with residential structures in Joplin. At a budget level \$181M, 109 Pareto optimal solutions are available for retrofitting the residential buildings. Block "290970101002040" appears in 59 of 109 solutions. However, Block "290970106003009" is only shown in 1 of 109 solutions. Therefore, we can suggest that block "290970101002040", which is retrofitted more often than block "290970106003009", can be prioritized before block "290970106003009".

Figure 3-19 describes the relative frequency of the residential blocks in Joplin that are retrofitted in 55 unique Pareto optimal solutions with a budget of \$9M. The blocks in dark red indicate these blocks appear in 44 out of 55 solutions in the worst cases (80% of 55 solutions). The blocks in yellow (relative frequency is approximately 0) means there is no retrofitting across all optimal solutions. If the budget is increased up to \$90M, it is evident that more blocks are retrofitted (Figure 3-20). The frequency of the blocks in dark red in the Figure 3-20 is over 80% of total solutions, meaning with \$90M budget, 87 out

of 109 retrofitting solutions retrofitted the blocks in dark red. By applying the restrictive budget, the most vulnerable blocks are pinpointed in the community. By increasing the priority of retrofitting interventions on these blocks, potentially, less direct economic loss, less household dislocation, and higher building functionality would happen after tornado hazard.

Priority analysis expands the options on decision-making by using geographical technique and information. The prerequisite of priority analysis is that the geographic feature associated with decision level much be available to allow decision makers to explore the options.

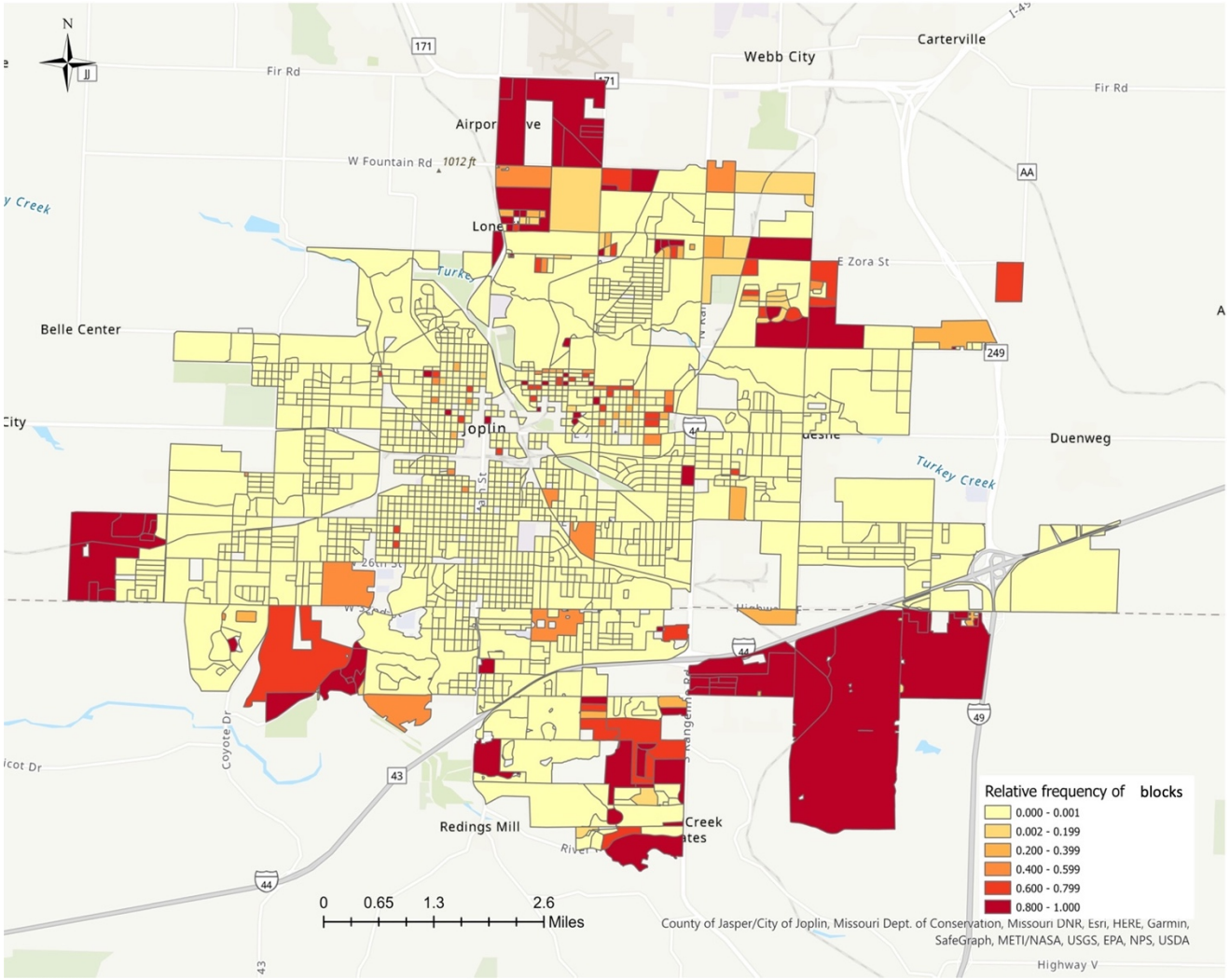

Figure 3-19. Identify vulnerable areas with $9M retrofitting budget

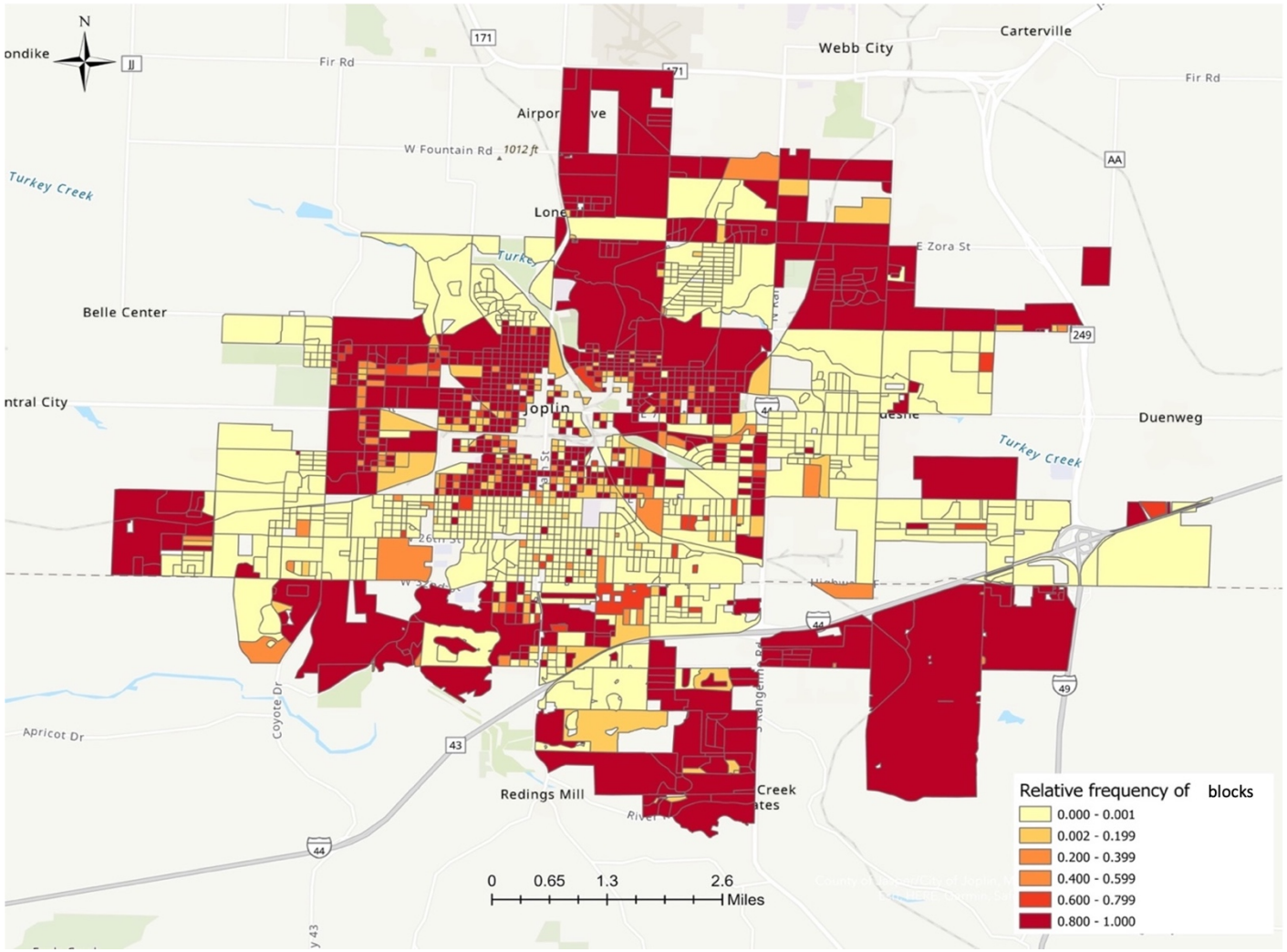

Figure 3-20. Identify vulnerable areas with $90M retrofitting budget

3.5.2 Decision-making on different budget

Budget B is the constraint that provides the threshold for retrofitting efforts. By adjusting the budget, we broaden the options for decision-making. Table 3-17 provides optimal values of three objective functions with three budgets: \$9M, \$90M, \$181M for a recovery time of 30 days. The range for each objective function is minimum and maximum values of the objective's values across all solutions. For instance, at budget level \$9M, there are a total of 55 solutions associated with 55 direct economic loss values, 55 population dislocation values, and 55 building functionality values. \$1.640M and \$1.643M are the smallest and the largest values out of the 55 direct economic loss values. Figure 3-21 depicts three Pareto curves between direct economic loss and population dislocation with \$9M, \$90M, and \$181M as budgets. The curve in blue located in the upper right corner of Figure 3-21 is the Pareto curve with \$9M budget, the curve in red is the Pareto curve with a \$90M budget, and the curve in green located in the lower left corner of the figure is the Pareto curve with a \$181M budget. It is observed that increasing the availability of retrofit budget can reduce the potential damage on direct economic loss and population dislocation. Figure 3-22 describes the Pareto curves between population dislocation and building functionality with three different budget levels. Increasing the retrofit budget improves building functionality as expected because if more buildings are retrofitted to higher strategies, the probability of damage of buildings after a tornado event will be less, which improves the building functionality in general.

The information provided on Table 3-17 can support decision-making on the following aspects: determination of availability of budget and the restricted budget. First, a decision-maker can use the range of each objective function to determine the availability

of funding. For instance, the goal of the mitigation effort for a community is to reduce the potential direct economic to $1.4M per block. Because $1.4M falls into the range with a budget of $181M ($1.378M to $1.414M), the retrofitting budget for the community can be defined as $181M. Similarly, such implications can apply to the other objectives in the model. Secondly, by decreasing the budget to a certain level, the range of the objectives will eventually become 0. We can call this budge level as the most restricted budget, which is the lower bound for the budget B. Using the most restricted budget, the decision-maker can identify the least investment for the community and the potential impacts on the primary community resilience goals given this budget.

The analysis based on different budgets add another layer of information to the array of options for decision-making. The decision makers can use such information on allocation the mitigation budget to target the desired performance of primary systems.

Table 3-17. Optimal values of three competing objectives with different budget levels

Budget	Objectives	Minimum	Maximum	Range
$9M	$Average direct economic loss per block($Million)	1.640	1.643	0.003
	Average population dislocation per block	26	27	1
	Average community building functionality (%)	8.8	0.2	8.6
$90M	$Average direct economic loss per block($Million)	1.514	1.534	0.02
	Average population dislocation per block	23	25	2
	Average community building functionality (%)	37	47	10
$181M	$Average direct economic loss per block($Million)	1.378	1.414	0.036
	Average population dislocation per block	21	23	2
	Average community building functionality (%)	56	69	13

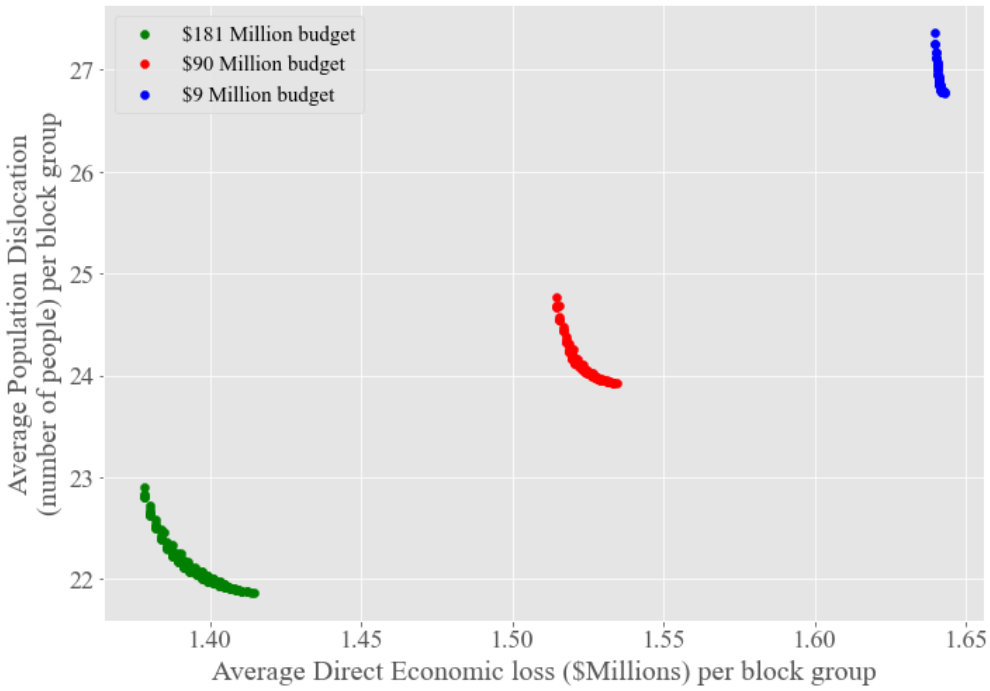

Figure 3-21. Pareto curves between direct economic loss and population dislocation with three different budgets

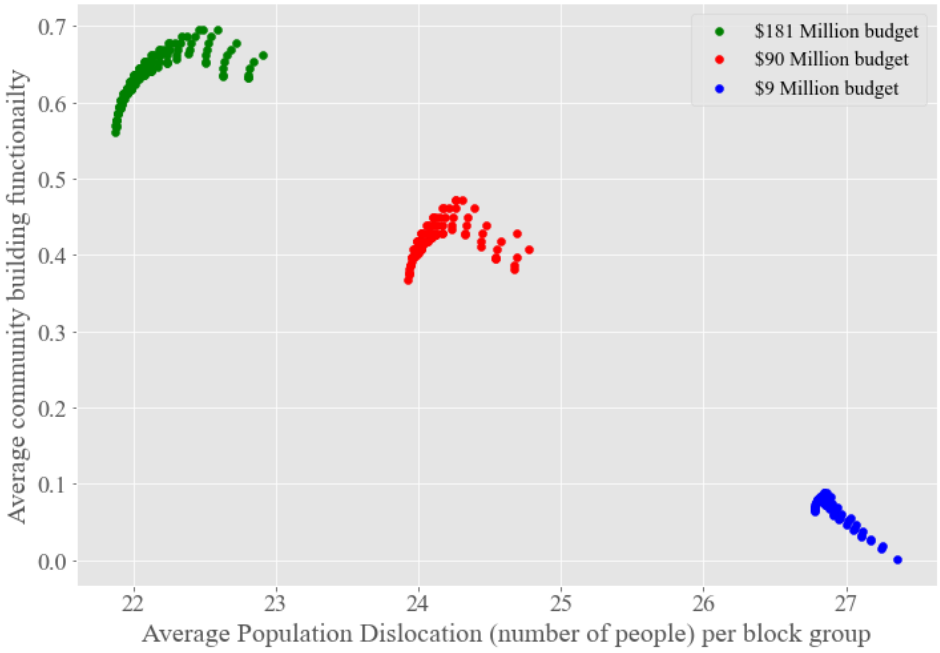

Figure 3-22. Pareto curves between population dislocation and building functionality with three different budgets

3.6 Case study through IN-CORE

To provide further analysis based on the results from the model, we can additionally utilized the computational platform, the Interdependent Networked Community Resilience Modeling Environment (IN-CORE) (Gardoni, et al., 2018), to simulate tornado scenarios and evaluate the effectiveness of the selected retrofit solutions. The optimal retrofitting solutions consider the wind speed 135 mph on all residential wood frame buildings without prior knowledge on where and when the tornado hazard will strike. In this section, we simulated several tornado scenarios through IN-CORE and provided the measurement for three competing objectives of the optimization model to evaluate the selected retrofit plans on all simulated tornado events.

This study is designed to mitigate the moderate to severe tornadoes in the Joplin area. The tornado scenarios are simulated from IN-CORE ranging from EF3 to EF5. We designed 66 scenarios including 20 EF3 tornadoes, 25 EF4 tornadoes, and 21 EF5 tornadoes. The current IN-CORE version allows modeling the building damage probability and population dislocation (Rosenheim, et al., 2021) while considering the designated hazard. The calculation of direct economic loss (Equation (3-1)) and buildings functionality (Equation (3-4)) will follow the methodology from Section 3.3.3. As we discussed in Section 3.3.5, there might be more than one optimal solution produced from the optimization model. Three retrofit plans were selected (Table 3-14) to incorporate with the tornado scenarios for further analysis.

To validate the selected retrofit plans from the model, we use the improvement on three objectives to evaluate the selected plans. Figure 3-23 reveals the process of computing the values of three objectives (i.e., direct economic loss, population dislocation,

building functionality right after the disruption). First, we applied 66 tornado events individually to the building inventory without any retrofit effort. Each tornado event resulted in building damage within the tornado path. Using the building damage analysis from IN-CORE, we computed direct economic loss, population dislocation, and building functionality after each tornado. The results included 66 values of direct economic loss that is denoted as $loss_h^0$, $h \in \{1,2,\dots,66\}$, 66 values of population dislocation that is denoted as $disl_h^0$, $h \in \{1,2,\dots,66\}$, and 66 values of building functionality that is denoted as $func_h^0$, $h \in \{1,2,\dots,66\}$. Second, we implemented Plan 1 on Joplin building inventory. Then we applied the tornado events on the new buildings inventory that is retrofitted according to Plan 1. Through IN-CORE building damage analysis on all tornado events, we computed the corresponding direct economic loss, population dislocation, and building functionality after each tornado event. Similarly, we have results for each objective. Let $loss_h^1$ denote direct economic loss of Plan 1, $disl_h^1$ denote population dislocation of Plan 1, and $func_h^1$ as building functionality of Plan 1 for $h \in \{1,2,\dots,66\}$. The same process was applied to Plan 2 and Plan 3. Three variables were created to represent the difference between before and after the retrofitting effort: Δ_{loss}, $\Delta_{disl.}$, and $\Delta_{func.}$ Table 3-18 describes the process to achieve the data used for the case study analysis. Table 3-19 provides expected values of three objectives across all tornado events on different retrofit plans. The percentage of the improvement was calculated as:

$$\frac{\text{Averge values of objective without retrofit} - \text{Average values of objective of retrofit plan}}{\text{Averge values of objective without retrofit}}.$$

The results from Table 3-19 revealed that the three retrofit plans reduced the potential damage from all tornado events. The average direct economic loss was reduced by approximately 12% on all three plans. The average population dislocation was reduced by approximately 17%. Average functionality was improved over 80%, which was be considered significant improvement. However, the average values of each objective had small difference across three retrofit plans, which was verified by the boxplot (Figure 3-24, Figure 3-26, Figure 3-28) and density plots (Figure 3-25, Figure 3-27, Figure 3-29) of Δ_{loss}, $\Delta_{disl.}$, and Δ_{func}.

Figure 3-24 is a boxplot that describes the distribution of each plan on the improvement of direct economic loss (Δ_{loss}). Figure 3-25 is the density plot that describes how the data is distributed. Plan 1 and Plan 3 had similar distributions on the reduction in term of direct economic loss. We observed similar improvement of population dislocation ($\Delta_{disl.}$) and for building functionality difference ($\Delta_{func.}$). Three one-way ANOVA tests were conducted on the results from each objective across three retrofit plans. The p-value from the ANOVA on direct economic loss across the three plans is 0.78, which suggested the means of improvement of direct economic loss between three retrofit plans were the same. The p-value from ANOVA on improvement of population dislocation was 0.86, which suggested there was no significant statistical difference in term of improvement of population dislocation across three retrofit plans. Similarly, the ANOVA test of improvement building functionality of three plan also suggested that the three retrofit plans had same impact on improving building functionality (p-value = 0.95%).

To conclude, the three selected retrofit plans showed the ability to reduce the potential impacts from all tornado events on the potential impact of physical, social, and

economic systems. Despite there was no significant difference between different plans, the analysis conducted on this section illustrate to evaluation of the retrofit plans from the statistical aspect.

Table 3-18. Relationship of the results from data computing for case study

Retrofit Plan	Metrics	Results $h \in \{1,2,\dots,66\}$	Data for evaluating retrofit plans (Δ) $h \in \{1,2,\dots,66\}$	
No retrofit	Direct economic loss: $loss_h^0$ Population dislocation: $disl_h^0$ Building functionality: $func_h^0$			
Plan 1	Direct economic loss	$loss_h^1$	$loss_h^0 - loss_h^1$	Δ_{loss}
Plan 2		$loss_h^2$	$loss_h^0 - loss_h^2$	
Plan 3		$loss_h^3$	$loss_h^0 - loss_h^3$	
Plan 1	Population dislocation	$disl_h^1$	$disl_h^0 - disl_h^1$	$\Delta_{disl.}$
Plan 2		$disl_h^2$	$disl_h^0 - disl_h^2$	
Plan 3		$disl_h^3$	$disl_h^0 - disl_h^3$	
Plan 1	Building functionality	$func_h^1$	$func_h^0 - func_h^1$	$\Delta_{func.}$
Plan 2		$func_h^2$	$func_h^0 - func_h^2$	
Plan 3		$func_h^3$	$func_h^0 - func_h^3$	

Table 3-19. Expected values of three objectives of different retrofit plan

Retrofit Plan	Metrics	Average result across all tornadoes	Percentage of improvement
No retrofit	Average direct economic loss across all events: $27,107,750 Average population dislocation across all events: 1,988 Average building functionality across all events: 20.6%		
Plan 1	Direct economic loss	$23,722,944	12.5%
Plan 2		$23,904,574	11.8%
Plan 3		$23,647,699	12.8%
Plan 1	Population dislocation	1,633	17.9%
Plan 2		1,654	16.8%
Plan 3		1,635	17.7%
Plan 1	Building functionality	37.2%	81.1%
Plan 2		37.5%	82.6%
Plan 3		37.7%	83.2%

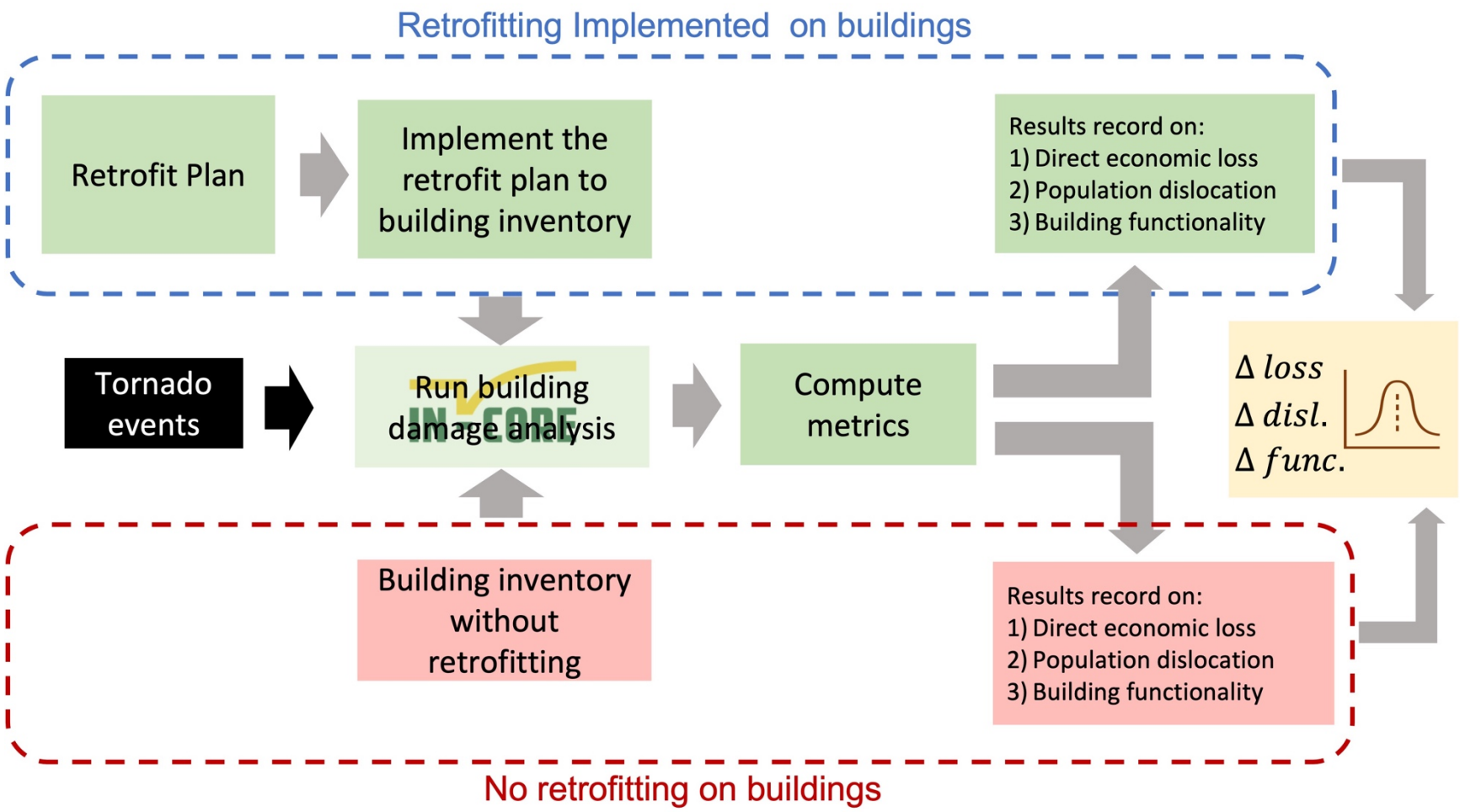

Figure 3-23. Flow chart of using IN-CORE to compute the improvement of three objectives between building inventory without retrofit plans and building inventory with retrofit plans across all tornado scenarios

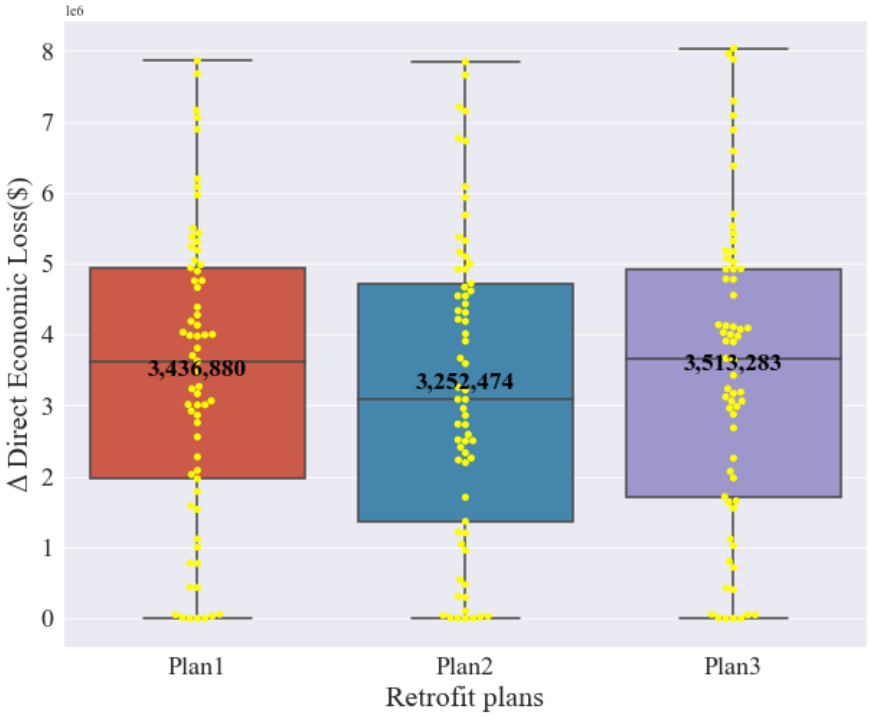

Figure 3-24. Boxplots of Δ_{loss} for three retrofit plans

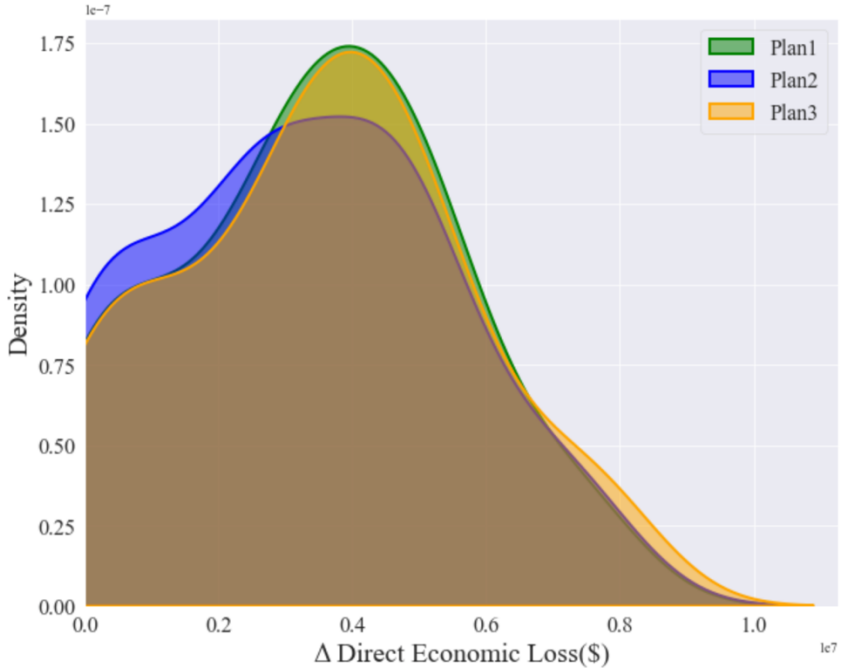

Figure 3-25. Density plots of Δ_{loss} for three retrofit plans

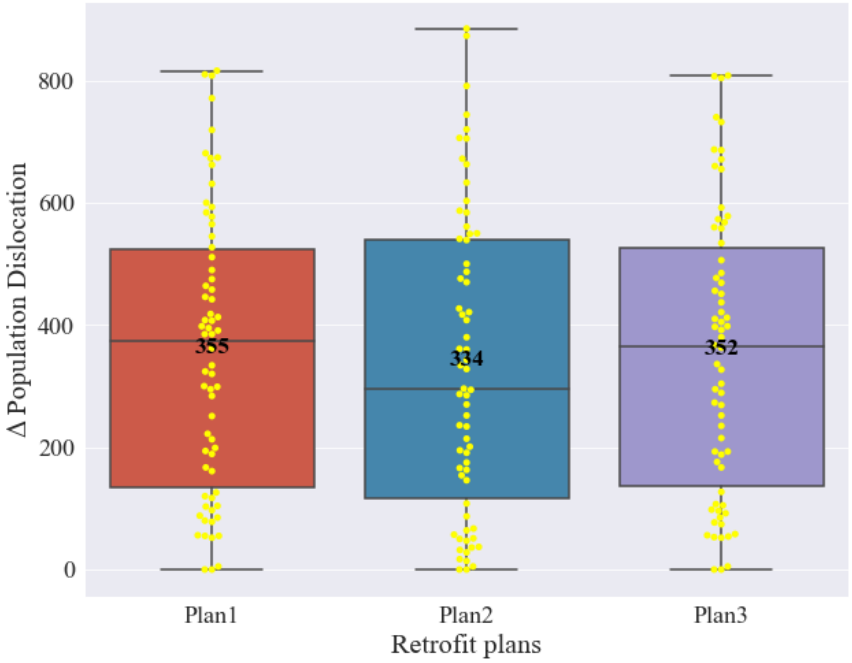

Figure 3-26. Boxplots of $\Delta_{disl.}$ for three retrofit plans

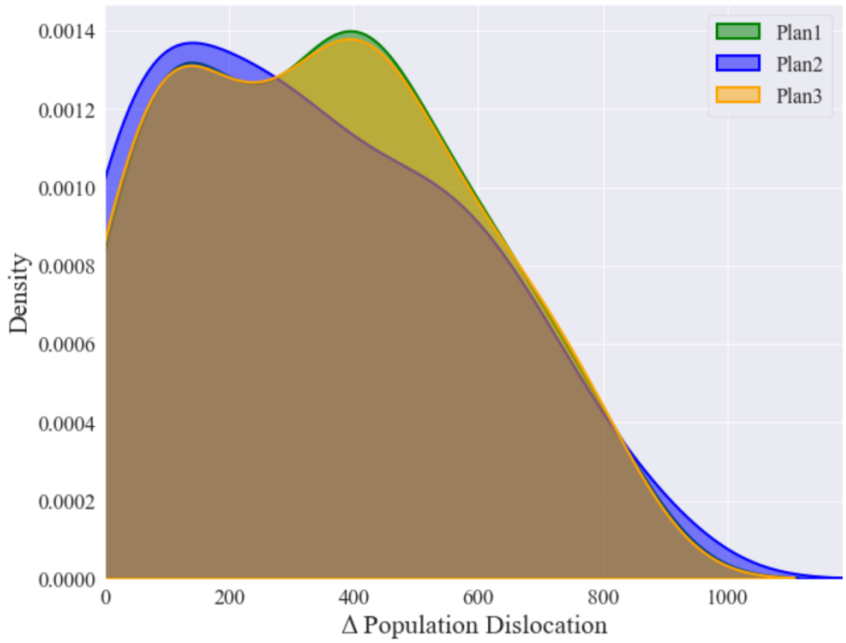

Figure 3-27. Density plots of $\Delta_{disl.}$ for three retrofit plans

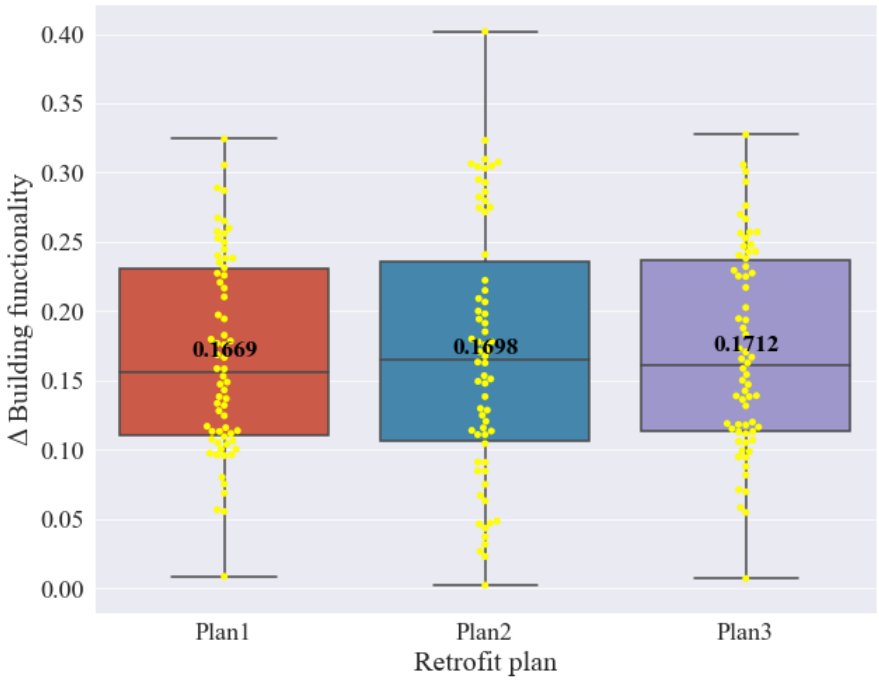

Figure 3-28. Boxplots of $\Delta_{func.}$ for three retrofit plans

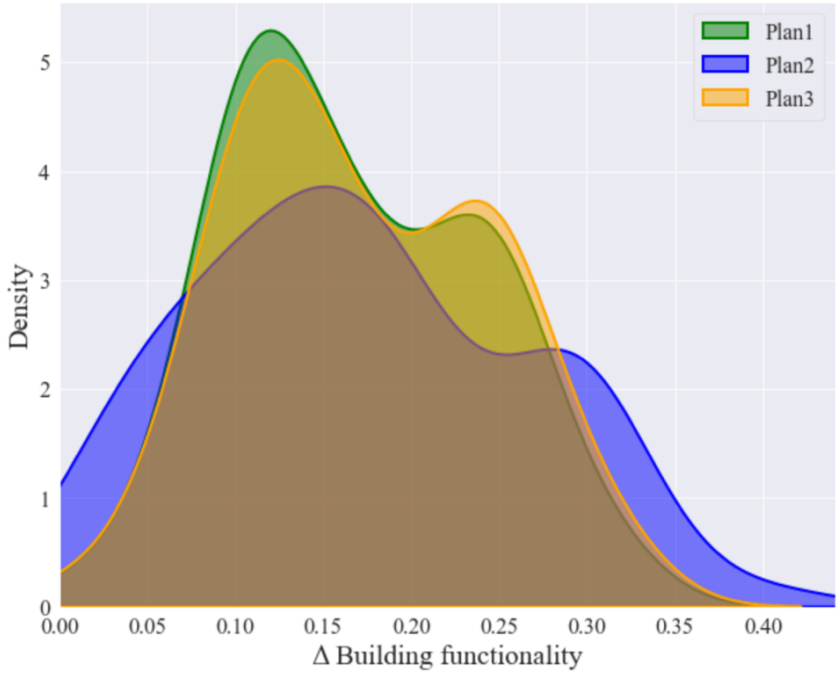

Figure 3-29. Density plots of $\Delta_{func.}$ for three retrofit plans

3.7 Summary

This chapter presents a study that an optimization model is implemented to provide mitigation plans on tornado mitigation at block levels considering the measurement of economic, social, and physical systems. The retrofit solutions are produced under the constraint of a limited budget that can be determined either by the actual needs or experimental purpose to evaluate the optimal solutions. The results analyses from this study can facilitate the decision-making from the following aspects:

- The tradeoff analysis allows comparing the retrofitting solutions with respect to the measurement of three competing objectives: economic, social, and physical systems of the community.
- By analyzing the granularity of retrofitting plans, we can identify the areas where can be considered most vulnerable in the community and to be mitigated with priority.
- The analysis based on the different budget levels allows the decision makers to allocate the budget on defined community resilience goals.
- Using the computational platform IN-CORE, we can apply simulated tornado events to the building inventory with the selected retrofit plan and evaluate the effectiveness of retrofit plans by comparing the values of three objectives before and after the retrofitting efforts.

4 A Hybrid Machine Learning and Optimization Modeling Application for Economic Analysis

4.1 Introduction

The occurrence of hazardous events, such as earthquakes, hurricanes, and tornadoes, is inevitable. The capacity of a country, state, city, or town to withstand and recover from such events is not: some communities are more resilient than others. The reasons, however, are not always easy to discern. Nor is it a trivial matter to determine how best to improve one's resilience to significant disruptive events. A community is a complex system of systems composed of a vast array of physical infrastructures (e.g., building portfolio, transportation systems, electric power networks, etc.) and the socio-economic systems they support. Due to this complexity, immediate impact from hazard events (e.g., initial damage to structures), may have indirect effects that propagate through the community (e.g., an important business sector may be negatively impacted causing job losses, population migration, and loss of tax revenue). Community resilience modeling and analysis is a highly interdisciplinary field of study.

Economic resilience refers to how well an economy responds to exogenous shocks. In the case of major hazard events, these shocks come in many forms, including an immediate loss of capital stock (e.g., capital goods, real capital, capital assets) due to building damage and /or their content losses. Input-Output (IO) economic models have been used by economists to study the indirect economic losses from disasters (Boisvert, 1992; Okuyama, et al., 2004; Wang, et al., 2017). However, to capture the realistic complexity in economic systems, researchers turn to more sophisticated modeling,

including the computable general equilibrium (CGE) model (West, 1995; Rose and Guha, 2004; Rose and Liao, 2005; Cutler and Davies, 2010).

The CGE approach provides a framework that allows for modeling price sensitivity and substitution possibilities for markets and economic agents, the importance of intermediate inputs, factors demand, tax payments, and imports, etc. Furthermore, the CGE model can provide estimates on the impact to various economic indicators such as domestic supply, employment levels, household income, and population migration due to hazard events (Cutler, et al., 2016a).

One method to mitigate such effects is developing and implementing a pre-disaster plan to protect the critical assets that support a community's economic well-being. The protection can be accomplished by retrofitting existing structures (e.g., buildings) associated with various economic sectors. Improving a structure's building code can improve its ability to withstand the effects of a hazard event, therefore reduce the expected loss of capital stock measured as direct damage and content loss. Such interventions may be costly in terms of time and money. An optimal allocation of a community's limited resources to best enhance its economic resiliency is desirable. Zhang and Nicholson (2016) considered a closely related problem. Their work determined an optimal allocation of resources to retrofit buildings to higher building code levels using mathematical program to minimize two competing objectives of expected direct loss due to damage and population dislocation. However, a critically important element is missing. That is, the direct damage is only one component of the economic impact. Given the nature of a community, one damage profile across the building portfolio may have an entirely different effect on total domestic supply than another damage distribution of equal magnitude.

Additionally, the long-term indirect effects, such as the loss of commerce, industry, and employment, must be considered. This complexity can be captured using a CGE model.

Mathematically, a CGE model is expressed as a simultaneous system of nonlinear equations. Unfortunately, the size of the model in terms of variables and equation, as well as the various critical parameters values that must be estimated (e.g., elasticities of substitution), can make the approach appear as a "black box" to researchers less familiar with the technique (Wing, 2004). Ideally, an optimal mitigation allocation of resources would directly minimize the effects of the key economic indicators available from the CGE model. However, due to the intractability of the approach, it cannot be easily incorporated into a traditional mathematical program.

4.2 Highlights

This study introduces a surrogate CGE model to effectively bridge this gap between the CGE outputs and a mathematical program optimization modeling paradigm (Figure 4-1). We discuss desirable characteristics of such a surrogate model and use a case study on Joplin, MO. We evaluate multiple machine learning approaches to construct surrogates based on CGE data that predict the hazard impacts on domestic supply, employment, migration, and household income. A selected ML model is used to predict the economic impact with a conditional wind speed 135 mph in the city of Joplin. A multi-objective optimization model is designed to demonstrate the possibility to connect CGE model with linear programming to link the economic impact with the retrofitting decision-making.

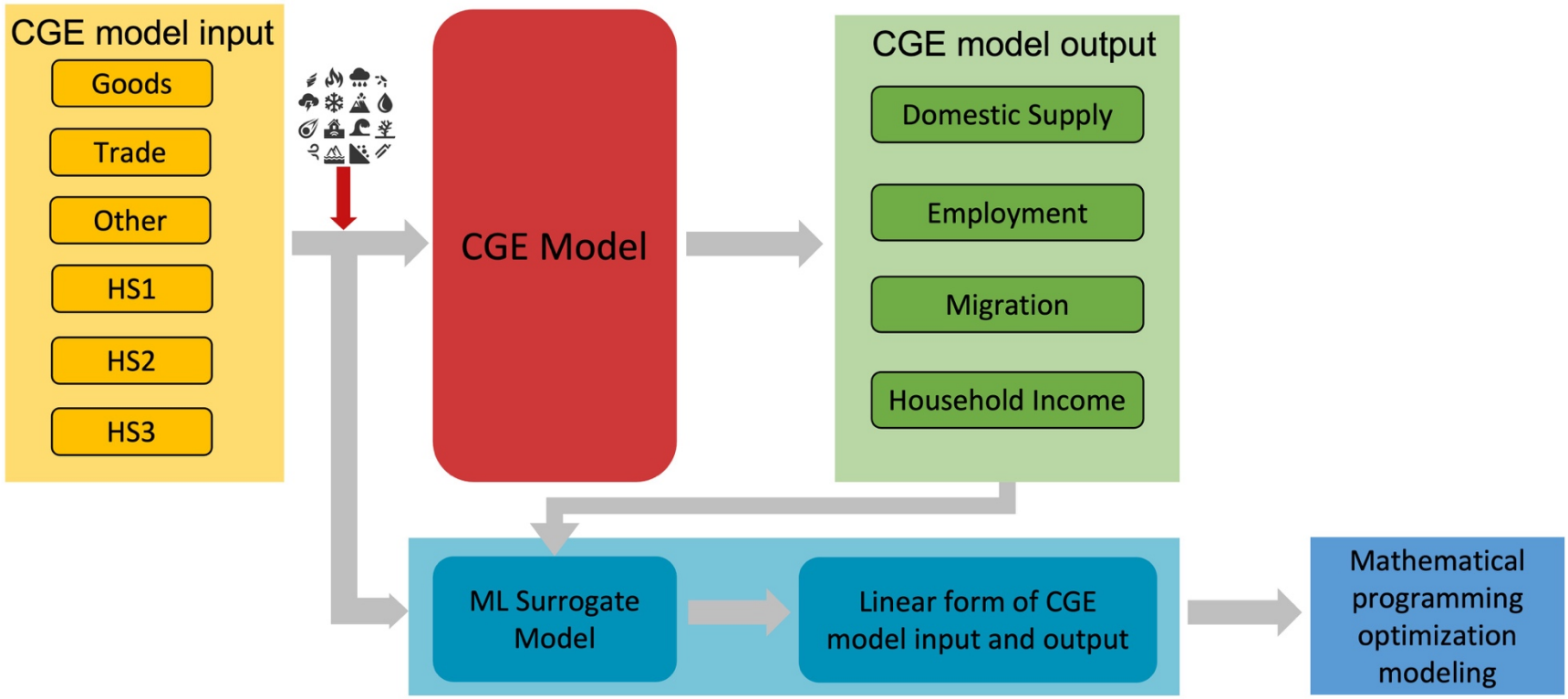

Figure 4-1. Flow chart of relationship between the CGE model and Surrogate mode

4.3 Approach

The CGE surrogate of interest is one that would be amenable to an optimization model for the building retrofits in a similar fashion to the work in Zhang and Nicholson (2016) to minimize the negative impact on community domestic supply. In this case, several factors should be considered, which are model-based form, input and decision variable consistency, functional form, and meaningfulness.

4.3.1 Model-based form

There are various machine learning (ML) approaches to choose from to estimate the economic value generated by the CGE model. However, certain approaches are not appropriate in light of the stated goal to build a surrogate model and incorporate it into a mathematical program.

Supervised learning techniques that produce a model with functional forms may be preferable. Lazy learning methods, such as the k-nearest neighbors algorithm (Altman, 1992) and local weighted regression (Cleveland and Devlin, 1988), do not produce functions that generalize inputs to expected outcomes but defer generalization of the training data until an explicit request for information is received. This results in potentially a large amount of memory required to store the training data (Bhatia, 2010). Additionally, unlike most eager learners (e.g., ordinary least squares regression, decision trees, neural networks, etc.), more effort is required for prediction than is required for training.

4.3.2 Input and decision variable consistency

There must be a consistency between the CGE model inputs, input features for the ML surrogate model, and decision variables in the optimization model. For example, if the CGE model considers shocks to capital stock at the sector level, then the input features for the surrogate model cannot be more granular than this. The decision variables in the optimization model must also ultimately affect these shock values. Retrofitting buildings can be an appropriate decision variable if the buildings are known to contribute to a given economic sector, and the retrofit actions will reduce (or at least probabilistically reduce) the impact of the capital shock.

Additionally, the scales of input features must be consistent with their usage in the optimization model. If the features are range-scaled prior to supervised learning, then the decision variables in the optimization model must be operated on the same scale.

4.3.3 Functional form

Besides desiring an accurate, model-based ML approach with consistent input features, the specific form of the model is also an important consideration. A linear model based on the ordinary least squares (OLS) regression could support a linear or integer programming model. This is also conditional on the feature construction and transformations used. For instance, to be consistent with linear programming, products and ratios of features and box-cox transformations cannot be used in order to keep the consistency between CGE mode, surrogate model, and optimization model.

Highly nonlinear techniques such as neural networks or support vector machines with a radial basis function kernel, would produce surrogate models that could only be

incorporated into nonlinear programs (unless they themselves were approximated) or require the use of advanced metaheuristics to produce near-optimal solutions. Other nonlinear approaches, such as decision trees, random forests, and gradient boosted trees, require the implementation of rule-based logic and would like to rely on metaheuristics approaches on the optimization side.

4.3.4 Meaningfulness

Since the functional form of the surrogate model will be used directly in an optimization model, it is important that the model is not simply predictive but also meaningful for this purpose. For instance, an Ordinary Least Squares (OLS) model with highly correlated input features relating to capital shock loss of economic sectors may have excellent predictive ability. However, due to the inflated variance, the parameter estimates themselves will be nearly meaningless. It is important to ensure that in such cases, the parameter estimates are directionally correct, and their relative magnitude is valid. Otherwise, the optimization model could be incentivized irrationally to increase expected damage to a given economic sector.

Additionally, in a method such as the least absolute shrinkage and selection operator (LASSO), one of two highly correlated variables might be included in the final model and other excluded. While the predictive accuracy could still be high, this is problematic from the perspective of the optimization model. There would be no reason to allocate resources to the economic sector eliminated from the surrogate model, even if doing so would produce nearly identical results in a more cost-effective manner.

4.4 Application

4.4.1 Joplin, MO

Joplin, MO, is located in Jasper and Newton counties in the Southwestern corner of state Missouri. The city's population is 50,073, according to the 2018 census. The largest industries in Joplin are health care & social assistance, manufacturing, and retail trade. Approximately 24,100 people are employed, and the median household income is $45,449 (Data USA).

For the CGE model used in this analysis, there are three household groups (i.e., HS1, HS2, HS3) distinguished by income levels who demand goods and services. The economic sectors are partitioned into Goods, Trade, and Other. The natural hazard shocks to the economy are represented as percent losses of the capital stocks at the sector level. Based on these six inputs, the CGE model computes the expected impact of Joplin's domestic supply, employment, migration, and household income.

4.4.2 Data Preparation

To train the ML surrogate models. 233 instances of potential tornado damage to Joplin, MO, are generated. The instances are designed based on likely tornado scenarios. These instances were randomized to some extent to provide variability for supervised learning methods. Using these 233 instances as input data that are percent losses of the capital stocks on Goods, Trade, Other, HS1, HS2, and HS3, CGE model provides the results on potential impact on domestic supply, employment, migration, and household income as output.

Figure 4-2 provides the analysis of the multicollinearity between the input features. The correlation between different features is not high. Therefore, OLS regression can be an option. Besides OLS, other techniques such as ridge regression that, LASSO, and elastic net regression that combines L1 and L2 regularization penalties to the loss function, can be considered as candidate models in the case that multicollinearity exists among the input features. Moreover, with the regularization method applied to the ML models, the complexity of the model can be reduced by coefficients shrinkage.

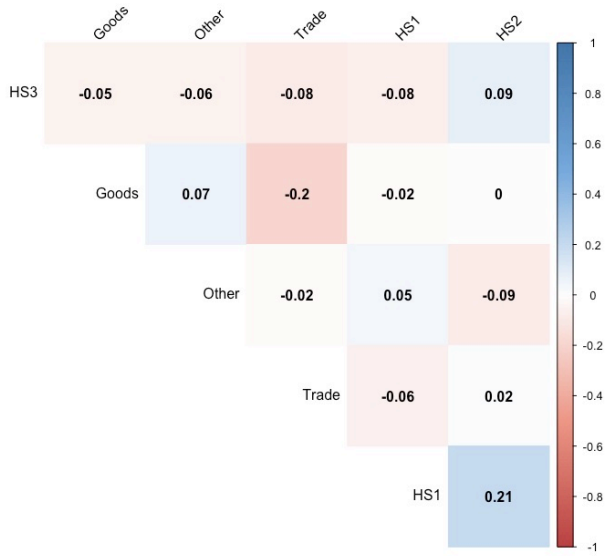

Figure 4-2. Correlation between input features

4.4.3 Model analysis

OLS is a type of linear least squares method to form a linear relationship between the observed independent variables and dependent variables. If the relationship is linear, a hyperplane can be drawn to model their relationship. The independent variables in this study encompass six economic sectors for Joplin, MO, including *Goods* (x_{Goods}), *Trades*

(x_{Trades}), *Other* (x_{Other}), *HS1* (x_{HS1}), *HS2* (x_{HS2}), *HS3* (x_{HS3}). The goal is to model the linear relationship to predict the economic impact on domestic supply (y_{des}), employment (y_{emp}), migration (y_{mig}), and household income (y_{hhinc}) from potential tornado hazard, which will be used as the coefficient for the objectives in the optimization model. The relationship can be is expressed as:

$$y_{sector} = a_{sector} + \beta_1 x_{Goods} + \beta_2 x_{Trades} + \beta_3 x_{Other} + \beta_4 x_{HS1} + \beta_5 x_{HS2} + \beta_6 x_{HS3} . \quad (4\text{-}1)$$

Ridge, LASSO, and elastic net regression are forms of penalized regression and can be explained by discussing the objective shown as:

$$minimize \sum_{i=1}^{n} (y_i - \hat{y}_i)^2 + \lambda \left(\alpha \sum_{j=1}^{p} |\beta_j| + (1-\alpha) \frac{1}{2} \sum_{j=1}^{p} \beta_j^2 \right) . \quad (4\text{-}2)$$

Assuming there are n observations and p input features, the left-most term in Equation (4-2) corresponds to the OLS objective of minimizing the sum of the squared difference between the actual outcome values y and the predicted values $\hat{y}$. The next terms are penalty is computed based on two parameters: the regularization parameter, $\lambda \geq 0$, and the mixing parameter, $0 \leq \alpha \leq 1$. If α is set to 1, Equation (4-2) is equivalent to the LASSO regression objective. If α is set to 0, then the result is the ridge regression objective. For any other value of α, the result is elastic net regression that effectively blends ridge and LASSO regression. As the value of λ increases, the coefficients will be smaller than then

ought to be in order to get the best predictive results, in LASSO, the coefficients will shrink to 0, but for ridge, the coefficients will not shrink to 0.

The dataset is partitioned into training and test data with split rate 75% (training set) and 25% (test set). Using 10-fold cross-validation and 1-SE rule on training data, we find the best values of λ for ridge regression, elastic net regression, and LASSO to build final models to predict the potential damage for domestic supply, employment, migration, and household income, respectively. The α values for elastic net regression are found through 10-fold cross-validation. The hyperparameter setting for ridge regression, elastic net regression, and LASSO is provided in Table 4-1. The results described in Table 4-2 are the prediction of test data. Overall, the predicted results on domestic supply and employment are highly closed to the actual values (Adjusted R^2 aprroximately 99%), and the adjusted R^2 on migration and household income are over 80%. The performance from OLS regression surpasses the performance from the Ridge, Elastic net regression, and LASSO on prediction of Domestic Supply, Employment, and Household Income. However, LASSO outperforms on prediction of migration. Figure 4-3 – Figure 4-6 visually provide results on all four models. Predicted domestic supply and employment are very close to the actual values.

Table 4-3 provides the coefficients of the ML models. For most of the features, the coefficients across all four models have the same sign and similar magnitude. With regularization techniques, the input feature *Other* sector shows less importance for prediction on migration damage. Moreover, the coefficient of *Other* and *HS3* sectors are shrinking from the Elastic Net and LASSO model to predict the damage on household income. All four models reveal that the damage estimates on domestic supply, employment,

migration, and household income should be revised downward if the economic area is severely damaged.

A subject-matter expert in CGE modeling should be engaged to help determine if one model is more intuitive than the others. The evaluation based on adjusted R^2 and RMSE reflects subtle differences from all four models. The linear model with regularization technique can be a better candidate for the dataset containing multicollinearity and providing the importance of input features.

Table 4-1. Model hyperparameter choice

	Ridge	Elastic Net	LASSO
Domestic Supply	λ = 7.861414 upper.limits = 0 Cross-validation fold =10	α = 0.0246 λ = 0.0285 upper.limits = 0 Cross-validation fold =10	λ = 0.2457 upper.limits = 0 Cross-validation fold =10
Employment	λ = 69.25332 upper.limits = 0 Cross-validation fold =10	α = 0.0368 λ = 0.397 upper. limits = 0 Cross-validation fold =10	λ = 2.375714 upper. limits = 0 Cross-validation fold =10
Migration	λ = 23.65865 upper.limits = 0 Cross-validation fold =10	λ = 3.73 α = 0.569 upper.limits = 0 Cross-validation fold =10	λ = 4.753574 upper. limits = 0 Cross-validation fold =10
Household Income	λ = 1.369627 upper. limits = 0 Cross-validation fold =10	λ = 0.0285 α = 0.0246 upper. limits = 0 Cross-validation fold =10	λ = 0.5277898 upper. limits = 0 Cross-validation fold =10

Table 4-2. Linear models evaluation

	OLS Regression		Ridge		Elastic Net		LASSO	
	Adjusted R^2	RMSE	Adjusted R^2	RMSE	Adjusted R^2	RMSE	Adjusted R^2	RMSE
Domestic Supply	0.9946	6.1641	0.9908	8.0050	0.9943	6.2665	0.9943	6.3012
Employment	0.9902	78.0178	0.9869	90.3332	0.9900	78.8284	0.9899	79.1826
Migration	0.8875	87.4624	0.8772	91.3516	0.8884	87.4101	0.8881	87.16170
Household Income	0.8054	7.2156	0.8015	7.2880	0.8053	7.3364	0.8001	7.3246

Table 4-3. Coefficients from ML model candidates

Dependent variables	Sector	Regression Model Coefficients			
		OLS Regression	Ridge	Elastic Net	LASSO
Domestic Supply	(Intercept)	1161.490	1102.25343	1102.00985	1162.31507
	Goods	-110.021	-100.88081	-102.50165	-111.37803
	Trades	-39.774	-32.47595	-31.36060	-37.35812
	Other	-100.562	-94.17968	-94.38244	-101.58747
	HS1	-378.452	-348.65907	-351.05286	-371.31835
	HS2	-497.933	-474.19279	-472.52047	-508.05297
	HS3	-40.466	-32.47595	-36.57416	-39.04256
Employment	(Intercept)	9483.13	9009.8727	9407.3737	9400.1688
	Goods	-197.70	-176.1048	-181.9786	-177.6828
	Trades	-155.14	-127.1396	-137.1121	-132.3264
	Other	-404.02	-364.9699	-390.7885	-387.9615
	HS1	-4118.97	-3869.2068	-4098.8287	-4101.4132
	HS2	-4237.20	-3980.8549	-4220.2826	-4224.1646
	HS3	-462.77	-426.2697	-445.6315	-441.4221
Migration	(Intercept)	2464.203	2342.75796	2339.11150	2352.00454
	Goods	-58.593	-53.40886	-30.87602	-29.05218
	Trades	8.245	.	.	.
	Other	-143.732	-135.72206	-113.59959	-111.82292
	HS1	-1627.725	-1506.26080	-1576.61756	-1597.38501
	HS2	-549.580	-531.57981	-520.69134	-520.98200
	HS3	-123.671	-107.11697	-87.24081	-86.86515
Household Income	(Intercept)	187.684	178.963803	173.34545	173.133374
	Goods	-13.772	-12.755443	-10.54442	-9.963842
	Trades	-2.029	-1.432725	.	.
	Other	-18.258	-17.057216	-15.25856	-14.743473
	HS1	-86.820	-81.809047	-82.58124	-83.294189
	HS2	-65.315	-62.013338	-62.05967	-62.165685
	HS3	-3.360	-2.875389	.	.

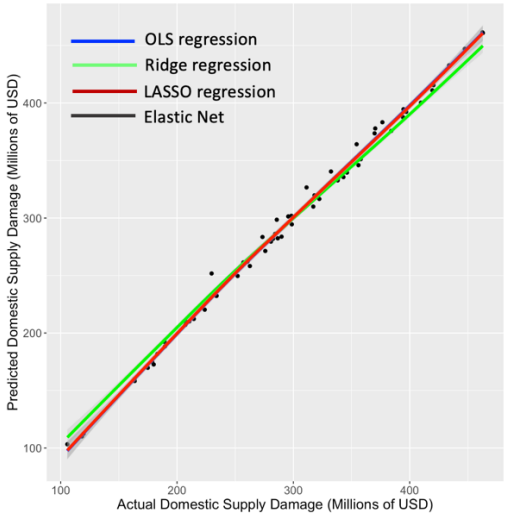

Figure 4-3. Predicted vs. Actual domestic supply damage

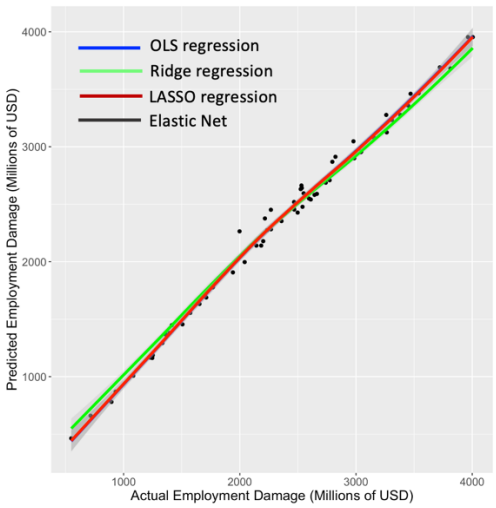

Figure 4-4. Predicted vs. Actual Employment Damage

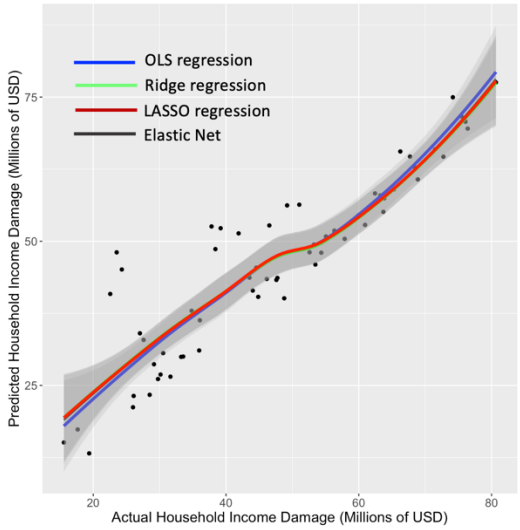

Figure 4-5. Predicted vs. Actual Household Income Damage

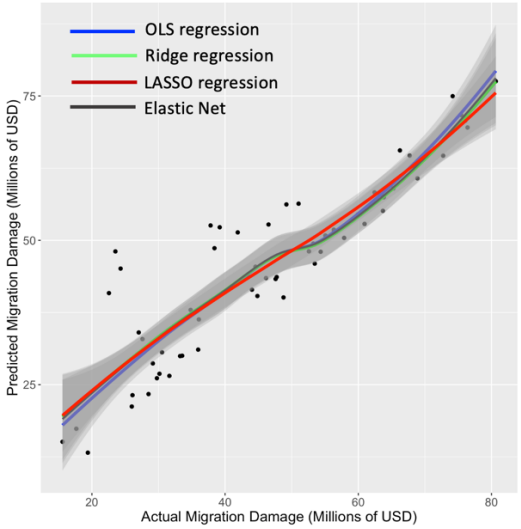

Figure 4-6. Predicted vs. Actual Migration damage

4.5 Connection to optimization models

The main contribution of this study is to reverse-engineer of CGE model to produce a linear relationship between the CGE inputs and outputs. If we know $d_j = f(x_j)$ is a linear function relating the expected damage to a set of decision variables x_j, the objective is complete as described in Figure 4-7. One of the benefits of this connection is that we can efficiently predict the appropriate coefficients of the objective functions of the optimization model with different hazard scenarios. Another benefit of utilizing this connection is that the decision-making of the optimization model can be traced back to different economic sectors, which provides multi-layer decision analysis.

4.5.1 Mathematical model

Model input

This model is the second application of the framework introduced in Chapter 2. The goal of this model is to minimize the potential economic impact of the economy of Joplin on tornado threat. The set $\mathcal{Z}$ in the model is defined as the economic sectors: Goods, Trade, Other, HS1, HS2, and HS3. Building type and retrofit strategy use the same input data from Chapter 3, which are residential building type $\mathcal{S}$ (single-family and multi-family building), and three retrofitting strategies (Table 3-3). After missing values were removed from the dataset that provides the mapping between the individual building and each sector, the final input data are as shown in Table 4-4. We assume that there is no prior retrofitting on the buildings in Joplin, which explains that all the values in the column "Strategy $k \in \mathcal{K}$" set to $k = 0$. The column "Building Counts b_{ijk}" provides the total number with building type

$j \in \mathcal{S}$ at each sector $i \in \mathcal{Z}$ with strategy $k \in \mathcal{K}$. For example, there are a total of 17,157 single family buildings in sector HS1 that indicate that majority of single-family buildings are accounted in lower income house service.

Retrofitting strategies cost $SC_{ijkk'}$ is computed by using the input data from Chapter 3. However, the data provided on Chapter 3 are calculated on block group level. To computer the retrofitting cost on sector level, we aggregated all buildings in the same building type $j \in \mathcal{S}$ for block group levels to each sector, which is as shown in Table 4-5. The column "Strategies Cost $SC_{ijkk'}$" is the expected retrofit cost for a building enhanced from the initial strategy $k \in \mathcal{K}$ to the final strategy $k' \in \mathcal{K}$ in the sector Goods and Trade. For instance, the average cost to retrofit a single-family building from the strategy 0 to the strategy 3 is \$35,301. To compute total retrofit costs of all single-family buildings retrofitted from the strategy 0 to the strategy 3 is \$4,447,926 that is the product of \$35,301 and 126 (from Table 4-4).

Table 4-4. Building stock input data file

Sector $i \in \mathcal{Z}$	Building type $j \in \mathcal{S}$	Strategy $k \in \mathcal{K}$	Building Counts b_{ijk}
Goods	Single-family	0	126
Goods	Multi-family	0	11
Trade	Single-family	0	19
Trade	Multi-family	0	2
Other	Single-family	0	83
Other	Multi-family	0	4
HS1	Single-family	0	17,157
HS1	Multi-family	0	6
HS2	Single-family	0	3,470
HS2	Multi-family	0	27
HS3	Single-family	0	135
HS3	Multi-family	0	28

Table 4-5. Strategy cost $SC_{ijkk'}$ data example file

Sector $i \in \mathcal{Z}$	Building type $j \in \mathcal{S}$	Initial Strategy $k \in \mathcal{K}$	Final Strategy $k' \in \mathcal{K}$	Strategies Cost $SC_{ijkk'}$ ($)
Goods	Single-family	0	0	0
Goods	Single-family	0	1	11,401
Goods	Single-family	0	2	17,316
Goods	Single-family	0	3	35,301
Goods	Multi-family	0	0	0
Goods	Multi-family	0	1	22,483
Goods	Multi-family	0	2	39,033
Goods	Multi-family	0	3	70,063
Trade	Single-family	0	0	0
Trade	Single-family	0	1	7,269
Trade	Single-family	0	2	11,040
Trade	Single-family	0	3	22,508
…	…	…	..	…

The coefficients of the mathematical model are defined by the mathematical form provided from the ML models. If we select the LASSO model as the final model to predict the potential damage on domestical supply (α_{ijk}^1), employment (α_{ijk}^2), migration (α_{ijk}^3), and household income (α_{ijk}^4), the parameters can be expressed as:

$$\alpha_{ijk}^1 = 1162 - 111h_{Goods} - 37h_{Trades} - 101h_{Other} - 371h_{HS1} - 508h_{HS2} - 39h_{HS3}\ , \quad (4\text{-}3)$$

$$\alpha_{ijk}^2 = 9400 - 178h_{Goods} - 132h_{Trades} - 388h_{Other} - 4101h_{HS1} - 4224h_{HS2} - 441h_{HS3}\ , \quad (4\text{-}4)$$

$$\alpha_{ijk}^3 = 2352 - 29h_{Goods} - 0h_{Trades} - 112h_{Other} - 15971h_{HS1} - 521h_{HS2} - 87h_{HS3}\ , \quad (4\text{-}5)$$

$$\alpha_{ijk}^{4} = 173 - 10h_{Goods} - 0h_{Trades} - 15h_{Other} - 83h_{HS1} - 62h_{HS2} - 0h_{HS3}. \quad (4\text{-}6)$$

In this study, we applied the same assumption stated in Chapter 3, which is that we assume that tornado events could occur any sector with the equal probability. We applied wind speed 135 mph on all buildings in the city Joplin to calculate the damage on domestic supply, employment, migration, and household income. First, wind speed 135 mph load was applied on all buildings without any retrofit effort, which is $k = 0$. Through IN-CORE, we calculated the building damage and ran CGE analysis according to the building damage caused by 135 mph wind speed. CGE module produced the capital remaining on six sectors after the shock from 135 mph wind speed on all buildings with strategy $k = 0$. Given the capital remaining on six sectors, which are h_{Goods}, h_{Trades}, h_{Other}, h_{HS1}, h_{HS2}, and h_{HS3} in Equation (4-3) – (4-6), we predicted the economic loss on domestical supply (α_{ijk}^{1}), employment (α_{ijk}^{2}), migration (α_{ijk}^{3}), and household income (α_{ijk}^{4}) at strategy $k = 0$. We computed these four coefficients using the same method at strategy 1, strategy 2, and strategy 3. The example of final data file is presented in Table 4-6.

Table 4-6. Example data file of coefficients of objects

Sector $i \in \mathcal{Z}$	Building type $j \in \mathcal{S}$	Strategy $k \in \mathcal{K}$	Building Counts b_{ijk}	α_{ijk}^{1}	α_{ijk}^{2}	α_{ijk}^{3}	α_{ijk}^{4}
Goods	Single-family	0	126	892	7,529	1,829	136
Goods	Single-family	1	0	892	7,529	1,829	136
Goods	Single-family	2	0	652	5,300	1,331	99
Goods	Single-family	3	0	649	5,265	1,326	99
HS1	Single-family	0	17,157	892	7,529	1,829	136
HS1	Single-family	1	0	892	7,529	1,829	136
HS1	Single-family	2	0	652	5,300	1,331	99
HS1	Single-family	3	0	649	5,265	1,326	99
…	…	…	…	…	…	…	…

The mathematical formulation of the model is presented in Table 4-7.

Table 4-7. Mathematical formulation of the model

Description	Equations	Eq.No.
Input Parameter	Set of unique economic sector $i \in \mathcal{Z}$ Set of building types $j \in \mathcal{S}$ Set of retrofitting strategies $k \in \mathcal{K}$ Domestic supply coefficient: α_{ijk}^{1} Employment coefficient: α_{ijk}^{2} Migration coefficient: α_{ijk}^{3} Household Income coefficient: α_{ijk}^{4} Retrofitting cost: $SC_{ijkk'}$ Retrofitting budget: B	(4-3) (4-4) (4-5) (4-6)
Decision Variable	The total number of buildings after the mitigation: $\boldsymbol{x_{ijk}}$ the total number of buildings retrofitted from strategy k to k': $\boldsymbol{y_{ijkk'}}$	
Objective 1 Minimize domestic supply loss	$\min \sum_{(i,j,k) \in \mathcal{T}_1} \alpha_{ijk}^{1} x_{ijk} \quad n = 1$	(2-7)
Objective 2 Minimize employment loss	$\min \sum_{(i,j,k) \in \mathcal{T}_2} \alpha_{ijk}^{2} x_{ijk} \quad n = 2$	(2-7)
Objective 3 Minimize migration	$\min \sum_{(i,j,k) \in \mathcal{T}_3} \alpha_{ijk}^{3} x_{ijk} \quad n = 3$	(2-7)
Objective 4 Minimize household income loss	$\min \sum_{(i,j,k) \in \mathcal{T}_4} \alpha_{ijk}^{4} x_{ijk} \quad n = 4$	(2-7)
Constraint 1 Retrofitting budget constraint	$\sum_{(i,j,k,k') \in \mathcal{U}} SC_{ijkk'} y_{ijkk'} \leq B$	(2-2)
Constraint 2 Building constraint of final state after intervention	$x_{ijk} = \sum_{k':\,(i,j,k',k) \in \mathcal{U}} y_{ijk'k} + b_{ijk} - \sum_{k':\,(i,j,k,k') \in \mathcal{U}} y_{ijkk'}$ $\forall (i,j,k) \in \mathcal{T}.$	(2-3)
Constraint 3 Building number balance constraint	$\sum_{k:\,(i,j,k) \in \mathcal{T}} x_{ijk} = \sum_{k:\,(i,j,k) \in \mathcal{T}} b_{ijk} \quad \forall i \in \mathcal{Z}, \forall j \in \mathcal{S}.$	(2-4)
Constraint 4 Non-negative constraint	$x_{ijk} \geq 0 \quad \forall (i,j,k) \in \mathcal{T}$	(2-5)
Constraint 5 Non-negative constraint	$y_{ijkk'} \geq 0 \quad \forall (i,j,k,k') \in \mathcal{U}.$	(2-6)

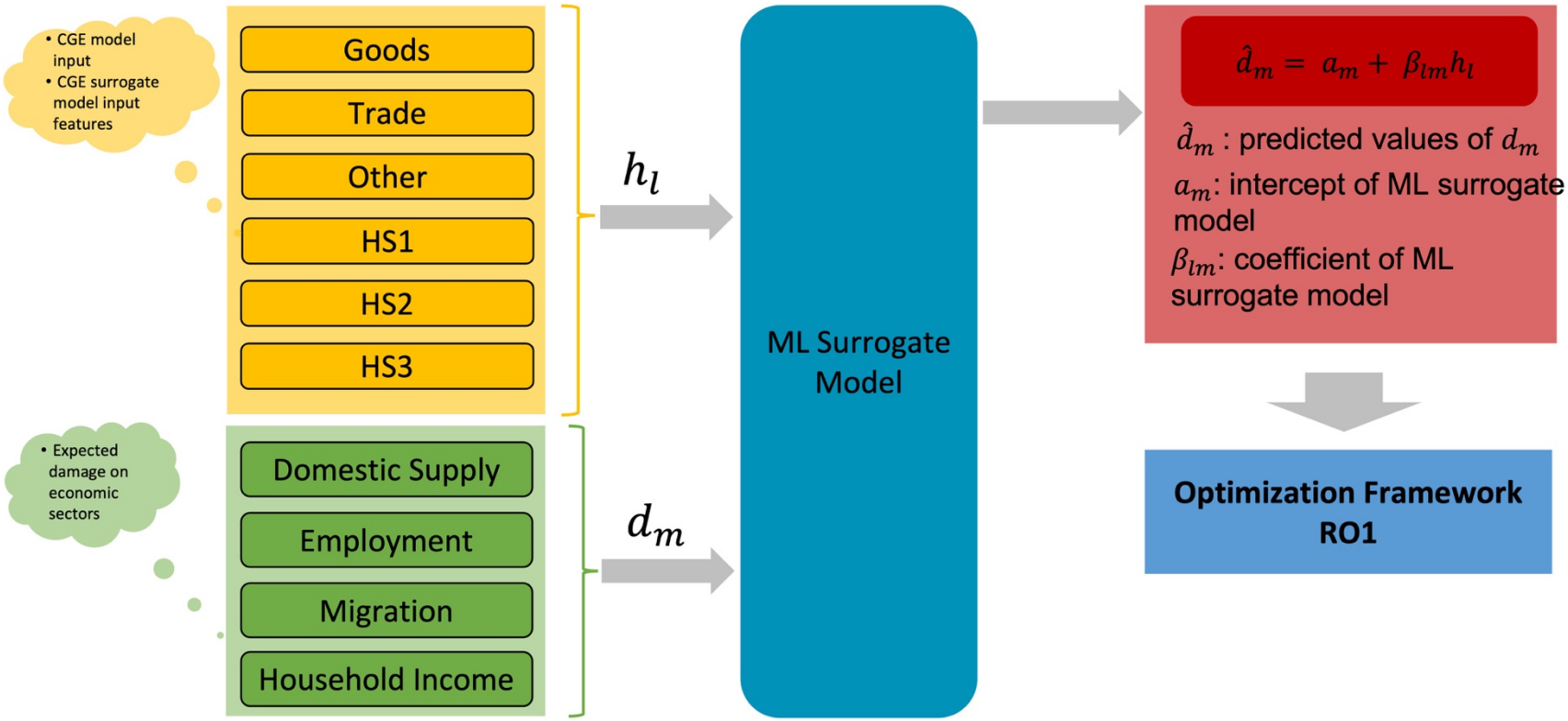

Figure 4-7. Flow chart of connection between surrogate model and optimization model

Model output

The mathematical model is coded in Python using Gurobi solver. Budget B represents the available fund for retrofitting plan. In this study, we calculated the maximum budget by retrofitting all the buildings to the highest strategy (Strategy 3) and apply fracture of the maximum budget as the retrofitting budget constraint (Equation (2-2)). However, from the most restrict budget (0.5% of maximum budget) to the maximum budget (100% of maximum budget), the results from the model showed that the four objective functions didn't have the competing relationship as we expected from multi-objective optimization model.

4.6 Summary

The potential for the CGE model to inform economic resilience decision-making is essential. One issue, however, is that the models can be hard to interpret and accommodate in traditional optimization paradigms such as integer linear programming. To circumvent this obstacle, we propose supervised learning to develop surrogate models that are amenable to optimization approaches. We discuss several characteristics of potential surrogate models that should be addressed if they are to be incorporated into mathematical program.

Using a case study based on a high fidelity CGE model developed by experts, we devise four appropriate machine learning models to act as a surrogate. All four models perform at a highly accurate level, and any of them could be chosen for optimization purposes: each has a linear functional form with meaningful parameter values and produces

reasonable accurate predictions for realistic tornado damage scenarios and expected impacts to domestic supply, employment, migration, and household income. Furthermore, the input features are logically aligned with the mitigation intervention strategy to be implemented. That is, building retrofits directly relate to protecting capital impact across economic sectors. Using the case study of Joplin, MO, we demonstrate that how to use the predicted results of ML model to design an optimization model from the proposed framework in Chapter 2. This model validates that the proposed framework can be adjusted by the actual need from the user. For example, in the case study, the granularity of decision level is the economic sectors in Joplin, and there is a total of four objective functions in the model. Despite the result from the case study did not show the competing effect of the four objectives, we demonstrate the process of developing an optimization model based on the research needs from the framework introduced in Chapter 2.

The ML modeling approach provides an effective way to intelligently use data to adjust this trend based on the complex nuances from the CGE model. We fully expect the integration of CGE surrogate models with optimization modeling to drive higher quality decision-making for community resilience.

5 Conclusions and future work

5.1 Contribution

This dissertation aims to develop a generic and hazard agnostic multi-objective optimization model to produce mitigation strategies to reduce potential impact from natural hazards and provide decision-making support for decision makers of the communities. The research goals listed in Chapter 1.2 are accomplished by developing a generalized optimization model that integrates multi-facet systems of a community in one framework, implementing the proposed framework on tornado mitigation, and developing a surrogate model to reverse engineer the CGE model and connect the CGE model with optimization model.

First, the newly introduced optimization framework is a well-defined framework that allows flexibility that is defined by decision makers. Such flexibility includes: (1) Level of decision granularity can be defined according to needs of the decision makers, ranging from PUMAs, census blocks to parcel, economic sectors, and building level. (2) The community-defined resilience objective functions are not bounded by the number of the objective or the type of objective. The decision makers can determine the objectives that fit the interests of the community. (3) The set of solutions returned from the model, including Pareto optimal solutions and objective functions, provides rich information to evaluate the solutions and facilitate the decision-making quantitively. (4) The framework is not limited to a specific type of hazard. If the input of the framework meets the requirement, the model can be applied to any hazard type. The allowed flexibility in this framework is not reflected in any existing multi-objective optimization framework of

community resilience. Furthermore, the availability of mitigation funds can be adjusted to facilitate decision-making and resource allocation.

Second, the city of Joplin, MO, is used as a testbed to illustrate the methodology by using three competing objectives to measure the impact on social, economic, and physical systems on tornado mitigation. Three objectives (i.e., direct economic loss, population dislocation, building functionality) are computed as the conditional expected value of a building given an impact with 135 mph wind speed. The resulting analysis reveals that: (1) Priority analysis can help identify the vulnerable areas of the community that can be prioritized. (2) Tradeoff analysis allows evaluating selected objectives between different retrofit plans quantitatively. (3) Resources analysis increases the array of options of decision-making by exploring different budget options. 66 tornado events simulated through IN-CORE are applied to three selected retrofitting plans. The impact on three objectives shows reduction from all retrofitting plans. By implementing selected retrofit plans, the community will expect less damage to economic, social, and physical systems from tornado threats.

Finally, ML models are designed as surrogate model of the CGE model to predict potential damage on the economic system of a community from a disruptive event. The surrogate model uses the input data from the CGE model as the input features and predicts the output of the CGE model. By producing a mathematical formation between the CGE inputs and outputs, the ML models allow the non-CGE expert to interpret the correlation between economic sectors and economic damage from a hazard. The potential candidates of surrogate models are selected among the linear regression models such as OLS regression, Ridge, Elastics Net, LASSO. The results show that all candidate models can

produce the highly accurate results of economic damage on domestic supply and employment (approximately 0.99), and reasonable accuracy on migration (>0.88), and on household income (>0.80). The models with regularization technique can shrink the coefficient of features that have less influence on the prediction, such as LASSO, Ridge, and Elastics Net regression. Moreover, we demonstrate how to connect the output from the surrogate model to an optimization model. In the case study, a multi-objective optimization model is designed using the framework from Chapter 2. This optimization model further showcases the flexibility and generalization of the proposed framework.

5.2 Limitation and future work

The modeling of mitigation planning on community resilience covers a broad spectrum of research areas, and this study only discusses some components. The limitations of this study require further research on the following aspects.

First, the flexibility and generalization of the proposed framework come from the design of the input data, where decision makers are responsible for using the correct data and data sources. Such a design brings an underlying issue that the data provided by the decision makers might introduce biases into the final decision-making. For instance, the model introduced to calculate population dislocation in Chapter 3 only considered the black and Hispanic population in the city Joplin, MO, because Black (3.2% of total population) and Hispanic population (5.1% of total population) are ranked as top two ethnic minorities as compared with American Indian & Alaska Native (1.8%), Asian (2.3%), and Native Hawaiian and Other Pacific Island (0.1%) (Data USA). The Decision makers should be aware of such disparity introduced from the input data and any ethical implication resulted

from the decision-making. To address such an issue, there are two suggestions when using the proposed framework. First, the metrics selected as the coefficients of objectives are determined by the decision makers, who have the responsibility to ensure if the data are intuitively closed to the background of the community. Secondly, the related scientist/experts should involve into the design of appropriate method to calculate the metric representing the specific aspect of the community. For example, with the method used to calculate population dislocation in Chapter 3, the decision makers can involve social scientists/experts into the selection of an appropriate model to determine which ethnic groups should be included in the model according to the demographic structure of the city of Joplin.

Secondly, this application in Chapter 3 demonstrates how to apply the framework in Chapter 2 to the city of Joplin, MO. The coefficient associated with building functionality only considers the structural integrity of the buildings, which only provides the perspective of the structural damage on the buildings. However, the primary purpose of the buildings is to serve people in the community such as delivering essential services, supporting the social and economic interest, and providing shelters. The building functionality defined from Almufti and Willford (2013) considered the structural integrity and availability of utilities (e.g., water, power, etc.) of a building. In future work, two suggestions can be considered to address this limitation. The first suggestion is that the input data can include the functionalities of critical utilities as the coefficients of the objectives of the model. For example, the functionality of the power network can be designed as one of the objectives. Such a method does not provide an overall building functionality, but it allows the decision makers to include the factors that are appropriate

for the community. The second suggestion is that building functionality provided in the input data should include the building functionality calculated from damage on both structural and non-structural components of a building. Zhang, et al. (2018) demonstrated the possibility to estimate the building functionality loss affected by both the structural integrity and availability of the critical utilities.

Lastly, the framework proposed in this study only illustrates a case study with a single hazard in Chapter 3. However, a hazard triggered by other hazards is not uncommon. For example, the earthquakes with magnitude between 7.6 and 7.8 might produce destructive tsunamis, landslides that are frequently triggered by earthquakes, or floods can be a consequence of tropical cyclones (e.g., hurricane, typhoon, tropical storm). Future studies can consider the multiple hazards in one framework, but an in-depth discussion is recommended to consider three suggestions: (1) the relationship between the first and secondary hazard, (2) a method to determine the building's structural damage because of fragility curves associated with specific hazards, and (3) a method to combine the retrofit strategies from different hazards in one building type.

The novel design of the framework of multi-objective optimization from this study allows input data to reflect the characteristics of the hazards and the community resilience goals determined by the decision makers; however, if the input data could introduce the social bias into the model, future studies should identify the bias and reduce the influence on the decision-making. Moreover, in this study, the functionality of critical infrastructures can be introduced from input data but should not be limited by the availability of data. Future studies should expand the ability of the framework to include the interdependency

between critical systems (e.g., water, gas, power) and buildings into the framework. Lastly, the future works can consider applying the framework to multiple hazard events.

Reference

Adachi, T. & Ellingwood, B. R. (2008), Serviceability of Earthquake-Damaged Water Systems: Effects of Electrical Power Availability and Power Backup Systems on System Vulnerability, *Reliability Engineering & System Safety*, **93**(1), 78-88.

Almufti, I. & Willford, M. (2013), *Redi™ Rating System: Resilience Based Earthquake Design Initiative for the Next Generation of Buildings*, Arup Co.

Alshehri, S. A., Rezgui, Y. & Li, H. (2014), Delphi-Based Consensus Study into a Framework of Community Resilience to Disaster, *Natural Hazards: Journal of the International Society for the Prevention and Mitigation of Natural Hazards*, **75**(3), 2221-2245.

Altman, N. S. (1992), An Introduction to Kernel and Nearest-Neighbor Nonparametric Regression, *The American Statistician*, **46**(3), 175-185.

Amini, M. O. & van de Lindt, J. W. (2014), Quantitative Insight into Rational Tornado Design Wind Speeds for Residential Wood-Frame Structures Using Fragility Approach, *Journal of Structural Engineering*, **140**(7), 04014033.

Arca, B., Ghisu, T. & Trunfio, G. A. (2015), Gpu-Accelerated Multi-Objective Optimization of Fuel Treatments for Mitigating Wildfire Hazard, *Journal of Computational Science*, **11**, 258-268.

Bai, J.-W., Hueste, M. & Gardoni, P. (2009), Probabilistic Assessment of Structural Damage Due to Earthquakes for Buildings in Mid-America, *Journal of Structural Engineering*, **135**(10), 1155-1163.

Berke, P. & Stubbs, N. (1989), Automated Decision Support Systems for Hurricane Mitigation Planning, *SIMULATION*, **53**(3), 101-109.

Berke, P. R. & Beatley, T. (1992), A National Assessment of Local Earthquake Mitigation: Implications for Planning and Public Policy, *Earthquake Spectra*, **8**(1), 1-15.

Bhatia, N. (2010), Survey of Nearest Neighbor Techniques, *arXiv preprint arXiv:1007.0085*.

Boisvert, R. (1992), Indirect Losses from a Catastrophic Earthquake and the Local, Regional, and National Interest, *Indirect Economic Consequences of a Catastrophic Earthquake*, pp. 207-265.

Brody, S. D. & Highfield, W. E. (2013), Open Space Protection and Flood Mitigation: A National Study, *Land Use Policy*, **32**, 89-95.

Brody, S. D., Zahran, S., Highfield, W. E., Bernhardt, S. P. & Vedlitz, A. (2009), Policy Learning for Flood Mitigation: A Longitudinal Assessment of the Community Rating System in Florida, *Risk Analysis*, **29**(6), 912-929.

Bruneau, M., Chang, S. E., Eguchi, R. T., Lee, G. C., O'Rourke, T. D., Reinhorn, A. M., Shinozuka, M., Tierney, K., Wallace, W. A. & von Winterfeldt, D. (2003), A Framework to Quantitatively Assess and Enhance the Seismic Resilience of Communities, *Earthquake Spectra*, **19**(4), 733-752.

Calle, C. P. M. (2019), A Comparative of Population Dislocation Models for Multi-Objective Community Resilience Optimization, University of Oklahoma, Norman, Oklahoma.

Chang, S. E., Pasion, C., Tatebe, K. & Ahmad, R. (2008), Linking Lifeline Infrastructure Performance and Community Disaster Resilience: Models and Multi-Stakeholder Processes, *Washington, DC: National Science Foundation*.

Chang, S. E. & Rose, A. (2012), Towards a Theory of Economic Recovery from Disasters, *International Journal of Mass Emergencies & Disasters*, **30**(2).

Chowdhury, A. G., Simiu, E. & Leatherman, S. P. (2009), Destructive Testing under Simulated Hurricane Effects to Promote Hazard Mitigation, *Natural Hazards Review*, **10**(1), 1-10.

Cleveland, W. S. & Devlin, S. J. (1988), Locally Weighted Regression: An Approach to Regression Analysis by Local Fitting, *Journal of the American statistical association*, **83**(403), 596-610.

Concannon, P. R., Brooks, H. E. & Doswell III, C. A. (2000), Climatological Risk of Strong and Violent Tornadoes in the United States, *Second Symp. on Environmental Applications*, American Meteorological Society, Long Beach, CA,.

Cuny, F. C. (1991), Living with Floods: Alternatives for Riverine Flood Mitigation, *Land Use Policy*, **8**(4), 331-342.

Cutler, H. & Davies, S. (2010), The Economic Consequences of Productivity Changes: A Computable General Equilibrium (Cge) Analysis, *Regional Studies*, **44**(10), 1415-1426.

Cutler, H., Nicholson, C., Wang, N. & Zharan, S. (2016a), Merging Economic and Civil Engineering Models to Estimate the Impact of Earthquakes, *55th Annual Meeting of the Southern Regional Science Association*, Washington, DC.

Cutler, H., Shields, M., Tavani, D. & Zahran, S. (2016b), Integrating Engineering Outputs from Natural Disaster Models into a Dynamic Spatial Computable General Equilibrium Model of Centerville, *Sustainable and Resilient Infrastructure*, **1**(3-4), 169--187.

Cutter, S. L., Boruff, B. J. & Shirley, W. L. (2003), Social Vulnerability to Environmental Hazardsn, *SOCIAL SCIENCE QUARTERLY*, **84**(2), 242-261.

Dahal, B. & Dahal, R. (2017), Landslide Hazard Map: Tool for Optimization of Low-Cost Mitigation, *Geoenviron Disasters*, **4**(1), 1-9.

Data USA. Joplin Mo, Date Accessed 27-September, 2021, **https://datausa.io/profile/geo/joplin-mo,**.

Deyle, R. E., Chapin, T. S. & Baker, E. J. (2008), The Proof of the Planning Is in the Platting: An Evaluation of Florida's Hurricane Exposure Mitigation Planning Mandate, *Journal of the American Planning Association*, **74**(3), 349-370.

Dodo, A., Davidson, R. A., Xu, N. & Nozick, L. K. (2007), Application of Regional Earthquake Mitigation Optimization, *Computers & Operations Research*, **34**(8), 2478-2494.

Dodo, A., Xu, N. & Davidson, R. A. (2005), Optimizing Regional Earthquake Mitigation Investment Strategies, *Earthquake Spectra*, **21**(2), 305-327.

Dong, Y., Frangopol, D. M. & Saydam, D. (2014), Pre-Earthquake Multi-Objective Probabilistic Retrofit Optimization of Bridge Networks Based on Sustainability, *Journal of Bridge Engineering*, **19**(6), 04014018.

Dueñas-Osorio, L., Craig, J. I. & Goodno, B. J. (2007), Seismic Response of Critical Interdependent Networks, *Earthquake Engineering & Structural Dynamics*, **36**(2), 285-306.

Ellingwood, B. R. (2007), Strategies for Mitigating Risk to Buildings from Abnormal Load Events, *International Journal of Risk Assessment and Management*, **7**(6-7), 828-845.

Ellingwood, B. R., Cutler, H., Gardoni, P., Peacock, W. G., van de Lindt, J. W. & Wang, N. (2016), The Centerville Virtual Community: A Fully Integrated Decision Model of Interacting Physical and Social Infrastructure Systems, *Sustainable and Resilient Infrastructure*, **1**(3-4), 95-107.

Ellingwood, B. R., van de Lindt, J. W. & McAllister, T. P. (2019), A Fully Integrated Model of Interdependent Physical Infrastructure and Social Systems, *The Bridge*, **49**(2), 43-51.

Fang, Y.-P. & Zio, E. (2019), An Adaptive Robust Framework for the Optimization of the Resilience of Interdependent Infrastructures under Natural Hazards, *European Journal of Operational Research*, **276**(3), 1119-1136.

Farokhnia, K., van de Lindt, J. W. & Koliou, M. (2020), Selection of Residential Building Design Requirements to Achieve Community Functionality Goals under Tornado Loading, *Practice Periodical on Structural Design and Construction*, **25**(1), 04019035.

Faturechi, R. & Miller-Hooks, E. (2013), A Mathematical Framework for Quantifying and Optimizing Protective Actions for Civil Infrastructure Systems, *Computer-Aided Civil and Infrastructure Engineering*, **29**(8), 572-589.

Federal Emergency Management Agency (FEMA). (1999), Hazus-Mh 2.1 Earthquake Model Technical Manual, Federal Emergency Management Agency Mitigation Division, Retrieved from https://www.fema.gov/sites/default/files/2020-09/fema_hazus_earthquake-model_technical-manual_2.1.pdf.

Federal Emergency Management Agency (FEMA). (2014), Homeowner's Guide to Retrofitting: Six Ways to Protect Your Home from Flooding, Retrieved from https://www.fema.gov/sites/default/files/2020-08/FEMA_P-312.pdf.

Filiatrault, A. & Sullivan, T. (2014), Performance-Based Seismic Design of Nonstructural Building Components: The Next Frontier of Earthquake Engineering, *Earthquake Engineering and Engineering Vibration*, **13**(S1), 17-46.

Fujimi, T. & Tatano, H. (2012), Estimation of Indirect Economic Loss Caused by House Destruction in a Natural Disaster, *Natural Hazards*, **61**(3), 1367-1388.

Gardoni, P., van de Lindt, J. W., Ellingwood, B., McAllister, T. P., Lee, J. S., Cutler, H., Peacock, W. G. & Cox, D. (2018), The Interdependent Networked Community Resilience Modelingenvironment (in-Core), *Proceedings of 16th European Conference on Earthquake Engineering*, Thessaloniki, Greece.

Gatzlaff, D., McCullough, K., Medders, L. & Nyce, C. M. (2018), The Impact of Hurricane Mitigation Features and Inspection Information on House Prices, *The Journal of Real Estate Finance and Economics*, **57**(4), 566-591.

Ge, Y., Peacock, W. G. & Lindell, M. K. (2011), Florida Households' Expected Responses to Hurricane Hazard Mitigation Incentives, *Risk Analysis*, **31**(10), 1676-1691.

Gilbert, S. W., Butry, D. T., Helgeson, J. F. & Chapman, R. E. (2015), Community Resilience Economic Decision Guide for Buildings and Infrastructure Systems, *Gaithersburg, MD: NIST Special Publication 1197*.

González, A. D., Dueñas-Osorio, L., Sánchez-Silva, M. & Medaglia, A. L. (2016), The Interdependent Network Design Problem for Optimal Infrastructure System Restoration, *Computer-Aided Civil and Infrastructure Engineering*, **31**(5), 334-350.

Gordon, P., Moore II, J. E., Richardson, H. W., Shinozuka, M. & Cho, S. (2004), Earthquake Disaster Mitigation for Urban Transportation Systems: An Integrated Methodology That Builds on the Kobe and Northridge Experiences, *Modeling Spatial and Economic Impacts of Disasters*, 205-232.

Guha, G.-S. (2011), Simulation of the Economic Impact of Region-Wide Electricity Outages from a Natural Hazard Using a Cge Model, *Southwestern Economic Review*, **32**, 101-124.

Guidotti, R., Chmielewski, H., Unnikrishnan, V., Gardoni, P., McAllister, T. & van de Lindt, J. (2016), Modeling the Resilience of Critical Infrastructure: The Role of Network Dependencies, *Sustain Resilient Infrastruct*, **1**(3-4), 153-168.

Gupta, A. & Shah, H. C. (1998), The Strategy Effectiveness Chart: A Tool for Evaluating Earthquake Disaster Mitigation Strategies, *Applied Geography*, **18**(1), 55-67.

Harrison, S., Silver, A. & Doberstein, B. (2015), Post-Storm Damage Surveys of Tornado Hazards in Canada: Implications for Mitigation and Policy, *International Journal of Disaster Risk Reduction*, **13**, 427-440.

Houston, J. B., Spialek, M. L., First, J., Stevens, J. & First, N. L. (2017), Individual Perceptions of Community Resilience Following the 2011 Joplin Tornado, *Journal of Contingencies and Crisis Management*, **25**(4), 354-363.

Jamieson, G. & Drury, C. (1997), Hurricane Mitigation Efforts at the U.S. Federal Emergency Management Agency, in Diaz, H. F. & Pulwarty, R. S. (eds.), *Hurricanes: Climate and Socioeconomic Impacts*, Springer Berlin Heidelberg, Berlin, Heidelberg, pp. 251-257.

Kanamori, H., Hauksson, E. & Heaton, T. (1997), Real-Time Seismology and Earthquake Hazard Mitigation, *Nature*, **390**(6659), 461-464.

Kantamaneni, K., Alrashed, I. & Phillips, M. (2017), Cost Vs. Safety: A Novel Design for Tornado Proof Homes, *HBRC Journal*, **13**(2), 223-232.

Karakoc, D. B., Almoghathawi, Y., Barker, K., González, A. D. & Mohebbi, S. (2019), Community Resilience-Driven Restoration Model for Interdependent Infrastructure Networks, *International Journal of Disaster Risk Reduction*, **38**, 101228.

Kim, A. A. & Reed, D. A. (2020), Interdisciplinary Approach to Building Functionality for Weather Hazards, *Risk Analysis*, **41**(7), 1213-1217.

Koliou, M. & van de Lindt, J. W. (2020), Development of Building Restoration Functions for Use in Community Recovery Planning to Tornadoes, *Natural Hazards Review*, **21**(2), 04020004.

Koliou, M., van de Lindt, J. W., McAllister, T. P., Ellingwood, B. R., Dillard, M. & Cutler, H. (2018), State of the Research in Community Resilience: Progress and Challenges, *Sustain Resilient Infrastruct*, **5**(3), 131-151.

Kopp, G. A., Morrison, M. J., Gavanski, E., Henderson, D. J. & Hong, H. P. (2010), "Three Little Pigs" Project: Hurricane Risk Mitigation by Integrated Wind Tunnel and Full-Scale Laboratory Tests, *Natural Hazards Review*, **11**(4), 151-161.

Kousky, C. & Walls, M. (2014), Floodplain Conservation as a Flood Mitigation Strategy: Examining Costs and Benefits, *Ecological Economics*, **104**, 119-128.

Kuligowski, E. D., Lombardo, F. T., Phan, L. T., Levitan, M. L. & Jorgensen, D. P. (2014), Final Report, National Institute of Standards and Technology (Nist) Technical Investigation of the May 22, 2011, Tornado in Joplin, Missouri., *National Construction Safety Team Act Reports (NIST NCSTAR)*, National Institute of Standards and Technology, Gaithersburg, MD.

Laumanns, M., Thiele, L. & Zitzler, E. (2006), An Efficient, Adaptive Parameter Variation Scheme for Metaheuristics Based on the Epsilon-Constraint Method, *European Journal of Operational Research*, **169**(3), 932-942.

Leatherman, S. P., Gan Chowdhury, A. & Robertson, C. J. (2007), Wall of Wind Full-Scale Destructive Testing of Coastal Houses and Hurricane Damage Mitigation, *Journal of Coastal Research*, **23**(5 (235)), 1211-1217.

Legg, M., Davidson, R. A. & Nozick, L. K. (2013), Optimization-Based Regional Hurricane Mitigation Planning, *Journal of Infrastructure Systems*, **19**(1), 1-11.

Li, Y. (2012), Assessment of Damage Risks to Residential Buildings and Cost-Benefit of Mitigation Strategies Considering Hurricane and Earthquake Hazards, *Journal of Performance of Constructed Facilities*, **26**(1), 7-16.

Lin, P. & Wang, N. (2016), Building Portfolio Fragility Functions to Support Scalable Community Resilience Assessment, *Sustainable and Resilient Infrastructure*, **1**(3-4), 108-122.

Lin, P. & Wang, N. (2017), Stochastic Post-Disaster Functionality Recovery of Community Building Portfolios I: Modeling, *Structural Safety*, **69**, 96-105.

Lin, Y. S. (2009), Development of Algorithms to Estimate Post-Disaster Population Dislocation-a Research-Based Approach, Texas A&M University.

Lin, Y. S., Peacock, W. G. & Zhang, Y. (2008), Household Dislocation Algorithm 3: A Logistic Regression Approach, Hazard Reduction and Recovery Center, Texas A&M University,HRRC Reports: 08-05R.

Liu, H. & Turner, E. J. (1990), Wind Damage Mitigation Strategies for the United States, *Journal of Wind Engineering and Industrial Aerodynamics*, **36**, 975-983.

Liu, Y., McNeil, S., Hackl, J. & Adey, B. T. (2020), Prioritizing Transportation Network Recovery Using a Resilience Measure, *Sustainable and Resilient Infrastructure*, 1-12.

Magis, K. (2010), Community Resilience: An Indicator of Social Sustainability, *Society & Natural Resources*, **23**(5), 401-416.

Maguire, B. & Hagan, P. (2007), Disasters and Communities: Understanding Social Resilience, *Australian Journal of Emergency Management*, **22**(2), 16-20.

Markhvida, M., Walsh, B., Hallegatte, S. & Baker, J. (2020), Quantification of Disaster Impacts through Household Well-Being Losses, *Nature Sustainability*, **3**(7), 538-547.

Martinelli, D., Cimellaro, G. P., Terzic, V. & Mahin, S. (2014), Analysis of Economic Resiliency of Communities Affected by Natural Disasters: The Bay Area Case Study, *Procedia Economics and Finance*, **18**, 959-968.

Masoomi, H., Ameri, M. R. & van de Lindt, J. W. (2018a), Wind Performance Enhancement Strategies for Residential Wood-Frame Buildings, *Journal of Performance of Constructed Facilities*, **32**(3), 04018024.

Masoomi, H. & van de Lindt, J. W. (2016), Tornado Fragility and Risk Assessment of an Archetype Masonry School Building, *Engineering Structures*, **128**, 26-43.

Masoomi, H. & van de Lindt, J. W. (2018), Restoration and Functionality Assessment of a Community Subjected to Tornado Hazard, *Structure and Infrastructure Engineering*, **14**(3), 275-291.

Masoomi, H., van de Lindt, J. W. & Peek, L. (2018b), Quantifying Socioeconomic Impact of a Tornado by Estimating Population Outmigration as a Resilience Metric at the Community Level, *Journal of Structural Engineering*, **144**(5), 04018034.

Mavrotas, G. (2009), Effective Implementation of the E-Constraint Method in Multi-Objective Mathematical Programming Problems, *Applied Mathematics and Computation*, **213**(2), 455-465.

McDonald, J. R., Mehta, K. C., Smith, D. A. & Womble, J. A. (2009), The Enhanced Fujita Scale: Development and Implementation, *Forensic Engineering 2009*, pp. 719-728.

Miles, S. B. & Chang, S. E. (2011), Resilus: A Community Based Disaster Resilience Model, *Cartography and Geographic Information Science*, **38**(1), 36-51.

NIST. (2015), Community Resilience Planning Guide for Buildings and Infrastructure Systems, Volumes I and Ii, *Community resilience planning guide for buildings and infrastructure systems, volumes I and II*, Gaithersburg, MD: NIST Special Publication 1190.

Oettle, N. K. & Bray, J. D. (2013), Geotechnical Mitigation Strategies for Earthquake Surface Fault Rupture, *Journal of Geotechnical and Geoenvironmental Engineering*, **139**(11), 1864-1874.

Okuyama, Y., Hewings, G. J. D. & Sonis, M. (2004), Measuring Economic Impacts of Disasters: Interregional Input-Output Analysis Using Sequential Interindustry Model, in Okuyama, Y. & Chang, S. E. (eds.), *Modeling Spatial and Economic Impacts of Disasters*, Springer Berlin Heidelberg, Berlin, Heidelberg, pp. 77-101.

Park, C. H., Joo, J. G. & Kim, J. H. (2012), Integrated Washland Optimization Model for Flood Mitigation Using Multi-Objective Genetic Algorithm, *Journal of Hydro-environment Research*, **6**(2), 119-126.

Peacock, W. G. (2003), Hurricane Mitigation Status and Factors Influencing Mitigation Status among Florida's Single-Family Homeowners, *Natural Hazards Review*, **4**(3), 149-158.

Pinelli, J.-P., Torkian, B., Gurley, K., Subramanian, C. & Hamid, S. (2009), Vulnerability Curves to Predict Loss on Mitigated Residential Buildings, *Proceedings of the 11th Americas Conference on Wind Engineering, San Juan*, Citeseer.

Pollyea, R. M., Mohammadi, N., Taylor, J. E. & Chapman, M. C. (2018), Geospatial Analysis of Oklahoma (USA) Earthquakes (2011–2016): Quantifying the Limits of Regional-Scale Earthquake Mitigation Measures, *Geology* **46**(3), 215–218.

Prevatt, D. O., Lindt, J. W. v. d., Back, E. W., Graettinger, A. J., Pei, S., Coulbourne, W., Gupta, R., James, D. & Agdas, D. (2012a), Making the Case for Improved

Structural Design: Tornado Outbreaks of 2011, *Leadership and Management in Engineering*, **12**(4), 254-270.

Prevatt, D. O., Roueche, D. B., Lindt, J. W. v. d., Pei, S., Dao, T., Coulbourne, W., Graettinger, A. J., Gupta, R. & Grau, D. (2012b), Building Damage Observations and Ef Classifications from the Tuscaloosa, Al, and Joplin, Mo, Tornadoes, *Structures Congress 2012*, pp. 999-1010.

Ramseyer, C., Holliday, L. & Floyd, R. (2016), Enhanced Residential Building Code for Tornado Safety, *Journal of Performance of Constructed Facilities*, **30**(4), 04015084.

Renschler, C. S., Frazier, A. E., Arendt, L. A., Cimellaro, G. P., Reinhorn, A. M. & Bruneau, M. (2010), Developing the 'Peoples' Resilience Framework for Defining and Measuring Disaster Resilience at the Community Scale, *9th US national and 10th Canadian conference on earthquake engineering (9USN/10CCEE).* Toronto, Ontario, Canada.

Ripberger, J. T., Jenkins-Smith, H. C., Silva, C. L., Czajkowski, J., Kunreuther, H. & Simmons, K. M. (2018), Tornado Damage Mitigation: Homeowner Support for Enhanced Building Codes in Oklahoma, *Risk Analysis*, **38**(11), 2300-2317.

Rose, A. & Guha, G.-S. (2004), Computable General Equilibrium Modeling of Electric Utility Lifeline Losses from Earthquakes, in Okuyama, Y. & Chang, S. E. (eds.),

Modeling Spatial and Economic Impacts of Disasters, Springer Berlin Heidelberg, Berlin, Heidelberg, pp. 119-141.

Rose, A. & Liao, S.-Y. (2005), Modeling Regional Economic Resilience to Disasters: A Computable General Equilibrium Analysis of Water Service Disruptions, *Journal of Regional Science*, **45**(1), 75-112.

Rosenheim, N., Guidotti, R., Gardoni, P. & Peacock, W. G. (2021), Integration of Detailed Household and Housing Unit Characteristic Data with Critical Infrastructure for Post-Hazard Resilience Modeling, *Sustainable and Resilient Infrastructure*, **6**(6), 385-401.

Sadeghi, M., Ghafory-Ashtiany, M. & Pakdel-Lahiji, N. (2017), Multi-Objective Optimization Approach to Define Risk Layer for Seismic Mitigation, *Geomatics, Natural Hazards and Risk*, **8**(2), 257-270.

Simmons, K. M., Kovacs, P. & Kopp, G. A. (2015), Tornado Damage Mitigation: Benefit–Cost Analysis of Enhanced Building Codes in Oklahoma, *Weather, Climate, and Society*, **7**(2), 169-178.

Smith, T. L., Perotin, M. & Walsh, E. (2012), Enhancing Tornado Performance of Critical Facilities: Findings and Recommendations of Fema's Mitigation Assessment Team, *Structures Congress 2012*, pp. 977-988.

Strader, S. M., Pingel, T. J. & Ashley, W. S. (2016), A Monte Carlo Model for Estimating Tornado Impacts, *Meteorological Applications*, **23**(2), 269-281.

Sutley, E. J., van de Lindt, J. W. & Peek, L. (2017a), Community-Level Framework for Seismic Resilience. I: Coupling Socioeconomic Characteristics and Engineering Building Systems, *Natural Hazards Review*, **18**(3), 04016014.

Sutley, E. J., van de Lindt, J. W. & Peek, L. (2017b), Community-Level Framework for Seismic Resilience. Ii: Multiobjective Optimization and Illustrative Examples, *Natural Hazards Review*, **18**(3), 04016015.

Tapia, C. & Padgett, J. E. (2016), Multi-Objective Optimisation of Bridge Retrofit and Post-Event Repair Selection to Enhance Sustainability, *Structure and Infrastructure Engineering*, **12**(1), 93-107.

Tasseff, B., Bent, R. & Van Hentenryck, P. (2019), Optimization of Structural Flood Mitigation Strategies, *Water Resources Research*, **55**(2), 1490-1509.

U.S. Census Bureau. (2011), 2010 Census Summary File 1, in Department of Commerce (ed.), Retrieved from https://www.census.gov/data/datasets/2010/dec/summary-file-1.html.

Unnikrishnan, V. U. & van de Lindt, J. W. (2016), Probabilistic Framework for Performance Assessment of Electrical Power Networks to Tornadoes, *Sustainable and Resilient Infrastructure*, **1**(3-4), 137--152.

Üstün, A. K. & Anagün, A. S. (2015), Multi-Objective Mitigation Budget Allocation Problem and Solution Approaches: The Case of İstanbu, *Computers & Industrial Engineering*, **81**, 118-129.

van de Lindt, J. W., Ellingwood, B., McAllister, T. P., Gardoni, P., Cox, D., Peacock, W. G., Cutler, H., Dillard, M. K., Lee, J. S., Peek, L. & Mitrani-Reiser, J. (2018), Modeling Community Resilience: Update on the Center for Risk-Based Community Resilience Planning and the Computational Environment in-Core, *17th U.S.-Japan-New Zealand Workshop on the Improvement of Structural Engineering and Resilience (ATC-15-16)*, Queenstown, New Zealand.

van de Lindt, J. W., Pei, S., Dao, T., Graettinger, A., Prevatt, D. O., Gupta, R. & Coulbourne, W. (2013), Dual-Objective-Based Tornado Design Philosophy, *Journal of Structural Engineering*, **139**(2), 251-263.

van der Veen, A. (2004), Disasters and Economic Damage: Macro, Meso and Micro Approaches, *Disaster Prevention and Management: An International Journal*, **13**(4), 274-279.

Van Zandt, S., Peacock, W. G., Henry, D. W., Grover, H., Highfield, W. E. & Brody, S. D. (2012), Mapping Social Vulnerability to Enhance Housing and Neighborhood Resilience, *Housing Policy Debate*, **22**(1), 29-55.

Walsh, E. & Tezak, S. (2012), Findings and Recommendations of Fema's Mitigation Assessment Team Investigations of the Spring 2011 Tornado Outbreaks, *Forensic Engineering 2012*, pp. 821-830.

Wang, G., Chen, R. & Chen, J. (2017), Direct and Indirect Economic Loss Assessment of Typhoon Disasters Based on Ec and Io Joint Model, *Natural Hazards*, **87**(3), 1751-1764.

Wang, W., van de Lindt, J. W., Cutler, H., Rosenheim, N., Koliou, M., Lee, J. S. & Calderon, D. (2020), Community Resilience Assessment of an Ef-5 Tornado Using the in-Core Modeling Environment, *Life-Cycle Civil Engineering: Innovation, Theory and Practice*, CRC Press, pp. 394-398.

Wang, W., van de Lindt, J. W., Rosenheim, N., Cutler, H., Hartman, B., Sung Lee, J. & Calderon, D. (2021), Effect of Residential Building Wind Retrofits on Social and Economic Community-Level Resilience Metrics, *Journal of Infrastructure Systems*, **27**(4), 04021034.

Wang, Y., Wang, N., Lin, P., Ellingwood, B., Mahmoud, H. & Maloney, T. (2018), De-Aggregation of Community Resilience Goals to Obtain Minimum Performance Objectives for Buildings under Tornado Hazards, *Structural Safety*, **70**, 82-92.

West, G. R. (1995), Comparison of Input–Output, Input–Output + Econometric and Computable General Equilibrium Impact Models at the Regional Level, *Economic Systems Research*, **7**(2), 209-227.

Wind, T. R., Fordham, M. & H. Komproe, I. (2011), Social Capital and Post-Disaster Mental Health, *Global Health Action*, **4**(1), 6351.

Wing, I. S. (2004), Computable General Equilibrium Models and Their Use in Economy-Wide Policy Analysis, *Technical Note, Joint Program on the Science and Policy of Global Change, MIT*.

Woodward, M., Gouldby, B., Kapelan, Z. & Hames, D. (2014), Multiobjective Optimization for Improved Management of Flood Risk, *Journal of Water Resources Planning and Management*, **140**(2), 201-215.

Xiao, Y. & Nilawar, U. (2013), Winners and Losers: Analysing Post-Disaster Spatial Economic Demand Shift, *Disasters*, **37**(4), 646-668.

Xie, J., Chen, H., Liao, Z., Gu, X., Zhu, D. & Zhang, J. (2017), An Integrated Assessment of Urban Flooding Mitigation Strategies for Robust Decision Making, *Environmental Modelling & Software*, **95**, 143-155.

Xu, N., Davidson, R. A., Nozick, L. K. & Dodo, A. (2007), The Risk-Return Tradeoff in Optimizing Regional Earthquake Mitigation Investment, *Structure and Infrastructure Engineering*, **3**(2), 133-146.

Yazdi, J. & Salehi Neyshabouri, S. A. A. (2014), Identifying Low Impact Development Strategies for Flood Mitigation Using a Fuzzy-Probabilistic Approach, *Environmental Modelling & Software*, **60**, 31-44.

Zahran, S., Brody, S. D., Peacock, W. G., Vedlitz, A. & Grover, H. (2008), Social Vulnerability and the Natural and Built Environment: A Model of Flood Casualties in Texas, *Disasters*, **32**(4), 537-560.

Zhang, W., Lin, P., Wang, N., Nicholson, C. & Xue, X. (2018), Probabilistic Prediction of Postdisaster Functionality Loss of Community Building Portfolios Considering Utility Disruptions, *Journal of Structural Engineering*, **144**(4), 04018015.

Zhang, W. & Nicholson, C. (2016), A Multi-Objective Optimization Model for Retrofit Strategies to Mitigate Direct Economic Loss and Population Dislocation, *Sustainable and Resilient Infrastructure*, **1**(3-4), 123-136.

Zhang, X. & Miller-Hooks, E. (2014), Scheduling Short-Term Recovery Activities to Maximize Transportation Network Resilience, *Journal of Computing in Civil Engineering*, **29**(6), 04014087.

Zhou, L. & Chen, Z. (2020), Are Cge Models Reliable for Disaster Impact Analyses?, *Economic Systems Research*, **33**(1), 20-46.